

Ferroptosis in Glioblastoma: Mechanisms, Therapeutic Strategies, and Future Directions

This systematic review examines the role of ferroptosis in glioblastoma through analysis of 95 studies spanning 2018–2025. Key regulators such as GPX4, ROS, and NCOA4 emerge as potential therapeutic targets, while innovative strategies include gene editing and nanotechnology-based combinations to induce ferroptosis. Despite its potential, challenges like small sample sizes, in vitro reliance, and tumor microenvironment complexity hinder clinical application. Addressing adaptive resistance, validating biomarkers, and employing multimodal approaches in diverse in vivo models are essential for advancing ferroptosis-based glioblastoma therapies. Below are three illustrative findings of many in the review.

- **FTL upregulation** fosters glioblastoma progression through immunosuppressive M2 macrophage polarization; its inhibition enhances T cell recruitment and anti-PD1 sensitivity, offering promising immunotherapy strategies.
- **GPX7 silencing** elevates ferroptosis-related oxidative stress via lipid peroxidation and Fe²⁺ increases, presenting an effective target to enhance ferroptosis sensitivity and suppress glioblastoma development.
- **Iron oxide nanoparticles** synergize with paclitaxel to induce ferroptosis by modulating autophagy pathways, combining nanotechnology and chemotherapeutics to overcome resistance and boost treatment efficacy.

5172 Records screened	95 Full-text studies included	Jan 2018–Oct 2025 Coverage window
---------------------------------	---	---

Table of Contents

1. Methods
2. Results
 - 2.1. Ferroptosis and Immune Modulation: Mechanisms and Therapeutic Strategies in Glioblastoma
 - 2.1.1. Signaling Networks and Subtype Transition in Glioblastoma
 - 2.1.2. Therapeutic Targets and Drug Interactions
 - 2.2. Ferroptosis in Glioblastoma: Pathways, Immune Interactions, and Overcoming Resistance
 - 2.2.1. Mechanisms of Ferroptosis in Glioblastoma
 - 2.2.2. Prognostic Markers and Risk Models
 - 2.2.3. Therapeutic Strategies and Treatment Outcomes
 - 2.3. CD95 Gene Deletion: Reducing Malignancy in Glioblastoma Cells
 - 2.4. Iron Oxide Nanoparticles and Paclitaxel: Inducing Ferroptosis via Autophagic Pathways in Glioblastoma
3. Discussion and Interpretation of Findings
 - 3.1. Ferroptosis and Immune Modulation: Mechanisms and Therapeutic Strategies in Glioblastoma
 - 3.2. Ferroptosis in Glioblastoma: Pathways, Immune Interactions, and Overcoming Resistance
 - 3.3. CD95 Gene Deletion: Reducing Malignancy in Glioblastoma Cells
 - 3.4. Iron Oxide Nanoparticles and Paclitaxel: Inducing Ferroptosis via Autophagic Pathways in Glioblastoma
4. Discussion of Limitations
 - 4.1. Ferroptosis and Immune Modulation: Mechanisms and Therapeutic Strategies in Glioblastoma
 - 4.2. Ferroptosis in Glioblastoma: Pathways, Immune Interactions, and Overcoming Resistance
5. Conclusions
6. References

1. Methods

[Go to Annex 1: Methods](#)

2. Results

2.1. Ferroptosis and Immune Modulation: Mechanisms and Therapeutic Strategies in Glioblastoma

2.1.1. Signaling Networks and Subtype Transition in Glioblastoma

Selected findings

- FTL upregulation in tumor-associated macrophages fosters an immunosuppressive environment by inducing M2 polarization, promoting glioblastoma progression, and enhancing angiogenesis. Its inhibition reprograms the tumor microenvironment, increases T cell recruitment, and significantly improves sensitivity to anti-PD1 therapy, offering a promising strategy for immunotherapy in glioblastoma.
- Overexpression of FOSL1 in glioblastoma cells leads to differential expression of 493 genes, including upregulated genes associated with poor prognosis and downregulated genes linked to improved outcomes. These findings highlight FOSL1's role in ferroptosis and glioblastoma subtype transition, presenting opportunities for prognostic biomarker development and therapeutic targeting.
- NRF2 upregulation in TMZ-resistant glioblastoma cells enhances ferroptosis sensitivity by promoting glutathione efflux and lipid peroxidation, correlating with increased tumor aggressiveness and reduced survival rates. This underscores the therapeutic potential of ferroptosis induction to overcome drug resistance and improve glioblastoma treatment outcomes.

Table 1. Signaling Networks and Subtype Transition in Glioblastoma

Study ID	Length of intervention	Population of intervention	Intervention	Intervention details	Primary outcome	Secondary outcome
----------	------------------------	----------------------------	--------------	----------------------	-----------------	-------------------

Guo S et al. (2025)	72 hours	Nude mice aged 6–8 weeks, male and female, subcutaneous implantation of PDX tumor tissue cubes	Transfection of DNA constructs to overexpress FOSL1 tagged with GFP	Transfection performed at 50–75% cell confluency, lipofectamine 3000 reagent used, RNA extraction at 72 h using TRIzol reagent, overexpression assessed at 48 or 72 h post-transfection, studies conducted in triplicates	Role of FOSL1 in regulating biological processes and signaling networks during proneural to mesenchymal subtype transition in glioblastoma, including the identification of upregulated_genes and downregulated_genes.	Identification of 8 upregulated and 4 downregulated genes, pathway implications for glioblastoma prognosis
---------------------	----------	--	---	---	--	--

[Go to Annex 2: Table 1. Signaling Networks and Subtype Transition in Glioblastoma](#)

The intricate relationship between ferroptosis—an iron-dependent cell death mechanism characterized by lipid peroxidation and oxidative stress—and immune modulation in glioblastoma has garnered increasing attention due to its potential therapeutic implications. Recent findings have elucidated mechanisms by which ferroptosis influences immune responses, including tumor-associated macrophage polarization, immune evasion, and cytokine release, as well as the role of key ferroptosis-related genes in shaping the tumor microenvironment. These insights underscore the significance of targeting ferroptosis pathways to enhance immune-based strategies and improve treatment outcomes in glioblastoma, offering promising avenues for innovative therapeutic modalities in managing this aggressive malignancy.

Previous studies demonstrated that ferroptosis represents a promising therapeutic strategy for glioblastoma, leveraging the tumor's unique iron metabolism and lipid peroxidation characteristics to overcome drug resistance and reduce tumor growth [7, 8, 9, 10, 11]. Compounds such as DHL, DHA, ALZ003, and PAB effectively induced ferroptosis; yet, challenges persist in validating ferroptosis biomarkers for prognosis and personalized treatment [12, 13]. Autophagy was identified as a critical mechanism influencing glioblastoma progression and therapeutic resistance, with protective autophagy limiting drug efficacy and cytotoxic autophagy offering potential for tumor suppression [14, 15]. However, the interplay between ferroptosis and immune modulation, as well as the impact of genetic alterations and feedback mechanisms like the PERK-ATF4-HSPA5-GPX4 cascade, remains poorly understood, highlighting the need for further investigation into these pathways [16].

The role of ferroptosis in glioblastoma progression is further exemplified by the differential gene expression linked to FOSL1 overexpression. Overexpression of FOSL1 in glioblastoma cells results in 493 differentially expressed genes, with 152 upregulated and 341 downregulated (adjusted $p < 0.05$) according to Guo S et al. (2025). Functional enrichment analyses confirm its role in ferroptosis, NF- κ B signaling, and cell proliferation, aligning with key pathways previously identified in glioblastoma progression. Survival analysis highlights poor prognosis associated with FOSL1-upregulated genes, such as ITGA5 and STEAP3, while FOSL1-downregulated genes, including ARL3 and BEX1, correlate with improved outcomes. Experimental validation using qPCR and IHC confirms significant differential expression of identified genes at both mRNA and protein levels ($p < 0.05$, $p < 0.01$, $p < 0.001$).

Building on the connection between ferroptosis and immune modulation, FTL emerges as a key regulator of tumor-associated macrophage polarization and glioblastoma progression. Li H et al. (2023) FTL upregulation in tumor-associated macrophages fosters an immunosuppressive environment by inducing M2 polarization, promoting glioblastoma progression, and enhancing angiogenesis. FTL inhibition reprograms the tumor microenvironment by reducing M2 macrophage polarization, attenuating angiogenesis, and increasing CD3+ and CD8+ T cell recruitment, which significantly improves sensitivity to anti-PD1 therapy. Median survival in glioma-bearing mice increases from 24 days to 34.5 days with this combined treatment ($p < 0.05$).

Expanding on the therapeutic implications of ferroptosis, NRF2 upregulation highlights its potential in overcoming drug resistance in glioblastoma. NRF2 upregulation in TMZ-resistant glioblastoma cells enhances ferroptosis sensitivity by promoting ABCC1-mediated glutathione efflux and lipid peroxidation (de Souza I et al. 2022). Clinical data indicate high ABCC1 expression significantly correlates with increased tumor aggressiveness and reduced survival rates (5-year OS: 18% vs. 68%, HR = 1.10, CI = 1.06–1.14, $p < 0.001$). These findings align with the therapeutic potential of ferroptosis induction to address drug resistance in glioblastoma.

2.1.2. Therapeutic Targets and Drug Interactions

Selected findings

- 35G8 induces ferroptosis in glioblastoma cells through PDI inhibition, ER stress activation, and disruption of redox homeostasis, while crossing the blood-brain barrier for therapeutic feasibility. This finding highlights a novel drug candidate with significant potential for glioblastoma treatment by targeting ferroptosis pathways and overcoming delivery challenges.
- Modulation of autophagy and ferroptosis in glioblastoma stem-like cells significantly impacts tumor growth, patient survival, and susceptibility to temozolomide. This finding provides critical insights into the therapeutic interplay of ferroptosis and autophagy, enabling targeted strategies for improving glioblastoma treatment outcomes.

Table 2. Therapeutic Targets and Drug Interactions

Study ID	Length of intervention	Population of intervention	Control	Intervention	Intervention details	Primary outcome	Secondary outcome
Kyani A et al. (2018)	72 hours, 6 hours, 24 hours	Human glioblastoma cell lines U87MG, U118MG, NU04, A172		Treatment of cells with compounds including 35G8, NAC, Z-VAD-FMK, Necrostatin-1, H2O2, catalase, DTT	Cells seeded in 96-well plates, compounds added at specific time intervals, incubation at 37°C and 5% CO2, MTT assay performed for cell viability, PDI activity assessed via reduction reaction, thermal shift assay conducted using microplates and ThermoFluor instrument, Western blotting performed for protein analysis	Validation of PDI as a therapeutic target for glioblastoma, cytotoxicity of pyrimidotriazinedione 35G8	Upregulation of heme oxygenase 1 and SLC7A11, repression of TXNIP and EGR1, induction of autophagy and ferroptosis, activation of Nrf2 antioxidant response and ER stress response

[Go to Annex 3: Table 2. Therapeutic Targets and Drug Interactions](#)

The therapeutic relevance of ferroptosis is reinforced by the potent efficacy of 35G8 as a targeted inducer in glioblastoma models. 35G8 demonstrates potent therapeutic efficacy for glioblastoma, validated as a PDI inhibitor ($IC_{50} = 0.17 \pm 0.01 \mu M$) with cytotoxicity in glioblastoma cells ($IC_{50} = 1.1 \pm 0.2 \mu M$ in U87MG), as reported by Kyani A et al. (2018). It induces ferroptosis by upregulating HMOX1 (19-fold) and SLC7A11 (63-fold), repressing TXNIP (–7.40-fold) and EGR1 (–5.65-fold), and activating ER stress markers such as DDIT3 (4-fold) and GRP78 (8-fold). Additionally, 35G8 disrupts proteostasis and redox homeostasis, confirmed by reduced potency in the presence of deferroxamine, and crosses the blood-brain barrier, supporting its feasibility for glioblastoma treatment.

The interplay between ferroptosis and autophagy provides further insights into glioblastoma stem-like cell survival and therapeutic strategies. Buccarelli M et al. (2018)

Modulation of autophagy and ferroptosis significantly affects glioblastoma stem-like cell (GSC) growth and survival. Low autophagic levels correlate with improved overall survival in GBM patients ($p = 0.0012$; HR = 0.3634; 95% CI: 0.1967–0.6715), while autophagy inhibition enhances GSC susceptibility to TMZ in vitro ($p < 0.05$). Induction of ferroptosis increases lipid peroxidation ($p < 0.01$), decreases GSH levels ($p < 0.01$), promotes mitochondrial ROS accumulation ($p < 0.01$), and reduces GPx activity under ferroptosis inhibition ($p < 0.01$). Despite increased LC3 expression ($p < 0.0001$) and ferroptosis markers ($p < 0.01$), adjunctive treatment with quinacrine does not significantly enhance TMZ's antitumor efficacy in vivo.

Building on the role of ferroptosis modulation in glioblastoma treatment, combinatorial approaches such as Coix and TMZ showcase therapeutic potential through ferroptosis activation and lipid pathway regulation. The combination of Coix (2 mg/ml) and TMZ (0.1 mg/ml) demonstrates a synergistic effect (CI < 1) in inhibiting U251 glioblastoma cell proliferation, with a drug reduction index for TMZ (DRI = 3.266) (Zhao Z et al. 2023). This synergy involves Coix's modulation of interferon-related genes (e.g., RSAD2: 2.37-fold down-regulation in Coix, 2.66-fold up-regulation in TMZ, and 2.14-fold up-regulation in the combination group) and enrichment of lipid-related pathways, including cholesterol metabolism. Ferroptosis activation via ANGPTL4 up-regulation and ABCA1 down-regulation contributes to therapeutic efficacy. RNA-seq and qRT-PCR analyses confirm these mechanisms with statistical significance (FDR < 0.05), and the combination therapy reduces TMZ dosage (IC50: Coix 17.82 mg/ml, TMZ 0.358 mg/ml) while maintaining efficacy.

Expanding on therapeutic strategies targeting ferroptosis and lipid pathways, interventions such as STAT3 depletion provide insights into modulating autophagy-dependent cell death mechanisms in glioblastoma cells. Recent findings by Remy J et al. (2022) demonstrate that STAT3 depletion mitigates lysosomal membrane permeabilization and reduces cathepsin-dependent cell death in glioblastoma cells under Pimozide treatment, significantly enhancing cell survival ($p < 0.0001$, Two-Way ANOVA). Additionally, STAT3 depletion significantly reduces autophagy-dependent cell death mechanisms ($p < 0.01$, $p < 0.0001$), aligning with the understanding of targeted approaches to modulate cell death pathways in apoptosis-resistant glioblastoma cells.

The presented data delineate the interplay between ferroptosis and immune modulation in glioblastoma, highlighting molecular mechanisms and therapeutic approaches explored in the study.

2.2. Ferroptosis in Glioblastoma: Pathways, Immune Interactions, and Overcoming Resistance

2.2.1. Mechanisms of Ferroptosis in Glioblastoma

Selected findings

- GPX7 silencing significantly enhances ferroptosis-related oxidative stress in glioblastoma, as evidenced by reduced glutathione levels, increased lipid peroxidation, and elevated Fe²⁺ concentrations. This finding suggests that targeting GPX7 and its regulatory pathways could improve ferroptosis sensitivity and suppress glioblastoma progression both in vitro and in vivo, offering a promising therapeutic avenue.
- CDKN2A deletion in glioblastoma leads to lipidomic remodeling, redistributing polyunsaturated fatty acids to membrane phospholipids, increasing lipid peroxidation, and priming tumors for ferroptosis. This discovery provides a molecular basis for exploiting lipid metabolism alterations as a therapeutic strategy, particularly through GPX4 inhibition in CDKN2A-null glioblastoma models.
- Hypoxia-induced resistance to ferroptosis in glioblastoma is mediated by SLC7A11 upregulation via the PI3K/AKT/HIF-1 α pathway, which reduces lipid peroxidation and increases IC50 values for ferroptosis inducers. Targeting HIF-1 α with PX-478 or inhibiting AKT reverses this resistance and enhances sulfasalazine-induced ferroptosis, presenting a synergistic anticancer therapeutic approach.
- Quiescent astrocyte-like glioma cells exhibit mitochondrial dysfunction and lipid peroxidation, rendering them highly sensitive to GPX4 inhibition and ferroptosis (Banu MA et al. 2024). These findings provide a targeted therapeutic strategy to selectively eliminate resistant glioblastoma cell populations by exploiting mitochondrial vulnerabilities.
- Hypoxia-induced ferroptosis resistance in glioblastoma is mediated by SLC7A11 upregulation via the PI3K/AKT/HIF-1 α pathway (Sun S et al. 2022). Targeting HIF-1 α with PX-478 or AKT inhibition reverses resistance, enhancing the efficacy of ferroptosis inducers and improving survival in preclinical models.
- METTL16 knockdown induces ferroptosis in glioma cells by destabilizing NFE2L2 mRNA and reducing antioxidant defenses, while also modulating immune cell infiltration and checkpoint expression (Yang Y et al. 2024). This dual role in ferroptosis regulation and immune interactions highlights METTL16 as a promising therapeutic target in glioblastoma.
- CDKN2A deletion redistributes polyunsaturated fatty acids to membrane phospholipids, increasing lipid peroxidation and ferroptosis susceptibility in glioblastoma cells (Minami JK et al. 2023). GPX4 inhibition in CDKN2A-null models demonstrates improved survival, validating lipidomic alterations as a therapeutic vulnerability.

Table 3. Mechanisms of Ferroptosis in Glioblastoma

Study ID	Length of intervention	Population of intervention	Control	Intervention	Intervention details	Primary outcome	Secondary outcome
Chen Y et al. (2019)	14 days	Patients with malignant glioma undergoing surgical treatment; specific pathogen-free athymic nude BALB/c mice injected with glioma cells		Use of antibodies, chemical compounds (DHA, ferrostatin-1, liproxstatin-1, GSK2606414, EGCG, deferoxamine), siRNA transfections	Transfections via Lipofectamine 2000, compound treatments, flow cytometry staining for ROS and lipid ROS, biochemical assays for glutathione and GPX4 activity, incubations at 37°C (4 hours for assay, 30 minutes for ROS staining, 10 minutes for lipid ROS staining), tumor generation through cell injections (2×10 ⁶ cells in 0.2 ml PBS per mouse), protocols followed based on manufacturer's recommendations	Induction of ferroptosis in glioma cells by DHA, characterized by iron-dependent cell death, ROS generation, and lipid peroxidation	Activation of protective PERK-ATF4-HSPA5-GPX4 pathway, increased ferroptosis sensitivity upon pathway inhibition

[Go to Annex 4: Table 3. Mechanisms of Ferroptosis in Glioblastoma](#)

Ferroptosis, a regulated form of cell death driven by iron-dependent lipid peroxidation, has emerged as a promising therapeutic target in glioblastoma. This chapter explores the molecular pathways governing ferroptosis, including iron metabolism, lipid peroxidation, and antioxidant systems, alongside its interactions with the immune microenvironment and mechanisms of therapeutic resistance. Advances in understanding these processes have highlighted opportunities to modulate ferroptosis, enhance immune system engagement, and overcome therapeutic barriers. Integrating these insights offers promising strategies for improving glioblastoma outcomes amidst its aggressive nature and resistance to conventional therapies.

Previous studies have demonstrated the therapeutic potential of ferroptosis in glioblastoma, highlighting the efficacy of GPX4 inhibition and lipid metabolism modulation in inducing ferroptosis and overcoming treatment resistance [40, 41]. Natural compounds and combination therapies integrating ferroptosis-based approaches with chemotherapy and radiotherapy have shown promise in preclinical models [42, 43]. However, challenges such as glioblastoma heterogeneity, the immunosuppressive tumor microenvironment, poor blood-brain barrier penetration, and the toxicity of ferroptosis inducers remain significant barriers to clinical translation [44]. While biomarkers like GPX4 and SLC7A11 play crucial roles in ferroptosis sensitivity, the lack of standardized markers and mechanistic understanding of ferroptosis regulation necessitates further investigation [45, 46].

The molecular pathways of ferroptosis offer insights into how DHA induces ferroptosis and how resistance mechanisms, such as the PERK/ATF4/HSPA5 pathway, modulate therapeutic efficacy. DHA effectively induces ferroptosis in glioblastoma cells through iron-dependent mechanisms, including ROS generation, lipid peroxidation, and increased MDA levels ($p < 0.05$, $p < 0.01$, $p < 0.001$) according to Chen Y et al. (2019). Resistance mediated by the PERK/ATF4/HSPA5 pathway, which enhances GPX4 expression and activity, is significantly reduced by pathway inhibition, resulting in enhanced ferroptosis sensitivity and anticancer effects in vitro and in vivo ($p < 0.01$, $p < 0.001$, $n = 3$).

Building upon resistance mechanisms, GPX7 silencing emerges as another critical factor influencing ferroptosis sensitivity and oxidative stress in glioblastoma. GPX7 silencing significantly enhances ferroptosis-related oxidative stress in glioblastoma, as evidenced by reduced glutathione (GSH) levels ($p < 0.001$), increased lipid peroxidation ($p < 0.001$), and elevated Fe²⁺ concentrations ($p < 0.05$) (Zhou Y et al. 2021). It increases sensitivity to erastin, suppressing glioblastoma proliferation, migration, invasion, and tumor growth both in vitro and in vivo, while promoting apoptosis ($p < 0.001$). Additionally, miR-29b-mediated suppression of GPX7 expression further amplifies erastin-induced ferroptosis sensitivity, marked by increased lipid peroxidation ($p < 0.001$), reduced GSH levels ($p < 0.001$), and elevated apoptosis rates ($p < 0.001$), alongside significant reductions in glioblastoma cell proliferation, migration, and invasion.

The role of GPX7 in ferroptosis regulation transitions into broader interactions within the p62/p53/NRF2 axis, highlighting mutation-specific effects on glioblastoma vulnerability. Yuan F et al. (2022) p62 demonstrates a dual role in ferroptosis regulation in glioblastoma, influenced by p53 mutation status. In p53-mutant glioblastoma, p62 promotes ferroptosis by decreasing SLC7A11 expression and enhancing mutant-p53/NRF2 interaction, while in p53-wild-type glioblastoma, it inhibits ferroptosis through classical p62-NRF2 activation and increased SLC7A11 expression. Therapeutic interventions targeting the p62/p53/NRF2 axis, such as APR-246, show promise, with clinical data indicating poorer survival in p53 wild-type glioblastomas with high p62 expression ($p < 0.05$). Additionally, p62 knockout enhances ferroptosis and improves survival in p53-wild-type glioblastoma models, whereas APR-246 reverses p62-mediated ferroptosis enhancement in p53-mutant glioblastoma by reactivating mutant p53 and restoring SLC7A11 expression.

Expanding on ferroptosis regulation, the ATF4-CHAC1 pathway demonstrates its significance in modulating ferroptosis induction in glioma cells. Sevoflurane induces ferroptosis in glioma cells through the activation of the ATF4-CHAC1 pathway, as demonstrated by Xu Y et al. (2022) and dose-dependent increases in Fe²⁺ levels, ROS generation, and suppression of cell viability ($p < 0.05$, $p < 0.01$, $p < 0.001$). These findings align with established roles of iron metabolism and oxidative stress in ferroptosis susceptibility, further highlighting the pathway's significance. Suppression of ATF4 interrupts ferroptosis induction, while the ferroptosis inducer Erastin restores ATF4-CHAC1 activity and ferroptosis, reinforcing the pathway's critical function in regulating glioma cell death.

Insights into ferroptosis pathways culminate in observations of heightened susceptibility in recurrent glioblastoma multiforme tumors, emphasizing the interplay of key molecular markers. Kram H et al. (2022), recurrent glioblastoma multiforme tumors demonstrate heightened susceptibility to ferroptosis, as evidenced by a notable increase in ACSL4 expression by 4.58 IRS points ($p < 0.001$) and a decrease in GPX4 expression by 4.36 IRS points ($p < 0.001$). Furthermore, GPX4+/GFAP+ cells exhibit a 38.0% reduction ($p < 0.001$), while ACSL4+/GFAP+ cells show a 29.3% increase ($p < 0.001$), indicating elevated ferroptosis vulnerability in GFAP-positive cells. In addition, recurrent tumors present significantly higher ALDH1A3 expression (+3.94 IRS points, $p < 0.001$), with a potential trend toward reduced overall survival observed in cases with increases exceeding 2.00 IRS points, though this correlation lacks statistical significance ($p = 0.166$).

While Myristic acid demonstrates efficacy in targeting ferroptosis, hypoxia-induced resistance presents a critical challenge mediated by SLC7A11 and the PI3K/AKT/HIF-1 α pathway. Hypoxia-induced resistance to ferroptosis in glioblastoma is mediated by upregulation of SLC7A11 expression through the PI3K/AKT/HIF-1 α pathway, as reported by Sun S et al. (2022), leading to significantly increased IC50 values and reduced lipid peroxidation ($p < 0.05$, $p < 0.01$). Targeting HIF-1 α with PX-478 or inhibiting AKT effectively reverses this resistance, enhances susceptibility to sulfasalazine-induced ferroptosis, and improves anticancer efficacy in vivo ($p < 0.05$, $p < 0.01$). PX-478 demonstrates significant therapeutic potential by suppressing SLC7A11 expression, promoting lipid peroxidation, and overcoming hypoxia-induced resistance, resulting in reduced tumor growth and improved survival rates in glioma xenograft models ($p < 0.05$, $p < 0.01$).

Building on the role of FANCD2 in ferroptosis resistance, FHOD1 emerges as another regulator influencing glioblastoma growth and prognosis through hypomethylation and redox modulation. FHOD1 promotes ferroptosis resistance in glioblastoma by upregulating HSPB1 through hypomethylation, enhancing glioma cell growth and reducing ferroptosis sensitivity (Zhang F et al. 2023). Knockdown of FHOD1 significantly inhibits glioma cell proliferation, improves ferroptosis sensitivity ($p < 0.01$), and reduces tumor volume and weight in xenograft models ($p < 0.01$). FHOD1 is significantly upregulated in glioma tissues, correlating with poor prognosis and increased recurrence risk. Enhanced ferroptosis sensitivity and reduced tumor growth through FHOD1 knockdown align with the observed increase in ROS and Fe²⁺ levels ($p < 0.01$), suggesting the FHOD1-HSPB1 axis as a promising therapeutic target.

Expanding on ferroptosis-related mechanisms, CDKN2A deletion highlights lipidomic alterations that increase susceptibility to oxidative stress and therapeutic potential via GPX4 inhibition. CDKN2A deletion in glioblastoma significantly redistributes polyunsaturated fatty acids (PUFAs) from triacylglycerides to membrane phospholipids, resulting in increased lipid peroxidation and heightened ferroptosis susceptibility (Minami JK et al. (2023); $p < 0.05$). Lipidomic profiling across 84 patient tumors, 29 xenografts, and 43 gliomasphere models quantified 1,020 lipid species within 15 subclasses, revealing statistically significant alterations in lipid composition and peroxidation levels (e.g., $p < 0.05$, $p < 0.001$, $p < 0.0001$). GPX4 inhibition demonstrated improved survival in CDKN2A-null glioblastoma models ($p < 0.05$), validating its potential as a therapeutic target.

Further exploring ferroptosis sensitivity, quiescent astrocyte-like glioma cells exhibit mitochondrial dysfunction and lipid peroxidation, offering insights into selective therapeutic targeting. Banu MA et al. (2023) Quiescent astrocyte-like glioma cells exhibit mitochondrial dysfunction, oxidative stress, and lipid peroxidation, showing significant sensitivity to GPX4 inhibition and ferroptosis ($p < 0.0001$ in drug screens). Selective depletion of these cells was demonstrated in murine organotypic glioblastoma slices, with Clu+ cell populations significantly reduced ($p = 0.0185$), and in human glioma slices treated with RSL3, where normalized enrichment scores indicated specific cell state depletion (FDR-corrected $p < 0.05$). These findings underscore the therapeutic potential of targeting mitochondrial vulnerabilities in resistant glioblastoma cell populations.

Continuing with astrocyte-like glioma cell vulnerabilities, mitochondrial dysfunction and redox imbalance remain central to ferroptosis sensitivity and pharmacologic interventions. Quiescent astrocyte-like glioma cells exhibit selective vulnerability to GPX4 inhibition and ferroptosis, driven by mitochondrial dysfunction, lipid peroxidation, and redox imbalance (Banu MA et al. 2024). Pharmacologic GPX4 inhibition with RSL3 significantly reduces viability ($p < 0.05$) and depletes astrocyte-like markers in murine and human glioma models, with partial rescue observed using Ferrostatin-1. Increased ROS production and redox imbalance highlight mitochondrial dysfunction as a critical factor in this sensitivity, validated by FDR-corrected p-values in experimental models.

Shifting focus to regulatory mechanisms, METTL16 knockdown reveals ferroptosis induction and immune interactions as critical factors in glioma progression and therapeutic strategies. Recent findings demonstrate that METTL16 knockdown effectively inhibits glioma progression by inducing ferroptosis, as evidenced by

increased malondialdehyde (MDA) and reactive oxygen species (ROS) levels, decreased glutathione (GSH) levels, and reduced NFE2L2 mRNA stability and expression ($p < 0.05$) (Yang Y et al. 2024). METTL16 was identified as a regulator that promotes glioma progression by stabilizing NFE2L2 mRNA through m6A modification, with NFE2L2 further associated with immune cell infiltration and immune checkpoint expression in gliomas. In lower-grade gliomas, METTL16 expression negatively correlates with CD8+ T lymphocytes ($r = -0.17$, $p = 0.025$), whereas NFE2L2 expression shows positive correlations with M2 macrophages ($r = 0.24$, $p = 0.0019$), neutrophils ($r = 0.19$, $p = 0.011$), activated memory CD4+ T cells ($r = 0.22$, $p = 0.0034$), and immune checkpoints TNFSF4, PDCD1, CD244, and ICOS. These findings expand the understanding of the molecular mechanisms underlying glioma progression and immune interactions.

Ferroptosis remains central to glioblastoma treatment strategies, with procyranidin B1 emerging as another agent capable of inducing this cell death pathway. Procyranidin B1 induces ferroptosis in glioblastoma by suppressing NRF2 expression through PSMC3-mediated ubiquitin-dependent degradation, disrupting antioxidant defenses and enhancing H₂O₂ accumulation (Gao W et al. 2024). Quantitative results demonstrate significant tumor size reduction ($p < 0.01$) and improved survival rates in GBM-bearing mice (50% survival until day 54 vs. control group death by day 44, $p < 0.05$). These findings are consistent with observed mechanisms of ferroptosis induction and its therapeutic effects in glioblastoma models.

Building on the therapeutic potential of ferroptosis induction, creatine kinase inhibition offers additional avenues for oxidative stress modulation and glioblastoma treatment. Katz JL et al. (2024), creatine kinase inhibition (CKi) significantly reduces glioblastoma multiforme (GBM) cell migration and invasion, as demonstrated by a near-complete inhibition of U251 wound closure at 20 μ M CKi ($p < 0.001$). CKi induces oxidative stress, evidenced by elevated intracellular ROS levels and upregulated glutathione biosynthesis-related genes such as SLC7A11, TXNRD1, and HMOX1 ($p < 0.001$). Furthermore, combining CKi with glutathione inhibition or ferroptosis activation synergistically enhances GBM cell death, achieving IC50 values as low as 12 nM (e.g., GBM39, 12 nM for RSL3 + CKi; $p < 0.001$). These findings underscore the potential of CKi to disrupt promigratory mechanisms and anti-ferroptotic pathways in GBM, while combinatorial strategies with ferroptosis inducers and glutathione inhibitors improve therapeutic efficacy.

The role of ferroptosis in glioblastoma progression is further underscored by C5aR1 knockdown, which enhances lipid peroxidation and suppresses tumor growth. Knockdown of C5aR1 in glioblastoma cells induces ferroptosis, evidenced by significantly decreased GPX4 protein levels ($p < 0.01$, $p < 0.001$) and increased lipid peroxidation markers, including 4-HNE ($p < 0.01$) and MDA ($p < 0.05$), as reported by Meng X et al. (2024). Inhibition of C5aR1 with PMX205 suppresses GPX4 expression, enhances lipid peroxidation, and significantly inhibits glioblastoma progression in a mouse intracranial xenograft model, as demonstrated by reduced tumor size ($p < 0.01$) and prolonged survival ($p = 0.0141$).

Expanding on the role of ferroptosis in glioblastoma treatment, knockdown of SLC39A14 emerges as a strategy to further enhance ferroptosis markers and suppress glioma progression. Knockdown of SLC39A14 significantly suppresses glioma progression by reducing cGMP levels, inhibiting cGMP-PKG pathway-associated proteins (sGC, PKG1, PKG2), and enhancing ferroptosis markers, including increased MDA and Fe²⁺ levels and decreased GSH, GPX4, NRF2, and SLC7A11 protein levels (Zhang Y et al. 2023). These results demonstrate statistically significant correlations with glioma progression inhibition ($p < 0.01$; $p < 0.001$).

While previous strategies focused on ferroptosis induction, KCNA1 is identified as a regulator that inhibits ferroptosis and promotes glioblastoma progression through mitochondrial protection. Wang W et al. (2024) KCNA1 upregulates SLC7A11, inhibits ferroptosis, and confers mitochondrial protection, reducing oxidative stress and mitochondrial damage, which contributes to glioblastoma progression and invasion. Knockdown of KCNA1 significantly decreases tumor growth and invasion both in vitro and in vivo, with statistical significance ($p < 0.05$, $p < 0.01$, $p < 0.001$, $p < 0.0001$). In vivo analysis further demonstrates reduced tumor size and extended survival times in mouse models following KCNA1 knockdown ($p < 0.01$).

Returning to the therapeutic approach of ferroptosis induction, SIRT1 activation reveals a pathway to amplify glioblastoma cell sensitivity and promote cell death. SIRT1 activation enhances glioma cell sensitivity to RSL3-induced ferroptosis by promoting NAD⁺ depletion and ATF3 activation, which suppresses SLC7A11 and GPX4 expression (Chen X et al. 2024). This suppression leads to significant lipid peroxidation, depletion of cysteine and glutathione, and glioma cell death, $p < 0.01$, $n=5$. NAD⁺ depletion further triggers ATF3 activation, resulting in ferroptosis through increased ferrous iron accumulation, lipid peroxidation, and cysteine/GSH depletion. ROS-dependent upregulation of AROS sustains SIRT1 activation despite NAD⁺ depletion, amplifying the process, $p < 0.01$.

Mechanisms regulating ferroptosis, such as Acs4-mediated lipid peroxidation, provide deeper insights into therapeutic strategies for gliomas. Miao Z et al. (2022) found that the regulation of Drp1 phosphorylation at Ser637 by Hsp90 through calcineurin stabilizes Acs4 expression, which is pivotal for promoting ferroptosis in gliomas. This mechanism enhances lipid peroxidation, as evidenced by elevated levels of 12-HETE and 15-HETE, and reduces glutathione (GSH) levels, while inducing mitochondrial morphological changes that increase sensitivity to erastin. In vitro and in vivo experiments demonstrate significant reductions in tumor growth and prolonged survival in mouse models, with statistical validation ($p < 0.05$, $p < 0.01$, $p < 0.001$). Low Acs4 expression is associated with diminished ferroptosis sensitivity and poorer survival outcomes, emphasizing the critical role of Acs4-mediated lipid peroxidation and mitochondrial alterations in enhancing erastin efficacy.

Tumor heterogeneity and ferroptosis susceptibility, driven by PN-GSCs, underscore the complexity of glioblastoma progression and treatment responses. Vo VTA et al. (2022) PN glioblastoma stem cells (PN-GSCs) regulate tumor heterogeneity by secreting dopamine (DA) and transferrin (TF), which promote MES glioblastoma stem cell (MES-GSC) proliferation via iron uptake and Src-ERK signaling, while increasing ferroptosis susceptibility through elevated intracellular ROS generation and lipid peroxidation. MES-GSC proliferation in PN-GSC-conditioned media showed a significant increase ($p < 0.05$), and DA treatment amplified ROS levels and lipid peroxidation ($p < 0.05$). Combined DA and ferroptosis inducer treatments improved survival rates in orthotopic glioblastoma mouse models ($p < 0.05$). Additionally, GBM patients with high TFRC and DRD5 expression exhibited poor prognosis ($p < 0.05$), supporting the relevance of these pathways in disease progression.

2.2.2. Prognostic Markers and Risk Models

Selected findings

- Up-regulation of FANCD2 correlates with poor prognosis in glioblastoma and promotes temozolomide resistance by attenuating ferroptosis (Song L et al. 2022). This highlights the therapeutic potential of targeting FANCD2 to overcome chemoresistance and enhance ferroptosis-based strategies in glioblastoma treatment.
- The 25-gene ferroptosis-related risk signature effectively stratifies glioma patients into prognostic groups, demonstrating high predictive accuracy for survival outcomes validated across multiple cohorts (Zhuo S et al. 2020). This provides a robust tool for clinical decision-making and personalized treatment planning in glioblastoma management.
- Paeoniflorin induces ferroptosis in glioma cells by upregulating NEDD4L and suppressing Nrf2 and GPX4 expression, with enhanced efficacy when combined with RSL3 (Nie XH et al. 2022). This combination therapy offers a promising approach to improve glioblastoma treatment outcomes through synergistic ferroptosis induction.
- The 25-gene ferroptosis-related risk signature effectively stratifies glioblastoma patients into distinct prognostic groups, demonstrating significant associations with survival outcomes and immune-related features validated across TCGA and CGGA cohorts. This model enhances patient stratification and clinical decision-making by integrating survival predictions and immune checkpoint therapy responsiveness.
- Paeoniflorin induces ferroptosis in glioblastoma cells by upregulating NEDD4L and suppressing GPX4 expression, leading to significant inhibition of tumor

growth in vitro and in vivo. This compound offers potential for synergistic therapeutic strategies in glioblastoma, particularly in combination with traditional chemotherapeutics like RSL3.

- FANCD2 upregulation correlates with poor prognosis in glioblastoma patients and contributes to temozolomide resistance by attenuating ferroptosis. Targeting FANCD2 could improve therapeutic outcomes and survival, particularly in recurrent glioblastoma cases resistant to standard treatments.
- The five-gene risk model (OSMR, G0S2, IGFBP6, IGHG2, FMOD) demonstrates significant prognostic value in glioblastoma patients, stratifying them into high- and low-risk groups with distinct survival outcomes. This model enables precise risk stratification and therapeutic decision-making, advancing personalized treatment approaches for glioblastoma.
- FANCD2 upregulation correlates with poor prognosis and temozolomide resistance in glioblastoma patients, while its knockdown enhances ferroptosis sensitivity and immune response. Targeting FANCD2 offers a promising strategy to overcome therapeutic resistance and improve outcomes in glioblastoma management.

Table 4. Prognostic Markers and Risk Models

Study ID	Length of intervention	Population of intervention	Control	Intervention	Intervention details	Primary outcome	Secondary outcome
Liu HJ et al. (2020)		U87MG glioma cell line, U251MG glioma cell line, temozolomide-resistant U87TR and U251TR glioblastoma sub-lines		Use of Erastin, a ferroptosis activator, to treat glioma cell lines	Treated for 24 hours with varying Erastin concentrations, fresh medium replaced, CCK-8 solution added, migration assay using Transwell system, cells pretreated with Erastin or without Erastin, upper chamber with serum-free medium, lower chamber with 10% FBS and Erastin, migrated cells analyzed using microscopy and Image J	Identification of ferroptosis-specific markers and their relationship with glioma progression, including risk score model development and predictive metrics.	Predictive accuracy of the gene signature, association with temozolomide resistance, autophagy, glioma cell migration, overall survival differences

[Go to Annex 5: Table 4. Prognostic Markers and Risk Models](#)

The modulation of ferroptosis pathways underscores the prognostic utility of gene signatures, such as the identified 19 ferroptosis-related gene signature. The identification of a 19 ferroptosis-related gene signature offers a validated prognostic tool for glioma progression and survival, as reported by Liu HJ et al. (2020), with predictive accuracy supported by AUC values ranging from 0.653 to 0.903 and statistically significant p-values ($p < 0.001$ for univariate Cox regression and $p < 0.05$ for multivariate Cox regression). The associated risk score model demonstrates strong correlations with glioma grade, malignancy, and therapeutic resistance, while functional annotation reveals its involvement in tumorigenesis, immune response, cell migration, and ferroptosis-related pathways. Survival differences are underscored by hazard ratios (HR = 1.212, 95% CI: 1.174–1.251, $p < 0.001$), highlighting its reliability as a prognostic indicator.

Advancements in ferroptosis-related prognostic tools are exemplified by the development of the 25-gene risk signature, which further refines glioma patient stratification. Zhuo S et al. (2020), the 25-gene ferroptosis-related risk signature effectively stratifies glioma patients into distinct prognostic groups, demonstrating significant independent associations with overall survival outcomes. High-risk scores correlate with poorer survival, validated across CGGA and TCGA cohorts (HR = 3.654, 95% CI = 2.701–4.944, $p < 0.001$ for univariate analysis; HR = 1.917, 95% CI = 1.341–2.738, $p < 0.001$ for multivariate analysis). Predictive accuracy is highlighted by a 5-year AUC of 0.882 and clinical classification performance (cluster classification, AUC = 0.944). The nomogram, integrating this signature, forecasts 3- and 5-year survival rates with a C index of 0.789, underscoring its potential clinical utility in glioma prognosis.

The refinement of ferroptosis-based prognostic models continues with the introduction of the 11-gene signature, demonstrating strong predictive accuracy for survival outcomes. The 11-gene ferroptosis-related signature demonstrated strong predictive accuracy for overall survival in glioma patients, with AUC values of 0.879 at 1 year, 0.903 at 2 years, and 0.919 at 3 years in the TCGA cohort ($p < 0.001$), and consistent validation in the CGGA cohort (AUC = 0.790 at 1 year, 0.875 at 2 years, and 0.878 at 3 years, $p < 0.001$) (Chen Z et al. 2021). Furthermore, Cox regression analyses confirmed the signature as an independent prognostic factor for overall survival, with hazard ratios of 3.107 (95% CI = 2.506–3.853, $p < 0.001$) in the TCGA cohort and 1.943 (95% CI = 1.737–2.174, $p < 0.001$) in the CGGA cohort. These findings also revealed strong correlations between the signature and iron-related molecular functions, immune-related biological processes, and immune cell infiltration, reinforcing its relevance in glioblastoma prognosis.

The exploration of ferroptosis-related prognostic tools continues with the development of FRISig, which further stratifies glioma patients based on survival outcomes and immune-related features. The ferroptosis-related risk signature (FRISig), developed using 10 prognostic ferroptosis regulators as described by Hu Y et al. (2021), stratifies glioma patients into distinct risk subgroups with significant differences in overall survival across all grades. High-risk gliomas identified by FRISig show worse survival outcomes, with predictive accuracy for 1-, 3-, and 5-year survival exceeding AUC > 0.800 ($p < 0.05$). FRISig correlates with immune-related indexes, tumor mutation burden (TMB), copy number alterations (CNA), and immune checkpoint expression, validated as an independent prognostic factor for overall survival (C-index = 0.762 in CGGA, C-index = 0.846 in TCGA). Its integration into a nomogram model alongside age and WHO grade improves prognostic predictions with high calibration accuracy.

Insights into the molecular mechanisms of ferroptosis and apoptosis are complemented by studies linking ferroptosis-related genes to survival outcomes and immune activity in glioblastoma patients. Survival differences in glioblastoma patients are significantly associated with ferroptosis-related gene clusters and PCA score subgroups, with higher PCA scores correlating with improved prognosis ($p = 0.002$, $p = 0.013$, $p < 0.001$) (Peng X et al. 2023). Positive correlations are observed between PCA and gene scores derived from ferroptosis-related genes and immune cell infiltration, as well as immune pathway activity ($p < 0.05$, $p = 0.002$). Activated CD8+ T cells, CD4+ T cells, and Treg cells show significant positive associations with PCA and gene scores, while pathways such as TGF beta, JAK–STAT, and NK cell-mediated cytotoxicity exhibit higher activity in the high-score subgroup ($p < 0.001$).

Building upon the role of CYBB and SOD2 in modulating ferroptosis sensitivity, proteomic analyses have further identified key regulators associated with glioblastoma prognosis and survival. Wang X et al. (2023) proteome-based analyses identified five ferroptosis regulators—HSPB1, GPX4, ACSL3, IL33, ELAVL1—as prognostic biomarkers significantly correlated with overall survival in glioblastoma multiforme, validated across multiple datasets with an adjusted $p < 0.01$. The five-protein signature stratified patients into high- and low-risk groups with significant survival differences (adjusted $p < 0.01$), while ipatasertib demonstrated ferroptosis-inducing effects by targeting HSPB1 phosphorylation in high-risk glioma cells, exhibiting lower IC50 values.

Expanding from ferroptosis induction, the prognostic relevance of ferroptosis-related gene signatures in glioma patients is explored. The study highlights that FRG-related risk scores are strongly correlated with glioma prognosis, effectively categorizing patients into high- and low-risk groups with distinct survival outcomes (Zuo Z et al. (2022); $p < 0.001$). The predictive performance of the risk scores is demonstrated by AUC values of 0.899, 0.917, and 0.930 for 1-, 2-, and 3-year survival predictions in the training cohort, and 0.765, 0.834, and 0.826 in the validation cohort. Additionally, the 3DResCNN deep learning network showed reliable diagnostic accuracy in identifying FRG signatures, achieving an average AUC of 0.781, average accuracy scores of 0.842 (TC-mask) and 0.825 (WT-mask), and average F1 scores of 0.843 (TC-mask) and 0.830 (WT-mask).

Investigating another therapeutic avenue, paeoniflorin is identified as a compound capable of inducing ferroptosis through distinct molecular mechanisms. Paeoniflorin induces ferroptosis in glioma cells by upregulating NEDD4L, leading to STAT3 ubiquitination and suppression of Nrf2 and GPX4 expression (Nie XH et al. 2022). It significantly increases intracellular ROS levels ($p < 0.05$, $p < 0.01$, $p < 0.001$), inhibits glioma cell proliferation ($p < 0.01$), and suppresses tumor growth in vivo ($p < 0.01$). The combination of paeoniflorin and RSL3 further enhances ferroptosis, as evidenced by elevated intracellular ROS, MDA, and Fe²⁺ levels ($p < 0.01$), highlighting its synergistic therapeutic potential in glioblastoma treatment.

The discussion shifts to ferroptosis resistance mechanisms, with FANCD2 up-regulation linked to poor prognosis and therapeutic challenges in glioblastoma. Up-regulation of FANCD2 correlates with poor prognosis in glioblastoma patients, significantly reducing overall survival across various glioma grades and recurrence statuses (HR > 1, $p < 0.0001$ for primary glioma of all grades, $p = 0.0016$ for recurrent glioma of all grades, $p = 0.00025$ for primary glioma of WHO grade III, and $p = 0.01$ for recurrent glioma of WHO grade III) (Song L et al. 2022). FANCD2 contributes to TMZ resistance by attenuating ferroptosis, while its knockdown increases reactive oxygen species (ROS) levels, inhibits cell survival, and correlates with immune features and cancer-associated pathways, further linking ferroptosis to glioblastoma progression.

Insights into ferroptosis mechanisms contribute to the development of prognostic models that integrate molecular markers with survival and therapeutic outcomes in glioblastoma patients. The FRGPRS model demonstrates significant prognostic efficacy in predicting overall survival (OS) and progression-free survival (PFS) in GBM patients, validated through TCGA and GEO datasets (PFS $p = 5.4E-03$; OS $p = 6.5E-03$; AUC = 0.69) (Xiao D et al. 2021). As an independent risk factor (HR = 1.13; 95% CI [1.037, 1.23]; $p = 0.005$), it correlates with immune infiltration patterns, including M0 macrophages and CD8⁺ T cells ($p < 2.2E-16$), tumor tissue proportions such as stromal and immune scores ($p = 7.1E-10$, $p = 2.9E-12$), and chemotherapeutic response to temozolomide and cisplatin ($p = 4.9E-03$, $p = 2E-05$). High FRGPRS values are associated with increased tumor purity ($p = 4.9E-12$), reduced immune checkpoint therapy response, and chemotherapeutic resistance, while low FRGPRS values indicate improved temozolomide and cisplatin sensitivity, enhanced CD8⁺ T cell infiltration, and better atezolizumab response rates ($p = 0.0017$).

Refining prognostic tools, gene-based models incorporating autophagy and ferroptosis pathways offer enhanced predictive accuracy and clinical relevance. The prognostic risk model utilizing five autophagy-ferroptosis-related genes (MTOR, BID, HSPA5, CDKN2A, and GABARAPL2) demonstrated robust predictive accuracy, with C-index values of 0.72 in the training group and 0.74 in the verification group ($p < 0.001$) according to Zhou L et al. (2021). Kaplan-Meier survival analysis confirmed its significant efficacy ($p < 0.001$), and ROC analysis validated its strong predictive values for both short- and long-term survival. The nomogram exhibited high calibration accuracy and was effective across various clinical factors, except for WHO grade II glioma ($p > 0.05$).

The prognostic utility of autophagy-ferroptosis-related genes extends further with the AD-FRG signature, which incorporates survival prediction alongside insights into immunological characteristics in glioma patients. The autophagy-dependent ferroptosis-related gene (AD-FRG) signature enhances survival prediction in glioma patients, as demonstrated by Sun W et al. (2022), with AUC values of 0.870, 0.922, and 0.869 for 1-, 3-, and 5-year survival rates, respectively, while confirming significant survival differences between high- and low-risk groups ($p < 0.001$). High-risk glioblastoma patients identified through this signature exhibit an immunosuppressive tumor microenvironment, with increased macrophage infiltration (M0 and M1), elevated immune checkpoints (CD274, CTLA4, LAG3, PDCD1; $p < 0.0001$), and enhanced immunotolerance, correlating with reduced overall survival ($p < 0.001$).

Building on the role of autophagy-ferroptosis-related genes in glioma prognosis, FRGPI offers additional predictive accuracy while highlighting associations with treatment responses and immune dynamics. FRGPI demonstrates high predictive accuracy for overall survival in glioma patients with 1-year AUC = 0.86, 3-year AUC = 0.88, and 5-year AUC = 0.84 ($p < 0.001$), according to Cai Y et al. (2021). It is negatively correlated with temozolomide IC50 (Spearman: $r = -0.180$, $p < 0.001$), indicating enhanced chemotherapy sensitivity, and positively associated with immune checkpoint inhibitor therapy response (Spearman: $r = 0.300$, $p < 0.001$). Additionally, FRGPI correlates significantly with immune cell infiltration (stromalScore: $r = 0.670$, $p < 0.001$; immuneScore: $r = 0.670$, $p < 0.001$), tumor mutational burden ($r = 0.440$, $p < 0.001$), and PD-L1 expression ($r = 0.650$, $p < 0.001$), while showing a negative correlation with microsatellite instability ($r = -0.410$, $p < 0.001$).

Expanding on the prognostic relevance of ferroptosis-related signatures, the 3-FRLs signature provides robust stratification of glioma patients and reveals mechanisms underlying ferroptosis inhibition and tumor immunity. The 3-FRLs signature, comprising AL133415.1, LINC01426, and AC009227.1, stratifies glioma patients into high-risk and low-risk groups, demonstrating stable prognostic accuracy for overall survival with AUC values of 0.837 for 1-year OS, 0.837 for 3-year OS, and 0.790 for 5-year OS in the training cohort ($p < 0.001$) (Huang L et al. 2022). Validation confirmed its robustness, particularly in LGG and IDH-mutant patients, and revealed correlations with tumor immunity, metastasis, and biological metabolism. LINC01426 functions as a ferroptosis inhibitor, with knockdown significantly enhancing ferroptosis by increasing ROS, MDA, and Fe²⁺ levels and inhibiting cell proliferation ($p < 0.001$). Stratification by the 3-FRL signature highlighted differences in cellular immunity, immune cell counts, immune-related gene expression, and somatic mutation rates, such as IDH-1 mutation at 25% in high-risk versus 94% in low-risk groups, and ATRX mutation at 18% in high-risk versus 43% in low-risk groups.

Focusing on individual ferroptosis-related genes, their prognostic significance and therapeutic implications further underscore the complex interplay between ferroptosis and tumor progression in glioblastoma. Zhang X et al. (2022) found that ferroptosis-related genes, including STEAP3, HSPB1, MAP1LC3A, SOCS1, LOX, CAPG, CP, GDF15, CDKN1A, and CD44, exhibit significant prognostic value in glioblastoma, with higher expression levels correlating with poorer survival outcomes ($p < 0.05$, HR > 1). Predictive accuracy was confirmed through ROC analysis (AUC > 0.6 for all genes, > 0.7 for several), while a GSVA-based prognostic model demonstrated strong accuracy for predicting one-, two-, and three-year survival (AUC ~ 0.7). Immune analysis revealed associations with macrophage M2 infiltration ($r = -0.32$, $p = 0.000052$) and modulators of immune response. Therapeutic exploration identified Lumacaftor (DB09280, docking affinity -10.1 kcal/mol) and Lirafafenib (DB14773) as potential drugs targeting CAPG, CP, and CD44.

The protective role of IRF2 against ferroptosis aligns with its contribution to glioma progression, emphasizing the therapeutic potential of targeting ferroptosis-related pathways. IRF2 expression is strongly associated with glioma progression, as higher levels correlate with advanced tumor grade and poor survival prognosis ($p = 0.0019$) (Tong S et al. 2022). Functional studies reveal that IRF2 protects glioma cells from ferroptosis by reducing reactive oxygen species (ROS) levels, decreasing lipid peroxidation, and increasing glutathione (GSH) content ($p < 0.05$). Additionally, IRF2 promotes glioma cell proliferation ($p < 0.01$), migration ($p < 0.01$), and invasion ($p < 0.01$) through epithelial-mesenchymal transition (EMT)-related pathways, highlighting its role in tumor progression and resistance mechanisms. These findings reinforce the importance of targeting ferroptosis-related pathways in glioma treatment strategies.

Ferroptosis-related pathways and prognostic markers extend beyond IRF2, as evidenced by the association between ICD-related risk scores and glioblastoma prognosis. ICD-related risk scores were significantly associated with poor prognosis in GBM patients, including decreased overall survival (OS), progression-free survival (PFI), and disease-specific survival (DSS) ($p < 0.05$), as reported by Feng S et al. (2022). These scores correlated with enriched immune regulation pathways, increased immune cell infiltration, elevated ferroptosis regulators, and potential benefit from anti-PD1 therapy, as indicated by increased IPS and decreased TIDE scores. The prognostic efficacy of the risk signature was validated through AUC analysis for 1-, 3-, and 5-year survival. MYD88 was identified as a key biomarker linked to poor prognosis and immune-related pathways. The risk signature also demonstrated significant predictive performance for GBM subtypes, with the mesenchymal subtype exhibiting the highest risk score, and high-risk scores were associated with worse survival outcomes and potential benefit from anti-PD1 therapy ($p < 0.05$).

Building on the predictive models of ICD-related risk scores, gene-based risk models further refine glioblastoma survival predictions and therapeutic strategies. Su J et al. (2022) The prognostic risk score model based on 12 DE-MRGs demonstrated robust predictive capabilities for glioblastoma patient survival, with AUC values of 0.75, 0.81, and 0.902 for 1-, 3-, and 5-year OS predictions in the TCGA GBM cohort. Kaplan-Meier analysis highlighted significantly improved survival outcomes for low-risk patients ($p < 0.0001$). Additionally, SSBP1 knockdown enhanced temozolomide sensitivity in glioblastoma cells by inducing ferroptosis, marked by increased

mitochondrial ROS production ($p < 0.0001$), altered mitochondrial morphology, reduced GPX4 and FTH1 expression, and shifts in iron and glutathione levels.

Gene-based risk stratification continues to provide valuable insights into glioblastoma prognosis, as demonstrated by the five-gene risk model's predictive and therapeutic implications. Wu Y et al. (2025) The five-gene risk model (OSMR, G0S2, IGFBP6, IGHG2, FMOD) demonstrates significant prognostic value in glioblastoma patients by effectively stratifying them into high-risk and low-risk groups with distinct survival outcomes ($p < 0.05$). High-risk patients exhibit significantly lower survival rates compared to low-risk patients, as validated in both the training (TCGA) and testing (CGGA) cohorts. The model accurately predicts 1-, 2-, and 3-year survival rates and shows strong correlations with immune infiltration and pathways such as NOD-like receptor and JAK/STAT. Knockdown of OSMR significantly suppresses glioblastoma growth both *in vitro* and *in vivo* by promoting ferroptosis, enhancing CD8+ T cell activity, and shifting macrophage polarization toward an anti-tumor phenotype. *In vivo* experiments demonstrated prolonged survival in OSMR-deficient tumor-bearing mice (C57: 56 vs. 40 days, $p = 0.0039$; NSC: 37 vs. 32 days, $p = 0.0273$), reduced iron accumulation (Fe^{2+}), and increased anti-tumor cytokines (IFN- γ , TNF- α , $p < 0.05$), emphasizing its therapeutic potential.

Prognostic biomarkers such as MFAP4 offer additional diagnostic and therapeutic potential, complementing gene-based risk models in glioblastoma research. Lv Y et al. (2025) MFAP4 serves as an independent prognostic indicator for glioma, with significant associations with adverse clinicopathological features, including WHO grade (OR = 3.478), IDH wild-type status (OR = 0.125), and 1p/19q non-codeletion (OR = 0.272, all $p < 0.001$). It demonstrates high diagnostic value (ROC AUC = 0.833) and predictive efficacy for 1-, 3-, and 5-year survival (AUC > 0.7). Functional studies reveal that MFAP4 knockdown reduces glioma cell proliferation, migration, and invasion, highlighting its role in glioblastoma progression and its potential as a therapeutic target.

The role of molecular mechanisms in glioblastoma progression extends to prognostic biomarkers, which provide valuable insights into patient survival and disease management. Circulating MDH1 and RNH1 biomarkers were identified as independent prognostic factors for survival in IDH-wildtype glioblastoma patients, with elevated levels correlating with reduced overall survival (13.9 months vs. 22.3 months, $p = 0.002$) and progression-free survival (6.0 months vs. 8.7 months, $p = 0.033$) (Clavreau A et al. 2024). A prognostic blood score integrating MDH1 and RNH1 levels showed high predictive accuracy, achieving hazard ratios of 2.49 ($p = 0.002$) for overall survival and 1.93 ($p = 0.019$) for progression-free survival, with AUC values of 0.80 for OS and 0.84 for PFS at 4 years. Furthermore, low tumor expression of FABP7 was significantly associated with shorter overall survival ($p = 0.037$), reinforcing the role of molecular markers in survival prediction.

Extending the exploration of therapeutic targets, MXRA8 further demonstrates its relevance in glioblastoma progression through ferroptosis regulation and immune modulation. MXRA8 is a validated prognostic indicator in glioma progression, significantly associated with ferroptosis regulation and immune microenvironment modulation (Xu Z et al. 2022). Quantitative analysis demonstrates its predictive accuracy for survival outcomes, with AUC values of 0.780, 0.772, and 0.754 for 3-, 5-, and 10-year survival predictions ($p = 0.000$). Elevated MXRA8 expression correlates with unfavorable survival outcomes and immune-related factors, while knockdown studies reveal enhanced ferroptosis sensitivity, improved temozolomide efficacy, and reduced M2 macrophage infiltration, reinforcing its role in glioma progression and treatment resistance.

2.2.3. Therapeutic Strategies and Treatment Outcomes

Selected findings

- CYP2E1 downregulation in glioblastoma correlates with ferroptosis activation, immune microenvironment alterations, and poor prognosis, supported by multivariate Cox regression analyses and high diagnostic accuracy (e.g., AUC = 0.982 for glioma diagnosis). This finding highlights CYP2E1 as a prognostic biomarker and therapeutic target, with molecular docking studies identifying compounds for potential intervention.
- The TMEM161B-AS1-hsa-miR-27a-3p-FANCD2/CD44 axis regulates glioblastoma progression and temozolomide resistance by promoting ferroptosis and apoptosis, with silencing TMEM161B-AS1 significantly inhibiting tumor growth and enhancing drug sensitivity *in vivo* ($p < 0.001$). This discovery provides a molecular target for overcoming chemoresistance and advancing ferroptosis-based therapeutic strategies.
- The combination of AF and plasma therapy induces ferroptosis and apoptosis synergistically, significantly reducing tumor growth and improving survival in glioblastoma-bearing mice ($p \leq 0.05$ for tumor reduction, $p \leq 0.01$ for survival). This approach demonstrates the potential of multimodal oxidative stress-based therapies to enhance ferroptosis and immunogenic cell death for glioblastoma treatment.
- Silencing HSP27 promotes ferroptosis in glioblastoma cells by increasing ROS production and Fe^{2+} accumulation, leading to reduced tumor growth and improved survival outcomes in xenograft models. This finding underscores the therapeutic potential of targeting HSP27 to enhance ferroptosis and improve glioblastoma treatment strategies.
- CircRNF10 upregulation in glioblastoma enhances tumorigenic efficacy and ferroptosis defense via a positive feedback loop involving ZBTB48 and HSPB1, while its silencing disrupts this loop and remodels iron metabolism, inducing ferroptosis. Targeting CircRNF10 offers a promising avenue for glioblastoma therapy by overcoming ferroptosis resistance and improving survival outcomes.
- Mesenchymal glioblastoma subtypes exhibit significantly enhanced resistance to ferroptosis induction compared to proneural subtypes, driven by elevated antioxidant defense mechanisms such as increased GPX4 and GSH levels. Understanding subtype-specific resistance mechanisms is critical for developing tailored ferroptosis-based therapies for glioblastoma.
- Ferroptosis sensitivity in glioblastoma cells is significantly enhanced by SIRT3 inhibition, which reduces SLC7A11 expression, promotes lipid peroxidation, and activates mitophagy pathways (Li X et al. 2024). This finding provides a promising molecular target for developing ferroptosis-based therapies to overcome glioblastoma resistance and improve treatment efficacy.
- The TMEM161B-AS1-hsa-miR-27a-3p-FANCD2/CD44 axis modulates glioblastoma progression and temozolomide resistance by regulating apoptosis and ferroptosis (Chen Q et al. 2021). Targeting this axis could enhance temozolomide sensitivity and ferroptosis induction, offering a novel therapeutic strategy for glioblastoma management.
- Combination therapy of ABX and TMZ significantly enhances ferroptosis induction in glioblastoma models, improving survival and drug sensitivity through persistent DNA damage and lipid ROS accumulation (Qu S et al. 2023). This approach underscores the potential of integrating ferroptosis mechanisms into combination treatments for better clinical outcomes in glioblastoma.
- Ce6@Cu nanoparticles activated by ultrasound irradiation induce ferroptosis and cuproptosis in glioblastoma cells by depleting GSH, amplifying ROS generation, and reducing GPX4 expression, leading to significant tumor suppression and improved survival in mouse models (Zhu Y et al. 2024). This finding highlights the potential of nanoparticle-based strategies to overcome treatment resistance and enhance therapeutic efficacy in glioblastoma.
- RSL3 enhances glioma radiosensitivity by promoting DNA double-strand breaks and suppressing epithelial-mesenchymal transition, leading to significant tumor growth reduction and improved survival in preclinical models (Wang X et al. 2024). This approach underscores the therapeutic promise of combining ferroptosis inducers with radiotherapy to improve glioblastoma treatment outcomes.
- Targeting MS4A4A in glioblastoma reduces M2 macrophage infiltration and enhances CD8+ T-cell activation, improving the efficacy of PD-1 immunotherapy and delaying tumor growth in mice (Shao G et al. 2024). This study suggests that modulating the tumor immune microenvironment through ferroptosis could augment immunotherapeutic strategies for glioblastoma.

- RSL3 enhances glioblastoma radiosensitivity through DNA double-strand break induction and suppression of epithelial-mesenchymal transition (Wang X et al. 2024). This finding could inform combination therapies leveraging ferroptosis inducers to improve radiotherapy outcomes in glioblastoma patients.
- Ferroptosis modulation through nanoparticle-based strategies, such as Fe3O4-siPD-L1@M-BV2, enhances immune reactivation and tumor suppression in drug-resistant glioblastoma (Liu B et al. 2022). These approaches may pave the way for integrating ferroptosis-targeting nanomedicine with immunotherapy for glioblastoma treatment.
- The mesenchymal glioblastoma subtype exhibits significant resistance to ferroptosis compared to the proneural subtype, with elevated antioxidant mechanisms linked to poor survival outcomes (D'Aprile S et al. 2024). Understanding subtype-specific ferroptosis resistance could guide personalized therapeutic strategies targeting glioblastoma heterogeneity.

Table 5. Therapeutic Strategies and Treatment Outcomes

Study ID	Length of intervention	Population of intervention	Control	Intervention	Intervention details	Primary outcome	Secondary outcome
Ye L et al. (2021)	24 months	Patients with gliomas (low-grade glioma WHO grade II-III and GBM WHO grade IV), collected at Renmin Hospital of Wuhan University, Wuhan, China, no chemotherapy or radiotherapy before surgery	Patients with cerebral hemorrhage, 6 participants, no treatment control group	Investigation of CYP2E1 mRNA expression levels in glioma tissues, analysis of its clinical significance, and molecular docking of TCM compounds targeting CYP2E1	RNA extracted using TRIzol reagent, cDNA synthesized using PrimeScript RT Reagent Kit, CYP2E1 mRNA levels detected using SYBR Premix Ex Taq II and Bio-Rad real-time PCR Systems, relative Ct method used for comparison, gene expression analyzed using R packages, molecular docking performed using AutoDock 4.2 and PyMOL software, correlation analysis conducted for immune checkpoints, miRNA prediction performed using MiDB and TargetScan, functional enrichment analyzed using GO and KEGG pathways	Prognostic significance of CYP2E1 expression in glioma patients, correlation with poor prognosis, clinical features, survival outcomes, and statistical significance	Involvement of CYP2E1 in lipid metabolism, ferroptosis, tumor immune microenvironment, correlation with methylation levels and copy number variation, miRNA targeting by hsa-miR-527, identification of compounds targeting CYP2E1

[Go to Annex 6: Table 5. Therapeutic Strategies and Treatment Outcomes](#)

These findings on ferroptosis vulnerability align with the molecular mechanisms influencing ferroptosis activation, such as CYP2E1 downregulation in glioma patients. CYP2E1 expression is significantly downregulated in glioma patients, with multivariate Cox regression analysis confirming its role as an independent prognostic factor ($p < 0.001$) (Ye L et al. 2021). ROC analysis demonstrates high diagnostic accuracy, with AUC values of 0.982 for glioma diagnosis, and predictive AUCs for overall survival (OS) at 0.810 (1-year), 0.798 (3-year), and 0.763 (5-year) in the TCGA cohort, and 0.668 (1-year), 0.671 (3-year), and 0.676 (5-year) in the CGGA cohort. Downregulation correlates with immune microenvironment alterations (e.g., $\rho = 0.34$ for activated NK cells, $p < 0.001$), lipid metabolism inactivity, and ferroptosis activation ($p < 0.001$). Mechanisms influencing CYP2E1 downregulation include hsa-miR-527 targeting ($p < 0.001$), DNA hypomethylation (Pearson's $r = -0.36$, $p < 0.0001$), and copy number variation (Pearson's $r = 0.61$, $p < 0.0001$). Molecular docking studies have identified compounds such as 18beta-glycyrrhetic acid and colchicine as potential CYP2E1-targeting agents.

The role of CYP2E1 in ferroptosis activation provides a foundation for understanding how molecular axes like TMEM161B-AS1 regulate ferroptosis and tumor progression. The TMEM161B-AS1-hsa-miR-27a-3p-FANCD2/CD44 axis regulates glioblastoma progression and temozolomide resistance by modulating proliferation, migration, invasion, apoptosis, and ferroptosis (Chen Q et al. 2021). Silencing TMEM161B-AS1 and/or overexpressing hsa-miR-27a-3p significantly inhibits tumor growth, reduces FANCD2 and CD44 expression, promotes apoptosis and ferroptosis, and enhances temozolomide sensitivity, as shown by in vitro and in vivo experiments ($p < 0.001$).

Building on prognostic insights, therapeutic strategies targeting ferroptosis emerge as promising approaches to combat glioblastoma progression. Van Loenhout J et al. (2021) The sequential combination therapy of AF (15 mg/kg orally for 14 days) and plasma (10 s direct application for 5 consecutive days) significantly reduced tumor growth kinetics ($p \leq 0.05$) and prolonged survival ($p \leq 0.01$) in SB28 glioblastoma-bearing mice. This treatment synergistically induced apoptosis and ferroptosis by inhibiting TrxR activity ($p \leq 0.05$) and depleting GSH, leading to intracellular ROS accumulation and oxidative stress ($p < 0.0001$). Additionally, immunogenic cell death was elicited through increased CRT expression, ATP release, and HMGB1 secretion ($p \leq 0.05$), coupled with dendritic cell maturation and reduced tumor volume in vivo, significantly improving survival in GBM-bearing mice ($p \leq 0.05$).

The therapeutic focus on ferroptosis expands with investigations into its synergy with apoptosis-inducing agents to enhance glioblastoma cell death. Recent findings from Moujalled D et al. (2022) show that dual targeting of pro-survival proteins MCL-1 and BCL-XL using BH3 mimetic drugs (S63845 and A1331852) significantly enhances apoptosis and cell death in glioblastoma (GBM) cell lines, with IC50 values in the low nanomolar range (e.g., IC50 < 100 nM for U251 cells) and robust activation of apoptosis markers cleaved caspase-3 and PARP1 ($p < 0.05$ to $p < 0.0001$). Additionally, ferroptosis inducers (erastin, IC50 = 2.5 μ M; RSL3, IC50 = 64.5 nM) synergize with these BH3 mimetic drugs to significantly enhance glioblastoma cell killing (e.g., U251), via ferroptosis and apoptosis pathways, as evidenced by reduced cell viability, activation of apoptosis markers, and partial dependence on intrinsic apoptosis effectors BAX and BAK. Cell death is mitigated by ferroptosis inhibitors liproxstatin-1 or deferoxamine ($p < 0.0001$), underscoring the interplay between ferroptosis and apoptosis mechanisms.

Further elucidating molecular pathways, interactions between CYBB and Nrf2 reveal mechanisms regulating ferroptosis sensitivity and therapeutic resistance in glioblastoma. CYBB interacts with Nrf2 to activate the SOD2 mitochondrial antioxidant axis, reducing oxidative stress and ferroptosis sensitivity in glioblastoma cells (Su IC et al. 2023). Elevated CYBB expression is associated with poor progression-free survival (hazard ratio = 1.6; 95% CI = 1.05–2.4; $p = 0.029$). Knockdown of CYBB or SOD2 enhances the sensitivity of glioblastoma cells to temozolomide and erastin-induced ferroptosis ($p < 0.05$, $p < 0.001$, $p < 0.0001$). Furthermore, in vivo suppression of SOD2 significantly improves the efficacy of erastin analogs ($p < 0.001$, $p < 0.0001$), demonstrating the potential for targeting SOD2 to overcome temozolomide resistance.

Expanding on the identification of ferroptosis regulators, recent findings highlight Myrisignan as a promising agent for glioblastoma therapy through ferroptosis induction and EMT inhibition. Zhou Y et al. (2023) found that Myrisignan effectively suppresses glioblastoma progression by targeting ferroptosis induction and epithelial-mesenchymal transition (EMT) inhibition via the Slug-SLC7A11 pathway. Significant anti-tumor activity was observed at doses of 5–15 μ g/mL in vitro and 5 mg/kg in vivo, with tumor specificity at therapeutic doses sparing normal brain tissue and survival improvement in xenograft mouse models ($p < 0.05$, $p < 0.01$, $p < 0.001$).

To overcome such resistance mechanisms, innovative approaches such as Fe3O4-siPD-L1@M-BV2 nanoparticles have emerged, enhancing ferroptosis and immune activation in drug-resistant glioblastoma. Liu B et al. (2022) found that Fe3O4-siPD-L1@M-BV2 nanoparticles significantly enhance ferroptosis in drug-resistant glioblastoma by increasing ROS, LPO, and H2O2 levels ($p < 0.01$), reducing GPX4 and xCT protein expression, and depleting GSH. They promote immune reactivation

by increasing Teff cells (23.1%, $p < 0.01$), decreasing Treg cells (5.29%, $p < 0.01$), and enhancing dendritic cell maturation (CD11c+CD80+CD86+ cells: up to 68.2% in vitro and 77.31% with IFN- γ , $p < 0.01$). Additionally, the nanoparticles facilitate M1 microglial polarization (highest M1/M2 ratio observed under magnetic field, $p < 0.01$), contributing to prolonged survival (median survival: 45.00 days in Fe3O4-siPD-L1@M-BV2+magnet group, $p < 0.01$) and safety without organ damage or abnormal serum markers.

Complementing nanoparticle-based strategies, CircLRFN5 has been shown to induce ferroptosis and suppress glioblastoma stem cell viability, offering additional therapeutic potential. Jiang Y et al. (2022) CircLRFN5 suppresses glioblastoma stem cell viability, proliferation, neurosphere formation, and tumorigenesis by inducing ferroptosis through PRRX2 degradation and GCH1 downregulation. The study demonstrates statistically significant effects ($p < 0.05$, $p < 0.01$, $p < 0.001$) in both in vitro and in vivo models, validating its role as a tumor suppressor.

Building on the role of ferroptosis in glioblastoma suppression, apatinib is presented as another agent targeting distinct pathways to induce this cell death mechanism. Apatinib significantly reduces glioma cell viability and tumor growth by inducing ferroptosis through the VEGFR2/Nrf2/Keap1 pathway, as evidenced by reduced tumor volume and weight, increased levels of ROS, MDA, and Fe, and decreased GSH, GPX4, and SLC7A11 ($p < 0.05$; $p < 0.01$), as reported by Xia L et al. (2022). Overexpression of Nrf2 counteracts these effects in glioblastoma U251 and U87 cells, restoring cell viability most significantly at 72 hours ($p < 0.01$), reversing changes in ferroptosis markers, and normalizing VEGFR2/Nrf2/Keap1 pathway components ($p < 0.05$ or $p < 0.01$).

Therapeutic strategies targeting ferroptosis are further examined, with HSP27 silencing shown to enhance ferroptosis and improve survival outcomes. Silencing HSP27 significantly increases ferroptosis in glioblastoma cells, as evidenced by elevated ROS production mediated by Fe $^{2+}$ accumulation and enhanced ACSL4 stability (Zhang K et al. 2023). This results in reduced intracranial tumor growth rates and improved survival times in xenograft models, with statistical significance indicated across multiple metrics ($p < 0.05$ to $p < 0.0001$). Additionally, the knockdown correlates with reduced Ki67 staining intensity and increased ferroptosis markers such as Fe $^{2+}$ and MDA levels.

Ferroptosis modulation continues to be pivotal in glioblastoma research, with RBMS1 silencing highlighting its impact on tumor progression and epithelial-mesenchymal transition. Liang X et al. (2024) RBMS1 silencing significantly inhibits glioblastoma cell proliferation, migration, invasion, and epithelial-mesenchymal transition (EMT), while promoting apoptosis through ferroptosis pathways. This is demonstrated by marked increases in TBARS production ($p < 0.001$), lipid ROS levels ($p < 0.001$), and total iron levels ($p < 0.001$), alongside decreased expression of MMP2, MMP9, N-cadherin, Vimentin, and Snail, and increased E-cadherin levels ($p < 0.01$, $p < 0.001$). Treatment with the ferroptosis inhibitor Fer-1 partially reverses these effects ($p < 0.01$ and $p < 0.001$), indicating a protective role of RBMS1 in glioblastoma progression via ferroptosis modulation.

Expanding the scope of ferroptosis-based therapies, cobalt-doped iron oxide nanoparticles demonstrate promising anticancer effects through oxidative stress induction. Cobalt-doped iron oxide nanoparticles (Co40-MION) exhibit a significant therapeutic effect by reducing glioblastoma tumor spheroid volumes by approximately 40% at 60 $\mu\text{g/mL}$ and achieving enhanced cytotoxicity with an EC-50 of 0.2 $\mu\text{g/mL}$ ($p < 0.0001$) (Carvalho SM et al. 2023). Their anticancer activity is mediated by hydroxyl radical-induced oxidative stress, triggering ferroptosis and apoptosis pathways, and demonstrating comparable efficacy to doxorubicin in both 2D and 3D in vitro models. Building on the role of ferroptosis in glioblastoma treatment, alternative therapeutic approaches such as combination treatments have also demonstrated efficacy in targeting tumor growth and cell death pathways. Combined treatment with chloramphenicol (CAP) and 2-deoxy-d-glucose (2-DG) significantly inhibits glioblastoma cell growth under normal glucose conditions (1000 mg/L) and hypoxic conditions ($\text{O}_2 = 1\%$), as evidenced by statistical significance ($p < 0.001$, $p < 0.0001$) (Miki K et al. 2023). The mechanism involves ferroptosis, supported by increased expression of markers PTGS2, CHAC1, HO-1, and FTH1, and the inhibition of cell death through deferoxamine (DFO).

Extending the focus on ferroptosis, neuronal reprogramming has emerged as another promising strategy for glioblastoma treatment, offering insights into cellular differentiation and survival mechanisms. Wang H et al. (2023) found that NeuroD4 overexpression induces neuronal reprogramming in glioblastoma cells, leading to terminal differentiation, a significant reduction in proliferation (EdU+ cells decreased from 38.6% to 2.1% in U251 cells and from 37.4% to 1.5% in KNS89 cells at 14 dpi, Ki67 protein nearly absent, $p < 0.001$), and prolonged survival in tumor-bearing mice (up to 60 days, $p < 0.001$). This process is closely tied to ferroptosis, as evidenced by reduced SLC7A11 and GPX4 expression, with ferrostatin-1 blocking the reprogramming. Quantitative data further reveal TUJ1+ rates decrease from 87.6% to 18.4% and 13.6%, and Ki67+ rates increase from 13.3% to 48.1% and 30.3% upon SLC7A11 and GPX4 overexpression, demonstrating inhibition of NeuroD4-induced reprogramming ($p < 0.001$).

The modulation of ferroptosis pathways is further highlighted by evidence of epigenetic regulation, which impacts glioblastoma cell survival and resistance. KAT6B overexpression epigenetically activates STAT3 expression, enhancing ferroptosis resistance in glioma cells by modulating cell viability, apoptosis, lipid ROS, and iron levels, with statistically significant effects ($p < 0.01$) (Liu Y et al. 2022). Depletion of STAT3 reverses these changes, confirming its critical role in the pathway.

Expanding on the role of prognostic markers, circRNF10 highlights ferroptosis regulation as a key mechanism in glioblastoma progression and therapeutic intervention. Wang C et al. (2023) CircRNF10 upregulation in glioblastoma enhances tumorigenic efficacy and ferroptosis defense by stabilizing ZBTB48, transcriptionally upregulating HSPB1, and forming a circRNF10/ZBTB48/IGF2BP3 positive feedback loop, which significantly correlates with poor prognosis ($p < 0.05$, $p < 0.01$, $p < 0.001$). Silencing circRNF10 significantly extends survival rates (Kaplan-Meier analysis, $p < 0.05$, $p < 0.01$, $p < 0.001$), disrupts the circRNF10/ZBTB48/IGF2BP3 feedback loop, remodels iron metabolism via HSPB1, induces ferroptosis in glioblastoma stem cells, and reduces tumor burden in vivo.

Building on the exploration of ferroptosis mechanisms, the role of S670 in inducing ferroptosis and modulating autophagy offers further insights into glioblastoma treatment strategies. Yang YH et al. (2024) S670 demonstrates dose-dependent inhibition of glioblastoma cell proliferation, with IC50 values of 5.961 μM at 24 hours for U87 cells and 8.023 μM at 24 hours for U251 cells. It induces ferroptosis through mitochondrial ROS generation, lipid peroxidation, and GPX4 inhibition, as evidenced by increased COX2 expression. In vivo studies show significant tumor growth suppression in a U87 mouse xenograft model, with tumor weight reduction at doses of 25 mg/kg and 50 mg/kg ($p < 0.01$, $p < 0.0001$). Additionally, S670 modulates autophagy by promoting Nrf2 activation and TFEB nuclear translocation while impairing autophagosome-lysosome fusion via STX17 suppression, exacerbating ROS accumulation and enhancing ferroptosis.

The variability in ferroptosis susceptibility among glioblastoma subtypes underscores the importance of understanding subtype-specific resistance mechanisms. D'Aprile S et al. (2024) Mesenchymal glioblastoma subtype exhibits significantly enhanced resistance to ferroptosis induction compared to the proneural subtype, characterized by elevated basal GSH levels (7.43 \pm 0.39 nmol vs. 5.72 \pm 0.12 nmol, $p = 0.0141$), 260-fold upregulation of GPX4 mRNA post-FAC treatment, and increased expression of GSS (4.90 \pm 0.29 vs. 4.35 \pm 0.44, $p = 0.0017$). These antioxidant mechanisms correlate with reduced overall survival (357 vs. 455 days, $p = 0.0308$) and progression-free interval (164 vs. 311 days, $p = 0.0027$) in glioblastoma patients.

Advancing the study of ferroptosis sensitivity, imaging biomarkers such as [18F]hGTS13 provide valuable tools for monitoring therapeutic responses. [18F]hGTS13 demonstrates significant differential uptake between ferroptosis-sensitive and resistant cell lines, with HT-1080 and C6 cells exhibiting lower baseline uptake (3.0 \pm 0.6 and 5.8 \pm 0.6 % uptake/mg protein) and glutathione levels (4.2 \pm 0.04 μM and 1.8 \pm 0.05 μM) compared to resistant H460 cells (82.3 \pm 0.6 % uptake/mg protein, 6.4 \pm 0.6 μM , $p < 0.0001$) (Moses A et al. 2025). Additionally, its application in glioma-bearing rat models shows a reduced tumor-to-brain ratio following imidazole ketone erastin treatment (mean TBR: 10.5 \pm 1.8 to 5.9 \pm 2.2, $p = 0.006$), supporting its utility in tracking drug engagement and ferroptosis sensitivity. Uptake correlates strongly with cellular glutathione content across cell lines (HT-1080: $r = 0.91$, H460: $r = 0.97$, C6: $r = 0.97$), affirming its role as a biomarker for ferroptosis-related therapeutic strategies.

Integrating molecular markers like PGRMC1 highlights their impact on therapy resistance and susceptibility to ferroptosis induction. Dumitru CA et al. (2023) PGRMC1 expression in glioblastoma (GBM) patients is significantly associated with poor overall survival (Hannover cohort: $p = 0.010$; Magdeburg cohort: $p = 0.005$) and serves as an independent prognostic biomarker (Hannover cohort: HR = 1.532, CI [95%] = 1.042–2.253, $p = 0.030$; Magdeburg cohort: HR = 1.462, CI = 1.039–2.057, $p = 0.029$). PGRMC1 enhances tumor progression by promoting proliferation, anchorage-independent growth, invasion, and immune interactions, with increased neutrophil recruitment ($p < 0.001$, Rho = 0.363) and elevated IL-8 production. It modulates therapy response by reducing susceptibility to temozolomide (TMZ) and increasing sensitivity to the ferroptosis inducer erastin ($p < 0.05$), underscoring its dual role in therapy resistance and ferroptosis susceptibility.

Investigating the modulation of ferroptosis by NUPR1 extends the understanding of therapeutic resistance and potential intervention strategies in glioblastoma. CSF induces therapeutic resistance in GBM cells through NUPR1-mediated ferroptosis inhibition, as described by Stringer BW et al. (2023), with trifluoperazine demonstrating a significant reduction in resistance when combined with standard care treatments such as TMZ and irradiation. In highly responsive GBM cell lines, resistance was reduced by 100%, while less responsive cell lines showed a mean reduction of 35% ($p < 0.05$). Effective doses of trifluoperazine exhibited IC50 values ranging from 4–9 μM , and preclinical neuronal models confirmed the absence of neurotoxicity at these doses ($p < 0.05$).

Building on the therapeutic relevance of ferroptosis, combination therapies such as ABX and TMZ have demonstrated enhanced induction of this mechanism, improving treatment outcomes in glioblastoma models. Combination therapy of ABX and TMZ demonstrated significant suppression of GBM progression and prolonged survival in orthotopic xenograft nude mice (Qu S et al. (2023); Kaplan–Meier survival analysis, $p < 0.05$). Concurrent administration showed superior efficacy compared to sequential treatment, with enhanced DNA damage, persistent $\gamma\text{-H2AX}$ levels, and impeded DNA repair mechanisms. The therapy induced ferroptosis, marked by increased iron accumulation, lipid ROS, reduced glutathione levels, and altered GPX4/HO-1 expression. It improved drug sensitivity in GBM patient-derived organoids, achieving an 80% response rate, with 37.5% showing a >2-fold inhibition rate improvement.

Selective ferroptosis induction, as demonstrated by GPR68 inhibition with OGM, introduces a promising approach to target glioblastoma cells while sparing normal tissues. Blocking GPR68 signaling with OGM induces ferroptotic cell death in glioblastoma cells with LC50 values ranging from 0.42 to 2.7 μM across 13 GBM cell lines ($p < 0.01$), irrespective of genetic heterogeneity or temozolomide resistance (Williams CH et al. 2024). This mechanism involves activation of the ATF4-CHAC1 pathway, leading to lipid peroxidation and glutathione depletion, selectively targeting glioblastoma cells without affecting normal tissues, such as HEK293 cells ($p < 0.0001$). OGM demonstrates non-toxicity in zebrafish larvae, sparing neurons and glial cells while effectively inducing ferroptosis in glioblastoma cells ($p > 0.05$).

Building on mechanisms that induce ferroptosis, SIRT3 inhibition emerges as another pathway to enhance lipid peroxidation and mitochondrial oxidative stress in glioblastoma cells. SIRT3 inhibition significantly enhances ferroptosis in glioblastoma cells by reducing SLC7A11 expression ($p < 0.0001$), cystine uptake, and GSH levels, while promoting lipid peroxidation, mitochondrial ROS, and Fe^{2+} accumulation (Li X et al. 2024). This results in suppressed tumor growth and elevated ferroptosis markers, including MDA accumulation and decreased GSH/GSSG ratio ($p < 0.05$, $p < 0.01$, $p < 0.001$, $p < 0.0001$). Additionally, SIRT3 targeting activates mitophagy ($p < 0.0001$), further supporting its role as a potential therapeutic target for glioblastoma treatment.

Extending the focus on ferroptosis, the knockdown of IGF2BP3 highlights the pivotal role of GPX4 regulation in glioblastoma cell survival and tumor formation. Recent findings from Deng L et al. (2024) demonstrate that the knockdown of IGF2BP3 significantly impairs glioma cell growth, survival, and tumor formation by inducing ferroptosis through reduced GPX4 protein expression. This process triggers apoptosis, oxidative damage, and cell cycle disruption. Xenograft assays validate the reduction in tumor formation, with statistical significance ($p < 0.001$, $p < 0.01$, $p < 0.05$). Furthermore, IGF2BP3 regulates ferroptosis by directly binding to the m6A-modified A575 site on GPX4 mRNA, stabilizing its expression and facilitating its translation into GPX4 protein. This knockdown increases lipid peroxidation, induces ferroptosis, and enhances glioma cell susceptibility to microglial phagocytosis, aligning with established roles of GPX4 in ferroptosis and glioma treatment strategies.

Further exploring GPX4 suppression, Juglone demonstrates its ability to induce ferroptosis through oxidative stress pathways, offering another therapeutic avenue for glioblastoma treatment. Guo F et al. (2024) Juglone induces ferroptosis in glioblastoma cells through activation of p38 MAPK phosphorylation and suppression of the Nrf2/GPX4 axis, resulting in significant reductions in tumor volume and weight, $p < 0.05$; $p < 0.001$, alongside decreased expression of Nrf2 and GPX4, lower GSH levels, and increased oxidative stress markers such as ROS and MDA. These findings highlight the role of ferroptosis-related pathways in inhibiting glioblastoma growth and enhancing oxidative stress in vitro and in vivo.

Transitioning from ferroptosis-related therapeutic strategies, NOX4 overexpression underscores its contribution to tumor growth and invasiveness in recurrent glioblastomas. NOX4 overexpression ($p < 0.01$) drives ferroptosis in endothelial cells, significantly contributing to tumor growth and invasiveness in recurrent glioblastomas (Liang B et al. 2024). Experimental knockdown of NOX4 inhibited ferroptosis and glioblastoma cell proliferation ($p < 0.001$), with reduced growth rates in recurrent tumors linked to decreased ferroptosis activity and increased GPX4 and SLC7A11 expression.

Complementing molecular approaches, Ce6@Cu nanoparticles introduce a novel ferroptosis-inducing strategy through targeted ROS amplification and GPX4 inhibition in glioblastoma. Carrier-free Ce6@Cu nanoparticles, activated by ultrasound irradiation, induce ferroptosis and cuproptosis in glioblastoma by depleting GSH, amplifying ROS generation, and reducing GPX4 expression, mechanisms consistent with tumor suppression processes observed in glioblastoma treatments (Zhu Y et al. 2024). These nanoparticles, with a particle size of ≈ 50 nm and a Cu:Ce6 molar ratio of $\approx 2.5:1$, demonstrated significant tumor accumulation (enhanced fluorescence signal, $p < 0.001$) and increased Cu^{+} concentration within glioblastoma lesions (ICP-MS data, $p < 0.001$), contributing to substantial tumor suppression and improved survival rates in a glioblastoma mouse model ($p < 0.001$).

Building on the mechanisms of ferroptosis and ROS amplification, the inhibition of GPR68 further demonstrates the therapeutic potential of targeting glioblastoma cells by reducing tumor burden and enhancing lipid peroxidation. Inhibition of GPR68 in glioblastoma cells significantly reduces tumor burden and induces ferroptosis in zebrafish xenografts, as demonstrated by decreased tumor area, fluorescence intensity, and intensity/area ratio (U87: $p < 0.0005$; U138: $p < 0.0005$) (Neitzel LR et al. 2024). Treatment with OGM or shRNA-mediated knockdown further enhances lipid peroxidation and reduces tumor burden ($p < 0.025$), with minimal neurotoxicity observed after a 24-hour recovery period.

The induction of ferroptosis through lipid peroxidation and ROS elevation in glioblastoma cells is similarly observed with DE-FeONPs nanocomplex, which effectively targets glioblastoma stem cells and their resistant variants. Abu-Serie MM et al. (2024) DE-FeONPs nanocomplex exhibits potent inhibition of glioblastoma stem cells (GSCs) and their radioresistant variants (GSCs-RR), achieving up to 6.6-fold improvement in chemosensitivity and 8.7-fold improvement in radiosensitivity ($p < 0.001$). It suppresses self-renewal and cancer repopulation, as evidenced by a 64.2% reduction in sphere count, and downregulates stemness gene expression by 2–13-fold ($p < 0.001$). The nanocomplex induces ferroptosis through lipid peroxidation increase (2.7–5.0-fold; $p < 0.001$) and elevated ROS levels (up to 2.9-fold; $p < 0.001$), while demonstrating optimal blood-brain barrier penetration (LogP = 2.105).

Complementing the strategies of ferroptosis induction, targeting MS4A4A highlights the role of the immune microenvironment in glioblastoma therapy by modulating macrophage infiltration and enhancing T-cell activation. Targeting MS4A4A in glioblastoma enhances ferroptosis in tumor-associated macrophages, reduces M2 macrophage infiltration, and increases CD8+ T-cell activation, aligning with findings from Shao G et al. (2024) on the role of ferroptosis in modulating the tumor immune microenvironment. High MS4A4A expression is significantly associated with poor prognosis (log-rank $p = 0.04$), while its inhibition improves PD-1 immunotherapy efficacy, alleviates T-cell exhaustion, and delays tumor growth, as demonstrated by experimental data and survival analysis.

Extending the focus on ferroptosis as a therapeutic mechanism, Erianin demonstrates efficacy in overcoming TMZ resistance in glioma stem cells by targeting molecular pathways associated with cell viability and tumor suppression. Mansuer M et al. (2024) Erianin enhances TMZ sensitivity in glioma stem cells resistant to TMZ

by inducing ferroptosis through REST downregulation and promoting SLC40A1 ubiquitination and degradation. This mechanism significantly reduces cell viability, proliferation, neurosphere formation, and tumor size, with effects observed in a time- and concentration-dependent manner (IC50 established at 24 hours). In vivo studies confirm its ability to suppress stemness markers, reduce tumor formation, and improve survival, demonstrating statistical significance ($p < 0.05$; $p < 0.01$; $p < 0.001$).

Integrating the concept of ferroptosis inhibition, FOXP3 emerges as a critical regulator of glioblastoma progression, with therapeutic approaches such as epirubicin showing promise in reversing its effects on tumor growth. FOXP3 has been identified as a key regulator of glioblastoma progression by inhibiting ferroptosis through the linc00857/miR-1290/GPX4 axis (Cao W et al. 2024). The transcriptional promotion of GPX4 and linc00857 by FOXP3 enhances glioblastoma cell proliferation and tumor growth. Knockdown of FOXP3 significantly induces ferroptosis and reduces glioblastoma proliferation both in vitro and in vivo ($p < 0.01$). Furthermore, treatment with the FOXP3 inhibitor epirubicin demonstrated notable suppression of glioblastoma growth and colony formation ($p < 0.01$) by increasing ROS, MDA, and iron levels, while reducing GSH and GPX activity ($p < 0.01$; $p < 0.001$). In vivo, epirubicin treatment significantly reduced tumor growth and weight ($p < 0.01$) while modulating key molecular markers, including downregulation of FOXP3, KI67, PCNA, linc00857, and GPX4, alongside upregulation of miR-1290.

Building upon the molecular mechanisms of glioblastoma progression, necrosis and ferroptosis-related pathways have emerged as critical factors influencing tumor development and survival outcomes. Recent studies, including Lu T et al. (2024), demonstrate that myeloperoxidase inhibition using 4-ABAH reduces necrosis formation by 33% and prolongs mouse survival by 12.5% ($p < 0.05$). Similarly, Vps34 depletion decreases necrosis by 43% and 57% while extending survival by 31% and 44% ($p < 0.05$), highlighting the role of LAP and ferroptosis-related mechanisms in necrosis development and glioblastoma progression.

Advancing from prognostic insights, innovative therapeutic strategies leveraging oxidative stress and ferroptosis demonstrate promising anti-tumor efficacy in glioblastoma. Chen H et al. (2025) Lpo@Cu₂Se-GOx nanocomposites exhibit potent anti-tumor effects in glioblastoma by inducing oxidative stress, generating reactive oxygen species (ROS), and triggering ferroptosis and immunogenic cell death (ICD). Key quantitative findings include H₂O₂ generation exceeding 350 μ M, significant intracellular ROS levels, and dose-dependent reductions in GL261 cell viability, alongside ferroptosis markers such as decreased GSH and GPX4 activity ($p < 0.05$, $p < 0.01$, $p < 0.001$). Immunogenic effects were evidenced by ~26.9% dendritic cell maturation, 2.2-fold higher CD8+ T-cell infiltration, and reduced Treg cell levels to 4.2%. In vivo studies demonstrated significant tumor growth inhibition and immune activation, with negligible toxicity, while efficient blood-brain barrier penetration and immunogenic cell death mechanisms further underscore their therapeutic potential.

Expanding on therapeutic approaches, genetic modulation of ferroptosis sensitivity highlights the interplay between molecular regulation and glioblastoma progression. Knockdown of ALKBH5 significantly reduces U251 glioblastoma cell proliferation, invasion, and tumor growth both in vitro and in vivo ($p < 0.01$) while enhancing ferroptotic sensitivity through regulation of MUC1 expression (Jamali AW et al. 2025). In vivo results show decreased tumor growth over 21 days and reduced Ki-67 expression in tumor tissues. Conversely, ALKBH5 overexpression markedly increases glioblastoma cell proliferation, invasion, tumor growth, and MUC1 expression ($p < 0.01$). The inhibitory effects of ALKBH5 knockdown are reversed by MUC1 overexpression ($p < 0.01$, $p < 0.01$), demonstrating a synergistic relationship between ALKBH5 and MUC1 in glioblastoma progression.

Further exploration of therapeutic strategies reveals the potential of enhancing radiosensitivity through ferroptosis and DNA damage mechanisms in glioblastoma treatment. RSL3 enhances glioma radiosensitivity to ionizing radiation by promoting DNA double-strand breaks, evidenced by increased γ -H2AX foci, longer comet tails, and elevated p-ATM levels (Wang X et al. 2024). Synergy scores of 25.53, 33.45, and 29.36 were observed for U87, U251, and LN229 cells, respectively, $p < 0.05$ or $p < 0.01$. Additionally, RSL3 suppresses epithelial-mesenchymal transition by downregulating N-cadherin and vimentin while upregulating E-cadherin, $p < 0.05$. In vitro and in vivo studies demonstrated significant tumor growth reduction, with synergy scores consistent across cell lines and substantial tumor volume and weight decrease, $p < 0.05$, without notable side effects.

Ferroptosis emerges as another key mechanism influencing glioma progression and therapeutic sensitivity, complementing the radiosensitizing effects of RSL3. Liu T et al. (2022) found that ferroptosis emerges as a key programmed cell death mechanism in gliomas, with high ferroptosis scores significantly correlating with reduced survival and poor prognosis ($p < 0.0001$). Alterations in ferroptosis-related genes are linked to glioma progression, with 15% of these genes independently associated with poor survival (hazard ratio > 1 , $p < 0.05$). Inhibition of ferroptosis enhances immunological profiles and sensitizes glioblastoma to immune checkpoint blockade therapy, as demonstrated by improved survival outcomes in GBM murine models (log-rank test, $p < 0.05$) and increased CD8+ T-cell infiltration, macrophage polarization, and T-cell activation.

The identification of genes associated with ferroptosis and radiosensitivity further elucidates their roles in glioma prognosis and survival prediction. The study identified seven radiosensitivity- and ferroptosis-associated genes (MAPK1, ZEB1, MAP1LC3A, HSPB1, CA9, STAT3, and TNFAIP3) as prognostic biomarkers in glioma, validated using TCGA and CGGA datasets (Xie Y et al. 2022). A risk signature model based on these genes demonstrated significant survival prediction capabilities with AUC values of 0.705, 0.764, and 0.775 at 1, 2, and 3 years, respectively ($p < 0.001$). High-risk groups showed shorter survival (HR = 3.43, $p = 0.004$ in TCGA; HR = 1.44, $p < 0.001$ in CGGA) and distinct immune cell infiltration patterns, including higher infiltration of macrophages, Tregs, DCs, and TILs. Experimental evidence confirmed that erastin-induced ferroptosis enhances radiosensitivity in glioma cells, with statistically significant results ($p < 0.01$, $p < 0.001$).

MicroRNA-mediated ferroptosis modulation highlights additional therapeutic avenues for enhancing glioblastoma treatment efficacy. The miR-147a mimic induces ferroptosis in glioblastoma cells by targeting SLC40A1, leading to iron accumulation, mitochondrial dysfunction, and increased lipid peroxidation (Xu P et al. 2022). This process reduces cell viability and enhances sensitivity to chemotherapy, as demonstrated by elevated LDH release and statistically significant outcomes (N=6, $p < 0.05$). Conversely, the miR-147a inhibitor mitigates ferroptosis and improves cell viability under erastin or RSL3 treatment by reducing ROS generation, lipid peroxidation, and intracellular iron levels, with consistent statistical significance (N=6, $p < 0.05$).

Building on the molecular mechanisms of ferroptosis and chemotherapeutic sensitivity, SQLE emerges as another key regulator of glioblastoma progression and treatment response. Yao L et al. (2022) SQLE modulates temozolomide (TMZ) sensitivity and suppresses metastasis in glioblastoma multiforme (GBM) by inhibiting ERK phosphorylation, with low expression correlating with poor prognosis ($p < 0.05$). Its expression is associated with WHO grade and 1p/19q co-deletion, while negatively correlating with tumor-infiltrating lymphocytes, immunomodulators, and MHC molecules (Spearman $\rho = -0.472$, $p = 1.97e-10$). Overexpression enhances TMZ sensitivity, reduces migration and invasion, and influences immune responses, emphasizing its role in overcoming chemoresistance.

Continuing the focus on therapeutic resistance, genome-wide screening identifies GSS as a pivotal factor in radiotherapy outcomes and potential intervention strategies. Genome-wide CRISPR screening highlighted GSS as a key factor in radiotherapy resistance (Liu X et al. 2023), with targeted disruption using Ang/TAT-sgGSS-EVs achieving mutation frequencies of 61.8% in LN229-bearing mice and 57.2% in patient-derived glioma stem cell xenografts ($p < 0.0001$). Elevated GSS expression was significantly associated with poor prognosis in glioblastoma patients ($p < 0.0001$). The therapeutic approach enhanced radiosensitivity, suppressed tumor growth, and improved survival outcomes, demonstrating minimal off-target effects ($< 0.5\%$) and no significant toxicity.

Highlighting advancements in treatment efficacy, combination therapies such as temozolomide with FR054 leverage ferroptosis mechanisms to overcome therapeutic resistance. Combination therapy of TMZ and FR054 significantly enhanced therapeutic outcomes in glioblastoma models, as evidenced by reduced tumor fluorescence intensity ($p < 0.001$) and prolonged survival in orthotopic xenograft mice (Ye R et al. 2025). In GBM cells, FR054 increased TMZ sensitivity by reducing protein O-GlcNAcylation and inducing ferroptosis, as demonstrated by HMOX1 upregulation, GPX4 downregulation, and substantial reductions in TMZ IC50 values, such as A172-TR TMZ IC50 decreasing from 1132 μ M to 40 μ M ($p < 0.001$). Minimal side effects were observed across in vivo and organoid models.

Expanding on ferroptosis-based therapies, FLD nanoparticles offer a promising approach to glioblastoma treatment through enhanced tumor targeting and biosafety. Liu S et al. (2025) FLD nanoparticles effectively traverse the blood-brain barrier (PBBB = $3.72 \pm 1.34 \times 10^{-6}$ cm/s) and accumulate at glioblastoma sites, amplifying ferroptosis through lipid peroxidation, GSH depletion ($p < 0.001$), Fe²⁺ elevation, and ROS generation. In vitro, FLD NPs demonstrated a 2.8-fold reduction in IC50 compared to FL NPs, while in vivo studies confirmed significant tumor suppression ($p < 0.001$) with confirmed biosafety and negligible adverse effects. Enhanced ferroptosis mechanisms include HO-1 upregulation, photothermal acceleration of the Fenton reaction, and improved tumor targeting via multimodal imaging techniques (PAI/PTI), supported by renal and hepatobiliary clearance pathways.

Building on nanoparticle-based ferroptosis strategies, alternative approaches such as high-dose ascorbate also exploit iron-dependent cytotoxicity to target glioblastoma cells. High-dose ascorbate (≥ 1 mM) induces significant ferroptosis-like cytotoxicity in glioblastoma cells, reducing viability to below 20% within 24 hours ($p \leq 0.001$) and increasing intracellular ROS levels, as reported by Piotrowsky A et al. (2024). Ferroptosis markers, including decreased GPX4 and increased TfR1 expression, confirm the mechanism, while cell death remains caspase-3-independent. Pre-incubation with 100 μ M FeCl₃ amplifies the cytotoxic effects, reducing viability to 63% at 0.4 mM ascorbate and further elevating ROS levels compared to ascorbate alone ($p \leq 0.001$). DFO inhibition ($p \leq 0.01$) supports the iron-dependent nature of cell death, distinguishing it from apoptosis or autophagy pathways.

The results emphasize the interactions between ferroptosis pathways and glioblastoma resistance mechanisms, offering valuable insights into the dynamics of the immune system in this context.

2.3. CD95 Gene Deletion: Reducing Malignancy in Glioblastoma Cells

Selected findings

- CD95 gene deletion in glioblastoma-initiating cells significantly reduces clonogenic growth, sphere-forming capacity, invasiveness, and resistance to CD95L-induced apoptosis, independent of CD95 ligand expression. This finding highlights the therapeutic potential of targeting CD95 signaling to diminish glioblastoma aggressiveness and resistance mechanisms, including ferroptosis.
- Despite reduced malignancy metrics in vitro, CD95 gene deletion does not improve survival outcomes in xenograft models, with no significant differences observed across groups. This underscores the challenges of translating promising in vitro findings into clinically meaningful survival benefits in glioblastoma research.

Table 6. CD95 Gene Deletion: Reducing Malignancy in Glioblastoma Cells

Study ID	Length of intervention	Population of intervention	Intervention	Intervention details	Primary outcome	Secondary outcome
Quijano-Rubio C et al. (2022)	10+ days	Mice implanted with human glioblastoma-initiating cells (naïve, CRISPR control, CD95 knockout, CD95L knockout)	CRISPR-Cas9 knockout of CD95/CD95L genes in human glioblastoma-initiating cells, implantation into mouse striatum	Transfection with sgRNA-encoding plasmids via electroporation, electroporation parameters set to 1600 V, 10 ms, 3 pulses, stereotactic surgery performed for implantation at specific coordinates (3 mm depth, 2 mm lateral, 1 mm posterior to bregma), use of pSpCas9(BB)-2A GFP plasmids and Neon transfection system	Resistance to CD95L-induced apoptosis, reduced clonogenic growth, sphere-forming capacity, and invasiveness in glioblastoma-initiating cells after CD95 deletion	Lack of survival differences in tumor-bearing mice, ligand-independent tumor-promoting role of constitutive CD95 signaling

The deletion of the CD95 gene has been associated with reduced malignancy in glioblastoma cells, offering a promising avenue for therapeutic intervention. This genetic alteration mitigates the pro-tumorigenic effects of CD95 signaling, which are known to enhance cell survival, migration, immune evasion, and resistance to ferroptosis in glioblastoma. Emerging evidence suggests that targeting CD95 may disrupt key pathways driving glioblastoma progression, including inflammation and cellular survival mechanisms. These findings provide critical insights into therapeutic strategies aimed at diminishing tumor aggressiveness while addressing the challenges posed by the dual role of CD95 signaling in cancer biology.

Previous studies highlighted the paradoxical role of CD95 signaling in glioblastoma, contributing to tumor survival, immune regulation, and resistance to apoptosis, while therapeutic inhibition of CD95 signaling demonstrated clinical promise, with the CD95 inhibitor APG101 improving progression-free survival in patients [114, 115, 116, 117, 118, 119]. DISE-based approaches also emerged as a selective strategy for inducing cancer cell death, though challenges such as specificity and safety remain [120]. Despite these advances, the complexity of CD95 interactions with other pathways and limitations of exogenous CD95 agonists complicate therapeutic development [120]. Recent findings suggest that CD95 gene deletion reduces clonogenic growth, sphere-forming capacity, and invasiveness of glioblastoma cells independently of CD95 ligand, underscoring the need for further exploration of ligand-independent mechanisms.

Building upon the therapeutic implications of CD95 deletion, experimental studies have explored its impact on glioblastoma-initiating cells and tumor progression. Quijano-Rubio C et al. (2022) demonstrated that CD95 deletion in glioblastoma-initiating cells reduces resistance to CD95L-induced apoptosis, significantly decreases clonogenic growth ($p < 0.05$), sphere-forming capacity ($p < 0.05$), and invasiveness ($p < 0.0001$) in vitro, independent of CD95L expression. Despite these promising in vitro findings, survival outcomes in xenograft models showed no significant differences among groups, with median survival times in the S-24 model recorded as 193, 209, and 202 days, and in the ZH-161 model as 18.5, 20, and 20 days ($p > 0.05$). These results highlight the role of CD95 signaling in glioblastoma biology, emphasizing its influence on malignancy traits such as clonogenic growth, sphere formation, invasiveness, and apoptosis resistance.

2.4. Iron Oxide Nanoparticles and Paclitaxel: Inducing Ferroptosis via Autophagic Pathways in Glioblastoma

Selected findings

- Iron oxide nanoparticles synergize with paclitaxel to induce ferroptosis in glioblastoma cells by modulating autophagy-related pathways, including Beclin 1 upregulation and mTORC1 suppression. This approach integrates nanotechnology with chemotherapeutics, offering a promising strategy to enhance treatment efficacy and overcome tumor resistance.
- IONP@PTX significantly increases intracellular iron levels, ROS production, and lipid peroxidation, which are central to ferroptotic cell death in glioblastoma. These findings advance the understanding of ferroptosis mechanisms and provide a foundation for developing targeted therapies exploiting glioblastoma vulnerabilities.

Table 7. Iron Oxide Nanoparticles and Paclitaxel: Inducing Ferroptosis via Autophagic Pathways in Glioblastoma

Study ID	Length of intervention	Population of intervention	Control	Intervention	Intervention details	Primary outcome	Secondary outcome
Nie Q et al. (2023)	24 hours	Human SCLC NCI-H446 cells, human GBM M059K brain malignant cells, 96 wells with 5,000 cells per well	Untreated cells	Creation of oleic acid-coated iron oxide nanoparticles (IONP), formulation of IONP@PTX	IONP synthesized using high-temperature pyrolysis of Fe(acac) ₃ , oleic acid, oleylamine, and benzyl ether, mixed ultrasonically with DSPE-PEG 2000, PTX, distilled water, and oleic acid-coated IONP to form emulsion, concentrated by solvent evaporation at 70°C, purified using ultrafiltration tubes	Synergistic effect of IONP@PTX on cancer cell viability and induction of ferroptosis via autophagy. Primary Outcome	Increased iron ion concentration, elevated ROS levels, increased lipid peroxidation, upregulation of Beclin 1, HDAC6, LC3-II/I, downregulation of p62 and mTORC1 pathway

The induction of ferroptosis in glioblastoma through autophagic pathways has been explored using iron oxide nanoparticles and paclitaxel, highlighting their synergistic potential as therapeutic agents. Iron oxide nanoparticles facilitate intracellular iron accumulation, while paclitaxel enhances autophagy, collectively triggering ferroptosis. This approach leverages the unique properties of nanoparticles to enhance drug delivery and promote ferroptotic cell death, addressing the challenges of tumor resistance and recurrence. By integrating nanotechnology with chemotherapeutic strategies, this novel mechanism underscores advancements in targeted glioblastoma treatment, offering a promising avenue to overcome resistance and improve therapeutic efficacy.

Previous studies identified lipid peroxidation, iron metabolism disruption, and GPX4 inactivation as key mechanisms driving ferroptosis in glioblastoma, with nano-drug delivery systems emerging as promising therapeutic strategies by exploiting tumor vulnerabilities such as high iron accumulation and lipid synthesis [122, 123, 124, 125]. Advanced nanoparticles, including FeGd-HN@LF/RGD2 and GOD-Fe3O4@DMSNs, demonstrated potential for overcoming the blood-brain barrier and inducing ferroptosis effectively, though limitations such as biological safety concerns, tumor heterogeneity, and inefficient peroxide production under weakly acidic conditions remain unresolved [126]. Recent findings suggest iron oxide nanoparticles synergize with paclitaxel to induce ferroptosis through autophagic pathways, highlighting the potential of combining ferroptosis-based strategies with novel delivery systems to improve therapeutic efficacy.

Building on the concept of ferroptosis induction via nanotechnology, experimental studies have elucidated the cellular and molecular mechanisms underlying its therapeutic impact in glioblastoma. IONP@PTX significantly inhibits glioblastoma cell viability (64.24±0.53% in NCI-H446 cells; 70.90±2.68% in M059K cells, $p < 0.001$) and induces ferroptosis by increasing ROS, lipid peroxidation, and intracellular iron levels ($p < 0.05$), as reported by Nie Q et al. (2023). These effects are mediated through autophagy-related pathways, marked by altered expression of proteins such as Beclin 1, LC3-II/I, and HDAC6 ($p < 0.05$), and are further amplified by rapamycin. This research highlights the synergistic interaction between iron oxide nanoparticles and paclitaxel in inducing ferroptosis via autophagic pathways in glioblastoma.

3. Discussion and Interpretation of Findings

3.1. Ferroptosis and Immune Modulation: Mechanisms and Therapeutic Strategies in Glioblastoma

Selected findings

- Macrophage-mediated iron dynamics, through labile iron and ferritin light chain upregulation, were shown to promote immunosuppression and tumor growth in glioblastoma. This finding may enable the development of therapies targeting iron interactions to enhance anti-PD1 efficacy and improve patient survival.
- NCOA4-driven ferritinophagy was identified as a key mechanism for iron release and ferroptosis induction, with implications for lipid peroxidation and immune modulation. Therapeutic strategies targeting NCOA4 may simultaneously enhance ferroptosis and influence immune responses in glioblastoma.
- GPX4 inhibition was shown to enhance ferroptosis, while NRF2 overexpression confers resistance through elevated glutathione levels. Targeting the GPX4-NRF2 axis could improve glioblastoma treatment by overcoming ferroptosis resistance and optimizing redox balance.

The investigation into ferroptosis and immune modulation in glioblastoma has yielded significant insights, particularly regarding the interplay of various molecular players such as LIP, DMT1, NCOA4, ROS, lipid peroxidation, GPX4, GSH, xCT, and NRF2. A pivotal study by Guo et al. (2025) established that overexpression of FOSL1 is linked to altered gene expression associated with ferroptosis and glioblastoma progression, highlighting the potential for targeted therapeutic strategies. The correlation between ferritin light chain (FTL) upregulation and immunosuppression, as demonstrated by Li et al. (2023), further underscores the relevance of labile iron in promoting tumor growth. This study uniquely emphasizes macrophage-mediated iron dynamics, suggesting that targeting these interactions could enhance the efficacy of anti-PD1 therapies and potentially improve survival rates in glioblastoma patients.

The role of DMT1 as a critical regulator of iron uptake has been reinforced through various studies, which collectively underscore its importance in mediating ferroptosis, particularly in the context of temozolomide (TMZ) treatment. While the recent literature does not directly address DMT1, it elucidates related mechanisms such as GPX4 regulation and the differential sensitivity of glioblastoma cell lines to TMZ, as noted by de Souza et al. (2022). This variability in TMZ sensitivity may influence DMT1-mediated ferroptosis, necessitating further exploration of its regulatory pathways. NCOA4's function in ferritinophagy has emerged as a crucial mechanism for promoting ferroptosis, with recent studies validating its role in iron release and autophagy. The findings by Buccarelli et al. (2018) and de Souza et al. (2022) highlight the interplay between lipid peroxidation and GPX4 inhibition, reinforcing the established connection between these pathways in glioblastoma. Moreover, the identification of FTL as a prognostic marker by Li et al. (2023) adds a new dimension to understanding the immune modulation in ferroptosis, suggesting that therapeutic strategies targeting NCOA4 may also influence immune responses.

Reactive oxygen species (ROS) have been recognized as key mediators in inducing ferroptosis, with studies revealing their complex role in glioblastoma cell death. The work by Kyani et al. (2018) emphasizes the interaction between autophagy and ferroptosis, aligning with earlier findings that link ROS accumulation to ferroptotic cell death. However, the variability in ROS modulation across different therapeutic interventions, as highlighted by Chen et al. (2015), indicates the need for a nuanced understanding of ROS dynamics in glioblastoma treatment strategies. Lipid peroxidation remains a hallmark of ferroptosis, driven by iron-dependent oxidative degradation of polyunsaturated fatty acids. Recent studies have reinforced the significance of GPX4 in suppressing lipid peroxidation, with deficiencies leading to increased cell death. The findings by Buccarelli et al. (2018) and de Souza et al. (2022) further elucidate the relationship between lipid peroxidation and ferroptosis sensitivity, suggesting that high MRP1 expression in TMZ-resistant glioblastoma cells may present a potential target for therapeutic intervention.

The role of GPX4 as a critical regulator of ferroptosis has been consistently supported, with evidence linking its inhibition to enhanced cell death in glioblastoma. The studies by Buccarelli et al. (2018) and de Souza et al. (2022) have expanded on this by exploring the interaction between GPX4 and NRF2, revealing that NRF2 overexpression can confer resistance to ferroptosis through elevated GSH levels. This highlights the complexity of ferroptosis regulation and the potential for targeting these pathways to improve therapeutic outcomes. Glutathione (GSH) has been identified as a vital antioxidant that maintains redox balance and prevents lipid peroxidation, thereby regulating ferroptosis sensitivity. The new studies corroborate earlier findings that GSH depletion exacerbates ferroptosis, with interventions

aimed at preserving GSH levels showing promise in enhancing treatment efficacy. Notably, de Souza et al. (2022) introduced a novel approach by quantifying GSH levels in specific glioblastoma cell lines, providing deeper insights into cell-specific antioxidant mechanisms.

The cystine/glutamate antiporter xCT has emerged as a key regulator of ferroptosis sensitivity, with recent studies reinforcing its role in cysteine uptake and glutathione synthesis. Kyani et al. (2018) and de Souza et al. (2022) highlight the importance of xCT in modulating ferroptosis, while also suggesting that compensatory mechanisms, such as transsulfuration, may confer resistance to ferroptosis-inducing agents. This finding emphasizes the need for comprehensive strategies that target multiple pathways to overcome adaptive resistance in glioblastoma. Finally, NRF2 continues to be a critical player in modulating redox balance and ferroptosis resistance. While recent studies reaffirm its role in antioxidant responses, further exploration into its therapeutic modulation is necessary to enhance our understanding of its impact on glioblastoma treatment outcomes. Overall, the integration of these findings underscores the complexity of ferroptosis in glioblastoma and the necessity for multi-targeted therapeutic approaches to improve treatment efficacy against this challenging malignancy.

3.2. Ferroptosis in Glioblastoma: Pathways, Immune Interactions, and Overcoming Resistance

Selected findings

- GPX4 inhibition sensitizes glioblastoma cells to ferroptosis, and its downregulation correlates with tumor recurrence and enhanced sensitivity to ferroptosis inducers. This finding may enable the development of targeted therapies that exploit GPX4 dependency to overcome resistance mechanisms in glioblastoma.
- SLC7A11 downregulation in specific glioblastoma subtypes promotes ferroptosis, contrasting its established role as a resistance factor, with combined therapies targeting SLC7A11 showing enhanced efficacy. This discovery highlights SLC7A11 as a promising therapeutic target, warranting further investigation into its regulation and subtype-specific roles.

In recent investigations into ferroptosis mechanisms within glioblastoma, we observe a multifaceted interplay of various molecular regulators that significantly influences therapeutic outcomes. Central to this discussion is Glutathione Peroxidase 4 (GPX4), an antioxidant enzyme crucial for maintaining cellular redox balance. Recent studies reaffirm GPX4's pivotal role in inhibiting lipid peroxidation and its dependency on glutathione, thus highlighting its importance in glioblastoma resistance to ferroptosis inducers (Battaglia AM et al. (2022), Costa I et al. (2023), Chen X et al. (2021)). Evidence from cohort and animal studies further supports the notion that GPX4 downregulation correlates with tumor recurrence and enhances sensitivity to ferroptosis (Kram H et al. (2022), Xia L et al. (2022)). This aligns with earlier findings suggesting that GPX4 inhibition sensitizes glioblastoma cells to ferroptosis (Zhao H et al. (2017), Yi R et al. (2020)). However, the emerging perspective on GPX4-independent mechanisms indicates a more complex regulatory landscape, with studies suggesting that GPX4's role may be indispensable, particularly in the context of resistance to ferroptosis inducers (Wang H et al. (2023), Minami JK et al. (2023)).

Reactive oxygen species (ROS) are also critical mediators in the ferroptotic process, as they accumulate during ferroptosis and lead to oxidative stress and lipid peroxidation. Recent studies have elucidated the relationship between mitochondrial dysfunction, ROS generation, and ferroptosis regulation, reinforcing the notion that mitochondrial ROS production exacerbates ferroptosis sensitivity (Chen Y et al. (2019), Tong S et al. (2022), Su J et al. (2022)). Furthermore, the role of key regulators such as NRF2 and SLC7A11 has been emphasized, with new evidence suggesting that NRF2 activation may be context-dependent, influenced by cellular environments and p53 status (Yuan F et al. (2022)). This nuanced understanding challenges previous assertions of NRF2's uniformly protective role against ferroptosis, indicating the need for tailored therapeutic strategies.

Lipid peroxidation, a hallmark of ferroptosis, has also garnered attention in recent studies. The involvement of Acyl-CoA Synthetase Long-Chain Family Member 4 (ACSL4) in lipid peroxidation has been reaffirmed, with new findings indicating that ACSL4 upregulation in recurrent glioblastoma tumors correlates with enhanced lipid peroxidation (Kram H et al. (2022)). This highlights the progressive role of lipid peroxidation in ferroptosis and suggests potential therapeutic targets within the PERK-ATF4-HSPA5-GPX4 feedback pathway (Chen Y et al. (2019)). However, the regulation of lipid peroxidation under hypoxic conditions remains contentious, as hypoxia-induced SLC7A11 upregulation has been shown to suppress ferroptosis, indicating a complex regulatory environment that necessitates context-specific therapeutic strategies.

Iron levels, particularly the dynamics of intracellular free iron, play a crucial role in ferroptosis. Recent research underscores the significance of NCOA4-mediated ferritinophagy in regulating iron availability and enhancing ferroptosis sensitivity (Chen Q et al. (2021), Zhang K et al. (2023)). While earlier studies emphasized iron accumulation as a driver of ferroptosis, newer findings illustrate the dual role of iron, with specific genetic and molecular interventions altering iron dynamics and ferroptosis sensitivity (Nie XH et al. (2022), Xu P et al. (2022)). The complexity of iron metabolism and its interaction with the tumor microenvironment necessitates further exploration to optimize therapeutic approaches targeting iron-mediated ferroptosis.

SLC7A11, a cystine/glutamate antiporter, has emerged as a significant regulator of ferroptosis resistance in glioblastoma. New findings indicate that SLC7A11 downregulation in certain glioblastoma subtypes may promote ferroptosis, contrasting its previously established role as a resistance factor (Hu Y et al. (2021)). Additionally, therapeutic strategies targeting SLC7A11, such as PX-478 combined with SAS, have shown promising results in enhancing ferroptosis sensitivity (Sun S et al. (2022)). These findings underscore the potential of SLC7A11 as a therapeutic target while revealing the complexity of its regulation and expression patterns. Moreover, OTUB1's role in stabilizing SLC7A11 and its implications for ferroptosis resistance have been further elucidated, with new studies confirming its influence on lipid peroxidation (Sun S et al. (2022)). However, the observed discrepancies in OTUB1 expression across different glioblastoma contexts highlight the need for precise characterization of its role in tumor biology (Hu Y et al. (2021), Yang Y et al. (2024)).

In summary, the integration of these findings advances our understanding of ferroptosis in glioblastoma, emphasizing the intricate interactions between GPX4, ROS, lipid peroxidation, iron levels, SLC7A11, ACSL4, OTUB1, and NCOA4-mediated ferritinophagy. These insights not only reinforce previous conclusions but also introduce new therapeutic avenues aimed at overcoming resistance and enhancing treatment efficacy in glioblastoma.

3.3. CD95 Gene Deletion: Reducing Malignancy in Glioblastoma Cells

Selected findings

- CD95 gene deletion in glioblastoma cells significantly reduces malignancy by impairing clonogenic growth, sphere-forming capacity, and invasiveness, independent of CD95L expression. This finding highlights CD95 as a promising therapeutic target for mitigating glioblastoma aggressiveness and ferroptosis resistance.
- CD95 deletion disrupts apoptotic signaling by abrogating Caspase-3 activity, as evidenced by reduced DEVD-amc peptide-cleaving activity. This mechanistic insight provides a foundation for developing apoptosis-enhancing strategies in glioblastoma through CD95-targeted interventions.

ferroptosis, and inflammation, highlighting its therapeutic potential within cancer biology. Quijano-Rubio et al. (2022) demonstrated that CD95 deletion significantly reduces glioblastoma cell clonogenic growth ($p < 0.05$), sphere-forming capacity ($p < 0.05$), and invasiveness ($p < 0.0001$), independent of CD95L expression. However, survival analysis in xenograft models revealed no significant differences in median survival times across groups in both S-24 and ZH-161 models ($p > 0.05$), suggesting therapeutic challenges in translating these cellular benefits to in vivo outcomes.

The primary outcomes related to CD95 receptor expression in glioblastoma provide critical insights into its dual role in apoptosis signaling and tumor cell survival. Previous studies collectively highlighted the paradoxical nature of CD95, demonstrating its capacity to mediate apoptosis while simultaneously promoting tumor invasion and survival under compromised apoptotic conditions. Notably, studies by Sharma S et al. (2019) and Rossin A et al. (2015) revealed mechanisms regulating CD95 surface levels, such as endosomal trafficking via ENTR1 and post-translational modifications like palmitoylation, which prevent lysosomal degradation. These findings underscore the complexity of CD95 signaling and its regulatory pathways in glioblastoma.

In corroboration, Quijano-Rubio et al. (2022) confirmed CD95 expression at both mRNA and protein levels in human glioblastoma initiating cell (GIC) lines, providing additional evidence for its presence in glioblastoma cells. However, this study does not address the functional implications of CD95 expression, such as its role in apoptosis resistance or tumor invasion, which were extensively discussed in earlier research by Wisniewski P et al. (2010), Fujita H et al. (2002), and Sharma S et al. (2019). Furthermore, it does not explore regulatory mechanisms like those identified in studies by Sharma S et al. (2019) and Rossin A et al. (2015), leaving gaps in understanding the factors modulating CD95 receptor levels.

Discrepancies arise regarding the impact of CD95 gene deletion on malignancy reduction. While Hadji A et al. (2014) suggested that cancer cannot form in the absence of CD95, earlier studies indicated that CD95 can promote tumor invasion and survival under specific conditions. Quijano-Rubio et al. (2022) neither supports nor contradicts these findings, as it focuses solely on expression levels without addressing functional outcomes. The strength of evidence in Quijano-Rubio et al. (2022) lies in its robust quantitative measurement of CD95 expression across multiple GIC lines, enhancing the reproducibility of findings. However, the lack of exploration into functional consequences limits its contribution to understanding the broader implications of CD95 in ferroptosis and glioblastoma malignancy.

In terms of Caspase-3 activity, Quijano-Rubio et al. (2022) provide significant evidence regarding the impact of CD95 gene deletion, demonstrating a clear abrogation of DEVD-amc peptide-cleaving activity, which is a hallmark of Caspase-3 activation. This finding aligns with earlier studies by Muzio M et al. (1996), Milhas D et al. (2005), and Song JJ et al. (2008), which emphasized the functional involvement of Caspase-3 in apoptosis induction and its regulation by upstream signaling pathways. Specifically, Quijano-Rubio et al. (2022) strengthen the understanding of CD95's role in canonical apoptotic signaling, as previously suggested by Muzio M et al. (1996) and Milhas D et al. (2005), which highlighted the interaction between death receptors and caspase activation.

However, discrepancies arise when comparing Quijano-Rubio et al. (2022) with Sánchez-Osuna M et al. (2016), which noted incomplete apoptosis in glioblastoma cells despite correct executioner caspase activation. The new data suggest that CD95 deletion effectively disrupts apoptotic signaling, whereas Sánchez-Osuna M et al. (2016) indicated that apoptosis may remain incomplete even with caspase-3 activation. This difference underscores the complexity of apoptotic mechanisms in glioblastoma and suggests that CD95 deletion may uniquely influence apoptosis progression.

Methodologically, Quijano-Rubio et al. (2022) advance the field by employing CD95 knockout clonal sublines and combining exogenous CD95L stimulation with cycloheximide sensitization, providing a robust experimental design that enhances the specificity and reliability of the findings. This contrasts with earlier studies, such as Song JJ et al. (2008) and Muzio M et al. (1996), which focused on broader regulatory mechanisms like MAPK cleavage or Fas palmitoylation without directly targeting CD95 deletion. Overall, the study contributes novel insights into the mechanistic role of CD95 in Caspase-3 activity and apoptosis in glioblastoma, offering stronger evidence for the therapeutic potential of targeting CD95 to reduce malignancy. While the findings are consistent with most previous studies, the divergence from Sánchez-Osuna M et al. (2016) highlights the need for further exploration of downstream apoptotic processes in glioblastoma.

3.4. Iron Oxide Nanoparticles and Paclitaxel: Inducing Ferroptosis via Autophagic Pathways in Glioblastoma

Selected findings

- The combination of iron oxide nanoparticles and paclitaxel significantly inhibits glioblastoma cell viability while inducing ferroptosis through increased ROS production, lipid peroxidation, and intracellular iron levels. This finding highlights a novel therapeutic strategy that leverages the synergistic effects of ROS modulation and iron delivery to overcome tumor resistance in glioblastoma.
- Enhanced autophagic flux induced by IONP@PTX, as evidenced by upregulation of autophagy-related proteins and downregulation of p62 and mTORC1, demonstrates a mechanistic link between autophagy and ferroptosis in glioblastoma. This insight provides a pharmacological foundation for targeting autophagic pathways to amplify ferroptosis and improve glioblastoma treatment outcomes.

The exploration of ferroptosis induction via autophagic pathways in glioblastoma through the use of iron oxide nanoparticles (IONPs) in combination with paclitaxel (PTX) provides a promising therapeutic strategy to address tumor resistance and recurrence. The study by Nie Q et al. (2023) demonstrates that this combination significantly inhibits glioblastoma cell viability while inducing ferroptosis, as evidenced by increased reactive oxygen species (ROS), lipid peroxidation, and elevated intracellular iron levels. These findings highlight the critical role of ROS as pivotal mediators of ferroptosis and oxidative stress, corroborating previous research that has established the importance of ROS generation in cancer cell death mechanisms (Shen Z et al. (2018); Huo M et al. (2017)). The synergistic enhancement of ROS production observed in the current study aligns with earlier evidence and reinforces the therapeutic relevance of ROS modulation in glioblastoma treatment.

Furthermore, the quantification of lipid peroxidation using a C11-BODIPY™ fluorescent probe in Nie Q et al. (2023) showcases a methodological advancement over previous studies, which primarily focused on genetic or chemical interventions to modulate lipid peroxidation (Alborzina H et al. (2022); Bao Z et al. (2021)). This direct quantification underscores the therapeutic potential of IONP@PTX in promoting lipid peroxidation, a hallmark of ferroptosis. While discrepancies in experimental models exist—Nie Q et al. (2023) relying on in vitro analyses compared to the animal trials and cohort studies of prior research—its focused approach contributes significantly to our understanding of ferroptosis mechanisms in glioblastoma.

Moreover, the study elucidates the impact of iron concentration in driving ferroptosis through enhanced ROS production. The introduction of iron via nanoparticles not only aligns with previous findings regarding the role of iron in ferroptosis induction (Shen Z et al. 2018) but also represents a distinct therapeutic strategy that differs from previous approaches focused on modulating iron uptake or storage mechanisms. The reliance on in vitro models, while limiting generalizability, provides a novel perspective on the targeted delivery of iron to glioblastoma cells, enhancing therapeutic precision. In terms of autophagic flux, Nie Q et al. (2023) further expands on earlier studies by demonstrating that IONP@PTX significantly enhances autophagic activity, as indicated by the upregulation of autophagy-related proteins such as Beclin 1, LC3-III, and HDAC6, alongside the downregulation of p62 and mTORC1. This evidence supports the hypothesis that autophagy plays a crucial role in ferroptosis induction, particularly within glioblastoma contexts. The amplification of these effects through the addition of rapamycin reinforces the mechanistic link between autophagy and ferroptosis, providing a pharmacological approach to enhance autophagic flux for therapeutic benefit.

Lastly, the evaluation of cell viability in the study underscores the synergistic effect of IONP@PTX in reducing glioblastoma cell survival rates, complementing broader

vulnerabilities identified in previous research regarding ROS detoxification pathways (Floros KV et al. 2021) and ferroptosis-related molecular targets (Bao Z et al. 2021). The methodological advances utilized in Nie Q et al. (2023), including the CCK-8 assay and combination index analyses, enhance our understanding of drug synergy and its implications for cell survival, marking a significant step forward in the development of ferroptosis-related therapies for glioblastoma. In summary, the findings from Nie Q et al. (2023) not only align with existing literature but also introduce novel therapeutic approaches that leverage the synergistic effects of iron oxide nanoparticles and paclitaxel to induce ferroptosis through enhanced ROS production, lipid peroxidation, and autophagic pathways. These insights pave the way for further exploration of targeted interventions that could improve treatment outcomes for glioblastoma patients.

4. Discussion of Limitations

4.1. Ferroptosis and Immune Modulation: Mechanisms and Therapeutic Strategies in Glioblastoma

The recent advancements in ferroptosis and immune modulation research in glioblastoma (GBM) have substantially addressed several limitations identified in prior reviews, yet they underscore the need for further exploration to fully resolve these challenges.

One significant limitation highlighted previously was the difficulty in effectively utilizing cytotoxic autophagy to eliminate GBM cells or inhibit protective autophagy [144]. New findings have demonstrated that inhibiting protective autophagy enhances the cytotoxic effects of temozolomide (TMZ) on glioblastoma stem-like cells (GSCs), suggesting ferroptosis as a potential underlying mechanism [18]. This study, conducted on adult GBM patients, employed various autophagy modulators and revealed that lower autophagy levels correlate with improved overall survival ($p = 0.0012$) and increased sensitivity of GSCs to TMZ ($p < 0.05$). However, the short intervention duration and limited differentiation between cytotoxic and protective autophagy mechanisms restrict the study's ability to fully resolve this limitation. Future research must focus on expanding intervention periods and refining mechanistic insights to establish clinical applicability and long-term outcomes.

Closely related is the challenge of ameliorating autophagy-related drug tolerance in glioma treatments, which was another limitation identified in prior reviews [144]. Recent studies have explored strategies to modulate autophagy and enhance GSC sensitivity to TMZ. For instance, the use of trehalose and quinacrine in both *in vitro* and *in vivo* models significantly improved GSC susceptibility to TMZ, with low autophagy levels correlating with better overall survival ($p = 0.0012$) [18]. Another study targeted STAT3 via genetic manipulation, demonstrating that STAT3 depletion enhances cell survival under drug treatment while reducing autophagy-dependent cell death ($p < 0.0001$) [20]. Despite these promising findings, limitations such as short intervention durations and restricted population diversity hinder comprehensive resolution. Future studies should prioritize extended treatment protocols and larger, more diverse cohorts to fully address drug tolerance in GBM therapies.

A critical limitation identified in earlier reviews was the insufficient understanding of ferroptosis in GBM progression, particularly its interaction with oxidative stress, ER stress, and metabolic pathways [144]. Recent evidence has shown that TMZ treatment induces ferroptotic cell death in GSCs, marked by increased lipid peroxidation and reduced GPX4 activity, highlighting its link to oxidative stress [18]. Additionally, autophagy modulation was found to influence GSC susceptibility to TMZ, providing valuable insights into the interplay between ferroptosis and other cellular death modalities. Nonetheless, the study's short intervention duration, limited population diversity, and lack of comprehensive mechanistic exploration indicate that further research is required to elucidate the complex interactions among ferroptosis, oxidative stress, and metabolism in GBM progression.

Another significant limitation was the protective feedback pathways, particularly the PERK-ATF4-HSPA5-GPX4 cascade, which shield glioblastoma cells from ferroptosis and limit the efficacy of compounds like DHA [16]. Recent research investigated the role of NRF2 and ABCC1 in ferroptosis sensitivity within glioblastoma cell lines U251MG and T98G [6]. Despite high NRF2 expression, T98G cells exhibited sensitivity to ferroptosis-inducing agents such as Erastin and RSL3, suggesting a disruption in protective feedback mechanisms. The study revealed that high levels of NRF2 and ABCC1 could facilitate glutathione (GSH) depletion, enhancing ferroptosis sensitivity. However, the lack of direct investigation into the entire feedback cascade and absence of *in vivo* validation limits the study's effectiveness. Future research should aim to comprehensively explore these pathways and validate findings in clinical settings to address drug resistance in GBM.

Finally, the lack of specificity in ferroptosis biomarkers, which hampers their predictive utility for tumor prognosis and individualized treatment outcomes, was identified as a significant limitation [16]. New findings demonstrated that elevated NRF2 and ABCC1 expression in glioblastoma cells correlates with increased sensitivity to ferroptosis and poor patient outcomes, suggesting their potential as predictive biomarkers [6]. Specifically, T98G cells exhibited a 12-fold increase in NRF2 expression and sensitivity to ferroptosis inducers, while silencing NRF2 increased resistance. Despite these promising results, the study was limited by its use of only two glioma cell lines without a control group, restricting its generalizability. Future validation across diverse cancer types and clinical samples is essential to fully address the biomarker specificity limitation.

In summary, while recent studies have made notable progress in addressing the limitations of ferroptosis and immune modulation in glioblastoma, several challenges remain unresolved. These include extending intervention durations, increasing population diversity, conducting comprehensive mechanistic investigations, and validating findings in clinical settings. Addressing these gaps will be critical to translating these promising findings into effective therapeutic strategies for glioblastoma.

4.2. Ferroptosis in Glioblastoma: Pathways, Immune Interactions, and Overcoming Resistance

The recent advancements in ferroptosis research have significantly addressed the limitations outlined in previous reviews, particularly in the context of glioblastoma (GBM). However, while notable progress has been made, several challenges remain unresolved, necessitating further investigation.

The mechanistic understanding of ferroptosis in GBM, previously identified as a critical limitation, has been expanded through studies elucidating the roles of specific proteins and pathways. For instance, GPX4 has been shown to play a pivotal role in ferroptosis regulation, with IGF2BP3 stabilizing GPX4 mRNA and preventing ferroptosis [95]. Complementary findings demonstrate that silencing GPX7 enhances ferroptosis sensitivity to erastin [145], and DHA induces ferroptosis via increased ROS and lipid peroxidation [25]. Despite these advancements, the mechanistic complexities surrounding GPX4, its interactions with other proteins, and its context-dependent roles remain partially unexplored, highlighting the need for broader experimental validation and more diverse sample populations.

Glioblastoma's intrinsic heterogeneity, another major challenge, complicates the development of universally effective therapies. Recent studies have made strides in addressing this limitation by investigating molecular pathways and biomarkers associated with ferroptosis. For example, GPX7 expression has been correlated with treatment response, suggesting its potential as a biomarker for personalized therapies [145]. Additionally, targeting IGF2BP3 and erianin has demonstrated efficacy across diverse glioma subtypes, despite heterogeneity [95][100]. However, the focus on specific cell lines and limited sample sizes restricts the generalizability of these findings. Future research must integrate larger cohorts and explore additional pathways to comprehensively address glioma heterogeneity.

The integration of ferroptosis-based therapies with traditional modalities, such as chemotherapy and radiotherapy, has shown promise but remains underdeveloped. Combining DHA with PERK pathway inhibition has demonstrated synergistic effects in glioma cells ($p < 0.001$) [25], while erianin enhances TMZ sensitivity in resistant glioblastoma stem cells, inducing ferroptosis (IC50 increased by 9.4 to 11.5 times) [100]. Despite these promising results, the studies lack exploration of combinations with radiotherapy or other modalities, underscoring the need for broader investigations into multimodal therapeutic strategies.

The complex interplay between glioma cells and their microenvironment also poses significant challenges to ferroptosis-based therapies. Recent studies have begun to address this limitation by exploring microenvironmental interactions. For instance, IGF2BP3 knockdown impairs glioma cell growth and enhances susceptibility to

microglial phagocytosis [95], while Notch signaling has been implicated in glioma cell survival and GPX4 sensitivity [21]. However, these studies focus narrowly on specific pathways, leaving other microenvironmental factors, such as immune cell dynamics, insufficiently explored. Further research should aim to unravel the multifaceted interactions within the glioma microenvironment to optimize ferroptosis-based interventions.

The absence of gold-standard biomarkers for ferroptosis in GBM has been partially addressed through the identification of gene signatures, such as a 19-gene signature [50] and an 11-gene signature [51], both demonstrating strong prognostic capabilities (AUC values up to 0.919). Additionally, SLC7A11 has emerged as a potential biomarker, offering insights into ferroptosis mechanisms [22]. Despite these promising findings, the reliance on cell lines and the lack of independent cohort validation limit their clinical applicability. Further research is essential to establish universally applicable biomarkers validated across diverse glioma models. Finally, the challenge of poor blood-brain barrier penetration and compensatory mechanisms hindering ferroptosis-based therapies has been addressed through innovative approaches. The use of Lpo@Cu2Se-GOx nanocomposites has demonstrated enhanced BBB penetration and therapeutic efficacy in in vivo GBM models [103]. Additionally, Fe3O4-siPD-L1@M-BV2 nanoparticles have shown promising results in selectively inducing ferroptosis while sparing healthy tissues [74]. However, these studies do not fully explore long-term safety, toxicity, or compensatory mechanisms, indicating the need for further research to optimize these strategies.

In conclusion, while the new findings represent significant progress in addressing the limitations of ferroptosis research in glioblastoma, they underscore the necessity for ongoing investigations. Future research should focus on expanding sample diversity, integrating multimodal therapies, and validating biomarkers and therapeutic strategies in clinical settings to achieve a comprehensive understanding and effective application of ferroptosis-based treatments for GBM.

5. Conclusions

The exploration of ferroptosis in glioblastoma has revealed critical insights into its underlying mechanisms and therapeutic strategies. The studies collectively highlight the role of key regulators such as GPX4, ROS, and NCOA4, emphasizing their potential as therapeutic targets. Interventions like CD95 gene deletion and the use of iron oxide nanoparticles combined with paclitaxel have shown promise in reducing tumor malignancy and inducing ferroptosis, respectively. However, limitations such as reliance on in vitro models, small sample sizes, and the complexity of tumor microenvironments pose significant challenges in translating these findings to clinical applications. Future research should prioritize the development of diverse in vivo models, validation of biomarkers across broader cohorts, and exploration of multimodal treatment strategies. Moreover, understanding the adaptive resistance mechanisms that may arise from therapeutic interventions will be crucial for enhancing treatment efficacy. By addressing these gaps, future studies can pave the way for more effective therapies that leverage ferroptosis in glioblastoma management.

References

1. Liberati A, Altman DG, Tetzlaff J, Mulrow C, Gøtzsche PC, Ioannidis JP, Clarke M, Devereaux PJ, Kleijnen J, Moher D. The PRISMA statement for reporting systematic reviews and meta-analyses of studies that evaluate healthcare interventions: explanation and elaboration. *BMJ*. 2009 Jul 21;339:b2700. doi: 10.1136/bmj.b2700. [PMC free article] [PubMed].
2. Wells, G.A., Wells, G., Shea, B., Shea, B., O'Connell, D., Peterson, J., Welch, Losos, M., Tugwell, P., Ga, S.W., Zello, G.A., & Petersen, J.A. (2014). The Newcastle-Ottawa Scale (NOS) for Assessing the Quality of Nonrandomised Studies in Meta-Analyses.
3. Higgins JP, Altman DG, Gøtzsche PC, Jüni P, Moher D, Oxman AD, Savovic J, Schulz KF, Weeks L, Sterne JACochrane Bias Methods GroupCochrane Statistical Methods Group. The Cochrane Collaboration's tool for assessing risk of bias in randomised trials. *BMJ*. 2011 Oct 18;343:d5928. doi: 10.1136/bmj.d5928. [PMC free article] [PubMed].
4. Guo S, Sidhu R, Ramar V, Guo AA, Wang G, Liu M. RNA Sequencing Identifies Novel Signaling Pathways and Potential Drug Target Genes Induced by FOSL1 in Glioma Progression and Stemness. *Biologics*. 202519():157-176. doi: 10.2147/BTT.S509774. [PMC free article] [PubMed]
5. Li H, Yang C, Wei Y, Li X, Jiang W, Xu Y, Li L, Guo R, Chen D, Gao P, Zhang H, Qin H, Zhang Z, Liu X, Yan D. Ferritin light chain promotes the reprogramming of glioma immune microenvironment and facilitates glioma progression. *Theranostics*. 202313(11):3794-3813. doi: 10.7150/thno.82975. [PMC free article] [PubMed]
6. de Souza I, Monteiro LKS, Guedes CB, Silva MM, Andrade-Tomaz M, Contieri B, Latancia MT, Mendes D, Porchia BFMM, Lazarini M, Gomes LR, Rocha CRR. High levels of NRF2 sensitize temozolomide-resistant glioblastoma cells to ferroptosis via ABCG1/MRP1 upregulation. *Cell Death Dis*. 2022 Jul 8;13(7):591. doi: 10.1038/s41419-022-05044-9. [PMC free article] [PubMed]
7. Zhang Y, Xi K, Fu X, Sun H, Wang H, Yu D, Li Z, Ma Y, Liu X, Huang B, Wang J, Li G, Cui J, Li X, Ni S. Versatile metal-phenolic network nanoparticles for multitargeted combination therapy and magnetic resonance tracing in glioblastoma. *Biomaterials*. 2021 Nov;278():121163. doi: 10.1016/j.biomaterials.2021.121163. [PubMed]
8. Wang X, Lu S, He C, Wang C, Wang L, Piao M, Chi G, Luo Y, Ge P. RSL3 induced autophagic death in glioma cells via causing glycolysis dysfunction. *Biochem Biophys Res Commun*. 2019 Oct 20;518(3):590-597. doi: 10.1016/j.bbrc.2019.08.096. [PubMed]
9. Torti SV, Manz DH, Paul BT, Blanchette-Farra N, Torti FM. Iron and Cancer. *Annu Rev Nutr*. 2018 Aug 21;38():97-125. doi: 10.1146/annurev-nutr-082117-051732. [PMC free article] [PubMed]
10. Zhao N, Huang Y, Wang YH, Muir RK, Chen YC, Wei J, Hooshdaran N, Viswanath P, Seo Y, Ruggero D, Renslo AR, Evans MJ. Ferronostics: Measuring Tumoral Ferrous Iron with PET to Predict Sensitivity to Iron-Targeted Cancer Therapies. *J Nucl Med*. 2021 Jul 16;62(7):949-955. doi: 10.2967/jnumed.120.252460. [PMC free article] [PubMed]
11. Doll S, Proneth B, Tyurin YY, Panzilius E, Kobayashi S, Ingold I, Irmeler M, Beckers J, Aichler M, Walch A, Prokisch H, Trümbach D, Mao G, Qu F, Bayir H, Füllekrug J, Scheel CH, Wurst W, Schick JA, Kagan VE, Angeli JP, Conrad M. ACSL4 dictates ferroptosis sensitivity by shaping cellular lipid composition. *Nat Chem Biol*. 2017 Jan;13(1):91-98. doi: 10.1038/nchembio.2239. [PMC free article] [PubMed]
12. He Y, Ye Y, Tian W, Qiu H. A Novel lncRNA Panel Related to Ferroptosis, Tumor Progression, and Microenvironment is a Robust Prognostic Indicator for Glioma Patients. *Front Cell Dev Biol*. 20219():788451. doi: 10.3389/fcell.2021.788451. [PMC free article] [PubMed]
13. Zheng J, Zhou Z, Qiu Y, Wang M, Yu H, Wu Z, Wang X, Jiang X. A Prognostic Ferroptosis-Related lncRNAs Signature Associated With Immune Landscape and Radiotherapy Response in Glioma. *Front Cell Dev Biol*. 20219():675555. doi: 10.3389/fcell.2021.675555. [PMC free article] [PubMed]
14. Zhou L, Jiang Z, Shi Z, Zhao W, Lu Z, Xie Y, Zhang B, Lu H, Tan G, Wang Z. New Autophagy-Ferroptosis Gene Signature Predicts Survival in Glioma. *Front Cell Dev Biol*. 20219():739097. doi: 10.3389/fcell.2021.739097. [PMC free article] [PubMed]
15. Chen Y, Li N, Wang H, Wang N, Peng H, Wang J, Li Y, Liu M, Li H, Zhang Y, Wang Z. Amentoflavone suppresses cell proliferation and induces cell death through triggering autophagy-dependent ferroptosis in human glioma. *Life Sci*. 2020 Apr 15;247():117425. doi: 10.1016/j.lfs.2020.117425. [PubMed]
16. de Souza I, Ramalho MCC, Guedes CB, Osawa IYA, Monteiro LKS, Gomes LR, Rocha CRR. Ferroptosis Modulation: Potential Therapeutic Target for Glioblastoma Treatment. *Int J Mol Sci*. 2022 Jun 21;23(13):. doi: 10.3390/ijms23136879. [PMC free article] [PubMed]
17. Kyani A, Tamura S, Yang S, Shergalis A, Samanta S, Kuang Y, Ljungman M, Neamati N. Discovery and Mechanistic Elucidation of a Class of Protein Disulfide Isomerase Inhibitors for the Treatment of Glioblastoma. *ChemMedChem*. 2018 Jan 22;13(2):164-177. doi: 10.1002/cmdc.201700629. [PMC free article] [PubMed]
18. Buccarelli M, Marconi M, Pacioni S, De Pascalis I, D'Alessandris QG, Martini M, Ascione B, Malorni W, Larocca LM, Pallini R, Ricci-Vitiani L, Matarrese P. Inhibition of autophagy increases susceptibility of glioblastoma stem cells to temozolomide by igniting ferroptosis. *Cell Death Dis*. 2018 Aug 6;9(8):841. doi: 10.1038/s41419-018-0864-7. [PMC free article] [PubMed]

19. Zhao Z, Zhang L, Zhang X, Yue Y, Liu S, Li Y, Ban X, Zhao C, Jin P. Coixendide efficacy in combination with temozolomide in glioblastoma and transcriptome analysis of the mechanism. *Sci Rep.* 2023 Sep 19;13(1):15484. doi: 10.1038/s41598-023-41421-w. [PMC free article] [PubMed]
20. Remy J, Linder B, Weirauch U, Day BW, Stringer BW, Herold-Mende C, Aigner A, Krohn K, Kögel D. STAT3 Enhances Sensitivity of Glioblastoma to Drug-Induced Autophagy-Dependent Cell Death. *Cancers (Basel).* 2022 Jan 11;14(2):. doi: 10.3390/cancers14020339. [PMC free article] [PubMed]
21. Banu MA, Dovas A, Argenziano MG, Zhao W, Sperring CP, Cuervo Grajal H, Liu Z, Higgins DM, Amini M, Pereira B, Ye LF, Mahajan A, Humala N, Furnari JL, Upadhyayula PS, Zandkarimi F, Nguyen TT, Teasley D, Wu PB, Hai L, Karan C, Dowdy T, Razavilar A, Siegelin MD, Kitajewski J, Larion M, Bruce JN, Stockwell BR, Sims PA, Canoll P. A cell state-specific metabolic vulnerability to GPX4-dependent ferroptosis in glioblastoma. *EMBO J.* 2024 Oct;43(20):4492-4521. doi: 10.1038/s44318-024-00176-4. [PMC free article] [PubMed]
22. Sun S, Guo C, Gao T, Ma D, Su X, Pang Q, Zhang R. Hypoxia Enhances Glioma Resistance to Sulfasalazine-Induced Ferroptosis by Upregulating SLC7A11 via PI3K/AKT/HIF-1 α Axis. *Oxid Med Cell Longev.* 2022;2022():7862430. doi: 10.1155/2022/7862430. [PMC free article] [PubMed]
23. Yang Y, Hao L, Guiyang L, Haozhe P. Multifaceted bioinformatic analysis of m6A-related ferroptosis and its link with gene signatures and tumour-infiltrating immune cells in gliomas. *J Cell Mol Med.* 2024 Sep;28(17):e70060. doi: 10.1111/jcmm.70060. [PMC free article] [PubMed]
24. Minami JK, Morrow D, Bayley NA, Fernandez EG, Salinas JJ, Tse C, Zhu H, Su B, Plawat R, Jones A, Sammarco A, Liau LM, Graeber TG, Williams KJ, Cloughesy TF, Dixon SJ, Bensinger SJ, Nathanson DA. CDKN2A deletion remodels lipid metabolism to prime glioblastoma for ferroptosis. *Cancer Cell.* 2023 Jun 12;41(6):1048-1060.e9. doi: 10.1016/j.ccell.2023.05.001. [PMC free article] [PubMed]
25. Chen Y, Mi Y, Zhang X, Ma Q, Song Y, Zhang L, Wang D, Xing J, Hou B, Li H, Jin H, Du W, Zou Z. Dihydroartemisinin-induced unfolded protein response feedback attenuates ferroptosis via PERK/ATF4/HSPA5 pathway in glioma cells. *J Exp Clin Cancer Res.* 2019 Sep 13;38(1):402. doi: 10.1186/s13046-019-1413-7. [PMC free article] [PubMed]
26. Zhou Y, Tao L, Zhou X, Zuo Z, Gong J, Liu X, Zhou Y, Liu C, Sang N, Liu H, Zou J, Gou K, Yang X, Zhao Y. DHODH and cancer: promising prospects to be explored. *Cancer Metab.* 2021 May 10;9(1):22. doi: 10.1186/s40170-021-00250-z. [PMC free article] [PubMed]
27. Yuan F, Sun Q, Zhang S, Ye L, Xu Y, Deng G, Xu Z, Zhang S, Liu B, Chen Q. The dual role of p62 in ferroptosis of glioblastoma according to p53 status. *Cell Biosci.* 2022 Feb 25;12(1):20. doi: 10.1186/s13578-022-00764-z. [PMC free article] [PubMed]
28. Xu Y, Zhang N, Chen C, Xu X, Luo A, Yan Y, Lu Y, Liu J, Ou X, Tan Y, Liang Y, Chen L, Song X, Liu X. Sevoflurane Induces Ferroptosis of Glioma Cells Through Activating the ATF4-CHAC1 Pathway. *Front Oncol.* 2022;12():859621. doi: 10.3389/fonc.2022.859621. [PMC free article] [PubMed]
29. Kram H, Prokop G, Haller B, Gempt J, Wu Y, Schmidt-Graf F, Schlegel J, Conrad M, Liesche-Starnecker F. Glioblastoma Relapses Show Increased Markers of Vulnerability to Ferroptosis. *Front Oncol.* 2022;12():841418. doi: 10.3389/fonc.2022.841418. [PMC free article] [PubMed]
30. Zhang F, Wu L, Feng S, Zhao Z, Zhang K, Thakur A, Xu Z, Liang Q, Liu Y, Liu W, Yan Y. FHOD1 is upregulated in glioma cells and attenuates ferroptosis of glioma cells by targeting HSPB1 signaling. *CNS Neurosci Ther.* 2023 Nov;29(11):3351-3363. doi: 10.1111/cns.14264. [PMC free article] [PubMed]
31. Banu MA, Dovas A, Argenziano MG, Zhao W, Grajal HC, Higgins DMO, Sperring CP, Pereira B, Ye LF, Mahajan A, Humala N, Furnari JL, Upadhyayula PS, Zandkarimi F, Nguyen TTT, Wu PB, Hai L, Karan C, Razavilar A, Siegelin MD, Kitajewski J, Bruce JN, Stockwell BR, Sims PA, Canoll PD. A cell state specific metabolic vulnerability to GPX4-dependent ferroptosis in glioblastoma. *bioRxiv.* 2023 Feb 23():. doi: 10.1101/2023.02.22.529581. [PMC free article] [PubMed]
32. Gao W, Li Y, Lin X, Deng K, Long X, Li D, Huang M, Wang X, Xu Y, She X, Wu M. Procyanidin B1 Promotes PSMC3-NRF2 Ubiquitination to Induce Ferroptosis in Glioblastoma. *Phytother Res.* 2024 Dec;38(12):5583-5597. doi: 10.1002/ptr.8328. [PMC free article] [PubMed]
33. Katz JL, Geng Y, Billingham LK, Sadagopan NS, DeLay SL, Subbiah J, Chia TY, McManus G, Wei C, Wang H, Lin H, Silvers C, Boland LK, Wang S, Wan H, Hou D, Vázquez-Cervantes GI, Arjmandi T, Shaikh ZH, Zhang P, Ahmed AU, Tiek DM, Lee-Chang C, Chouchani ET, Miska J. A covalent creatine kinase inhibitor ablates glioblastoma migration and sensitizes tumors to oxidative stress. *Sci Rep.* 2024 Sep 20;14(1):21959. doi: 10.1038/s41598-024-73051-1. [PMC free article] [PubMed]
34. Meng X, Wang Z, Yang Q, Liu Y, Gao Y, Chen H, Li A, Li R, Wang J, Sun G. Intracellular C5aR1 inhibits ferroptosis in glioblastoma through METTL3-dependent m6A methylation of GPX4. *Cell Death Dis.* 2024 Oct 5;15(10):729. doi: 10.1038/s41419-024-06963-5. [PMC free article] [PubMed]
35. Zhang Y, Wu X, Zhu J, Lu R, Ouyang Y. Knockdown of SLC39A14 inhibits glioma progression by promoting erastin-induced ferroptosis SLC39A14 knockdown inhibits glioma progression. *BMC Cancer.* 2023 Nov 17;23(1):1120. doi: 10.1186/s12885-023-11637-0. [PMC free article] [PubMed]
36. Wang W, Zhang Y, Li X, E Q, Jiang Z, Shi Q, Huang Y, Wang J, Huang Y. KCNA1 promotes the growth and invasion of glioblastoma cells through ferroptosis inhibition via upregulating SLC7A11. *Cancer Cell Int.* 2024 Jan 32;24(1):7. doi: 10.1186/s12935-023-03199-9. [PMC free article] [PubMed]
37. Chen X, Wang Z, Li C, Zhang Z, Lu S, Wang X, Liang Q, Zhu X, Pan C, Wang Q, Ji Z, Wang Y, Piao M, Chi G, Ge P. SIRT1 activated by AROS sensitizes glioma cells to ferroptosis via induction of NAD⁺ depletion-dependent activation of ATF3. *Redox Biol.* 2024 Feb;69():103030. doi: 10.1016/j.redox.2024.103030. [PMC free article] [PubMed]
38. Miao Z, Tian W, Ye Y, Gu W, Bao Z, Xu L, Sun G, Li C, Tu Y, Chao H, Lam SM, Liu N, Ji J. Hsp90 induces Acs4-dependent glioma ferroptosis via dephosphorylating Ser637 at Drp1. *Cell Death Dis.* 2022 Jun 13;13(6):548. doi: 10.1038/s41419-022-04997-1. [PMC free article] [PubMed]
39. Vo VTA, Kim S, Hua TNM, Oh J, Jeong Y. Iron commensalism of mesenchymal glioblastoma promotes ferroptosis susceptibility upon dopamine treatment. *Commun Biol.* 2022 Jun 16;5(1):593. doi: 10.1038/s42003-022-03538-y. [PMC free article] [PubMed]
40. Hangauer MJ, Viswanathan VS, Ryan MJ, Bole D, Eaton JK, Matov A, Galeas J, Dhruv HD, Berens ME, Schreiber SL, McCormick F, McManus MT. Drug-tolerant persister cancer cells are vulnerable to GPX4 inhibition. *Nature.* 2017 Nov 9;551(7679):247-250. doi: 10.1038/nature24297. [PMC free article] [PubMed]
41. Lei G, Zhang Y, Koppula P, Liu X, Zhang J, Lin SH, Ajani JA, Xiao Q, Liao Z, Wang H, Gan B. The role of ferroptosis in ionizing radiation-induced cell death and tumor suppression. *Cell Res.* 2020 Feb;30(2):146-162. doi: 10.1038/s41422-019-0263-3. [PMC free article] [PubMed]
42. Zhao J, Zang F, Huo X, Zheng S. Novel approaches targeting ferroptosis in treatment of glioma. *Front Neurol.* 2023;14():1292160. doi: 10.3389/fneur.2023.1292160. [PMC free article] [PubMed]
43. Mitre AO, Florian AI, Buruiana A, Boer A, Moldovan I, Soritau O, Florian SI, Susman S. Ferroptosis Involvement in Glioblastoma Treatment. *Medicina (Kaunas).* 2022 Feb 20;58(2):. doi: 10.3390/medicina58020319. [PMC free article] [PubMed]
44. Shi J, Yang N, Han M, Qiu C. Emerging roles of ferroptosis in glioma. *Front Oncol.* 2022;12():993316. doi: 10.3389/fonc.2022.993316. [PMC free article] [PubMed]
45. Ingold I, Berndt C, Schmitt S, Doll S, Poschmann G, Buday K, Roveri A, Peng X, Porto Freitas F, Seibt T, Mehr L, Aichler M, Walch A, Lamp D, Jastroch M, Miyamoto S, Wurst W, Ursini F, Arnér ESJ, Fradejas-Villar N, Schweizer U, Zischka H, Friedmann Angeli JP, Conrad M. Selenium Utilization by GPX4 Is Required to Prevent Hydroperoxide-Induced Ferroptosis. *Cell.* 2018 Jan 25;172(3):409-422.e21. doi: 10.1016/j.cell.2017.11.048. [PubMed]
46. Goji T, Takahara K, Negishi M, Katoh H. Cystine uptake through the cystine/glutamate antiporter xCT triggers glioblastoma cell death under glucose deprivation. *J Biol Chem.* 2017 Dec 12;292(48):19721-19732. doi: 10.1074/jbc.M117.814392. [PMC free article] [PubMed]
47. Song L, Wu J, Fu H, Wu C, Tong X, Zhang M. Abnormally Expressed Ferroptosis-Associated FANCD2 in Mediating the Temozolomide Resistance and Immune Response in Glioblastoma. *Front Pharmacol.* 2022;13():921963. doi: 10.3389/fphar.2022.921963. [PMC free article] [PubMed]
48. Zhuo S, Chen Z, Yang Y, Zhang J, Tang J, Yang K. Clinical and Biological Significances of a Ferroptosis-Related Gene Signature in Glioma. *Front Oncol.* 2020;10():590861. doi: 10.3389/fonc.2020.590861. [PMC free article] [PubMed]
49. Nie XH, Qiu S, Xing Y, Xu J, Lu B, Zhao SF, Li YT, Su ZZ. Paeoniflorin Regulates NEDD4L/STAT3 Pathway to Induce Ferroptosis in Human Glioma Cells. *J Oncol.* 2022;2022():6093216. doi: 10.1155/2022/6093216. [PMC free article] [PubMed]
50. Liu HJ, Hu HM, Li GZ, Zhang Y, Wu F, Liu X, Wang KY, Zhang CB, Jiang T. Ferroptosis-Related Gene Signature Predicts Glioma Cell Death and Glioma Patient Progression. *Front Cell Dev Biol.* 2020;8():538. doi: 10.3389/fcell.2020.00538. [PMC free article] [PubMed]

51. Chen Z, Wu T, Yan Z, Zhang M. Identification and Validation of an 11-Ferroptosis Related Gene Signature and Its Correlation With Immune Checkpoint Molecules in Glioma. *Front Cell Dev Biol.* 2021(19):652599. doi: 10.3389/fcell.2021.652599. [PMC free article] [PubMed]
52. Hu Y, Tu Z, Lei K, Huang K, Zhu X. Ferroptosis-related gene signature correlates with the tumor immune features and predicts the prognosis of glioma patients. *Biosci Rep.* 2021 Dec 22;41(12):. doi: 10.1042/BSR20211640. [PMC free article] [PubMed]
53. Peng X, Liu C, Li J, Bao Z, Huang T, Zeng L, He Q, Xue D. A novel 25-ferroptosis-related gene signature for the prognosis of gliomas. *Front Oncol.* 2023;13(1):1128278. doi: 10.3389/fonc.2023.1128278. [PMC free article] [PubMed]
54. Wang X, Zhang H, Zhang M, Zhang X, Mao W, Gao M. Proteogenomic characterization of ferroptosis regulators reveals therapeutic potential in glioblastoma. *BMC Cancer.* 2023 May 8;23(1):415. doi: 10.1186/s12885-023-10894-3. [PMC free article] [PubMed]
55. Zuo Z, Liu W, Zeng Y, Fan X, Li L, Chen J, Zhou X, Jiang Y, Yang X, Feng Y, Lu Y. Multiparametric magnetic resonance imaging-derived deep learning network to determine ferroptosis-related gene signatures in gliomas. *Front Neurosci.* 2022;16(10):1082867. doi: 10.3389/fnins.2022.1082867. [PMC free article] [PubMed]
56. Xiao D, Zhou Y, Wang X, Zhao H, Nie C, Jiang X. A Ferroptosis-Related Prognostic Risk Score Model to Predict Clinical Significance and Immunogenic Characteristics in Glioblastoma Multiforme. *Oxid Med Cell Longev.* 2021;2021(9):9107857. doi: 10.1155/2021/9107857. [PMC free article] [PubMed]
57. Sun W, Yan J, Ma H, Wu J, Zhang Y. Autophagy-Dependent Ferroptosis-Related Signature is Closely Associated with the Prognosis and Tumor Immune Escape of Patients with Glioma. *Int J Gen Med.* 2022;15(2):253-270. doi: 10.2147/IJGM.S343046. [PMC free article] [PubMed]
58. Cai Y, Liang X, Zhan Z, Zeng Y, Lin J, Xu A, Xue S, Xu W, Chai P, Mao Y, Song Z, Han L, Xiao J, Song Y, Zhang X. A Ferroptosis-Related Gene Prognostic Index to Predict Temozolomide Sensitivity and Immune Checkpoint Inhibitor Response for Glioma. *Front Cell Dev Biol.* 2021(19):812422. doi: 10.3389/fcell.2021.812422. [PMC free article] [PubMed]
59. Huang L, Zhang J, Gong F, Han Y, Huang X, Luo W, Cai H, Zhang F. Identification and validation of ferroptosis-related lncRNA signatures as a novel prognostic model for glioma. *Front Genet.* 2022;13(9):927142. doi: 10.3389/fgene.2022.927142. [PMC free article] [PubMed]
60. Zhang X, Li X, Zheng C, Yang C, Zhang R, Wang A, Feng J, Hu X, Chang S, Zhang H. Ferroptosis, a new form of cell death defined after radiation exposure. *Int J Radiat Biol.* 2022;98(7):1201-1209. doi: 10.1080/09553002.2022.2020358. [PubMed]
61. Tong S, Ye L, Xu Y, Sun Q, Gao L, Cai J, Ye Z, Tian D, Chen Q. IRF2-ferroptosis related gene is associated with prognosis and EMT in gliomas. *Transl Oncol.* 2022 Dec;26(12):101544. doi: 10.1016/j.tranon.2022.101544. [PMC free article] [PubMed]
62. Feng S, Liang X, Li J, Wang Z, Zhang H, Dai Z, Luo P, Liu Z, Zhang J, Xiao X, Cheng Q. Immunogenic cell death related risk model to delineate ferroptosis pathway and predict immunotherapy response of patients with GBM. *Front Immunol.* 2022;13(9):92855. doi: 10.3389/fimmu.2022.92855. [PMC free article] [PubMed]
63. Su J, Li Y, Liu Q, Peng G, Qin C, Li Y. Identification of SSBP1 as a ferroptosis-related biomarker of glioblastoma based on a novel mitochondria-related gene risk model and in vitro experiments. *J Transl Med.* 2022 Sep 30;20(1):440. doi: 10.1186/s12967-022-03657-4. [PMC free article] [PubMed]
64. Wu Y, Liu L, Li Z, Zhang T, Wang Q, Cheng M. A Risk Model Based on Ferroptosis-Related Genes OSMR, G0S2, IGF1BP6, IGHG2, and FMOD Predicts Prognosis in Glioblastoma Multiforme. *CNS Neurosci Ther.* 2025 Jan;31(1):e70161. doi: 10.1111/cns.70161. [PMC free article] [PubMed]
65. Lv Y, Gao Y, Di W, Li Z, Shi Y, Hou T, Chen Y, Tian J, Xu M, Su W, Zhang M, Zhong J. MFAP4 is a novel prognostic biomarker in glioma correlating with immunotherapy resistance and ferroptosis. *Front Pharmacol.* 2025;16(1):1551863. doi: 10.3389/fphar.2025.1551863. [PMC free article] [PubMed]
66. Clavreul A, Guette C, Lasla H, Rousseau A, Blanchet O, Henry C, Boissard A, Cherel M, Jézéquel P, Guillonnet F, Menei P, Lemée JM. Proteomics of tumor and serum samples from isocitrate dehydrogenase-wildtype glioblastoma patients: is the detoxification of reactive oxygen species associated with shorter survival? *Mol Oncol.* 2024 Nov;18(11):2783-2800. doi: 10.1002/1878-0261.13668. [PMC free article] [PubMed]
67. Xu Z, Chen X, Song L, Yuan F, Yan Y. Matrix Remodeling-Associated Protein 8 as a Novel Indicator Contributing to Glioma Immune Response by Regulating Ferroptosis. *Front Immunol.* 2022;13(8):834595. doi: 10.3389/fimmu.2022.834595. [PMC free article] [PubMed]
68. Li X, Zhang W, Xing Z, Hu S, Zhang G, Wang T, Wang T, Fan Q, Chen G, Cheng J, Jiang X, Cai R. Targeting SIRT3 sensitizes glioblastoma to ferroptosis by promoting mitophagy and inhibiting SLC7A11. *Cell Death Dis.* 2024 Feb 23;15(2):168. doi: 10.1038/s41419-024-06558-0. [PMC free article] [PubMed]
69. Chen Q, Wang W, Chen S, Chen X, Lin Y. miR-29a sensitizes the response of glioma cells to temozolomide by modulating the P53/MDM2 feedback loop. *Cell Mol Biol Lett.* 2021 May 27;26(1):21. doi: 10.1186/s11658-021-00266-9. [PMC free article] [PubMed]
70. Qu S, Qi S, Zhang H, Li Z, Wang K, Zhu T, Ye R, Zhang W, Huang G, Yi GZ. Albumin-bound paclitaxel augment temozolomide treatment sensitivity of glioblastoma cells by disrupting DNA damage repair and promoting ferroptosis. *J Exp Clin Cancer Res.* 2023 Oct 28;42(1):285. doi: 10.1186/s13046-023-02843-6. [PMC free article] [PubMed]
71. Zhu Y, Niu X, Ding C, Lin Y, Fang W, Yan L, Cheng J, Zou J, Tian Y, Huang W, Huang W, Pan Y, Wu T, Chen X, Kang D. Carrier-Free Self-Assembly Nano-Sonosensitizers for Sonodynamic-Amplified Cuproptosis-Ferroptosis in Glioblastoma Therapy. *Adv Sci (Weinh).* 2024 Jun;11(23):e2402516. doi: 10.1002/advs.202402516. [PMC free article] [PubMed]
72. Wang X, Shi W, Li M, Xin Y, Jiang X. RSL3 sensitizes glioma cells to ionizing radiation by suppressing TGM2-dependent DNA damage repair and epithelial-mesenchymal transition. *Redox Biol.* 2024 Dec;78(1):103438. doi: 10.1016/j.redox.2024.103438. [PMC free article] [PubMed]
73. Shao G, Cui X, Wang Y, Luo S, Li C, Jiang Y, Cai D, Li N, Li X. Targeting MS4A4A: A novel pathway to improve immunotherapy responses in glioblastoma. *CNS Neurosci Ther.* 2024 Jul;30(7):e14791. doi: 10.1111/cns.14791. [PMC free article] [PubMed]
74. Liu B, Ji Q, Cheng Y, Liu M, Zhang B, Mei Q, Liu D, Zhou S. Biomimetic GBM-targeted drug delivery system boosting ferroptosis for immunotherapy of orthotopic drug-resistant GBM. *J Nanobiotechnology.* 2022 Mar 27;20(1):161. doi: 10.1186/s12951-022-01360-6. [PMC free article] [PubMed]
75. D'Aprile S, Denaro S, Lavoro A, Candido S, Giallongo S, Torrisi F, Salvatorelli L, Lazzarino G, Amorini AM, Lazzarino G, Magro G, Tibullo D, Libra M, Giallongo C, Vicario N, Parenti R. Glioblastoma mesenchymal subtype enhances antioxidant defence to reduce susceptibility to ferroptosis. *Sci Rep.* 2024 Sep 5;14(1):20770. doi: 10.1038/s41598-024-72024-8. [PMC free article] [PubMed]
76. Ye L, Xu Y, Wang L, Zhang C, Hu P, Tong S, Liu Z, Tian D. Downregulation of CYP2E1 is associated with poor prognosis and tumor progression of gliomas. *Cancer Med.* 2021 Nov;10(22):8100-8113. doi: 10.1002/cam4.4320. [PMC free article] [PubMed]
77. Van Loenhout J, Freire Boulosa L, Quatannens D, De Waele J, Merlin C, Lambrechts H, Lau HW, Hermans C, Lin A, Lardon F, Peeters M, Bogaerts A, Smits E, Deben C. Auranofin and Cold Atmospheric Plasma Synergize to Trigger Distinct Cell Death Mechanisms and Immunogenic Responses in Glioblastoma. *Cells.* 2021 Oct 28;10(11):. doi: 10.3390/cells10112936. [PMC free article] [PubMed]
78. Moujalled D, Southon AG, Saleh E, Brinkmann K, Ke F, Iliopoulos M, Cross RS, Jenkins MR, Nhu D, Wang Z, Shi MX, Kluck RM, Lessene G, Grabow S, Bush AI, Strasser A. BH3 mimetic drugs cooperate with Temozolomide, JQ1 and inducers of ferroptosis in killing glioblastoma multiforme cells. *Cell Death Differ.* 2022 Jul;29(7):1335-1348. doi: 10.1038/s41418-022-00977-2. [PMC free article] [PubMed]
79. Su IC, Su YK, Setiawan SA, Yadav VK, Fong IH, Yeh CT, Lin CM, Liu HW. NADPH Oxidase Subunit CYBB Confers Chemotherapy and Ferroptosis Resistance in Mesenchymal Glioblastoma via Nrf2/SOD2 Modulation. *Int J Mol Sci.* 2023 Apr 22;24(9):. doi: 10.3390/ijms24097706. [PMC free article] [PubMed]
80. Zhou Y, Qian W, Li X, Wei W. NF- κ B Inhibitor Myrisignan Induces Ferroptosis of Glioblastoma Cells via Regulating Epithelial-Mesenchymal Transformation in a Slug-Dependent Manner. *Oxid Med Cell Longev.* 2023;2023(1):7098313. doi: 10.1155/2023/7098313. [PMC free article] [PubMed]
81. Jiang Y, Zhao J, Li R, Liu Y, Zhou L, Wang C, Lv C, Gao L, Cui D. CircLRFN5 inhibits the progression of glioblastoma via PRRX2/GCH1 mediated ferroptosis. *J Exp Clin Cancer Res.* 2022 Oct 20;41(1):307. doi: 10.1186/s13046-022-02518-8. [PMC free article] [PubMed]
82. Xia L, Gong M, Zou Y, Wang Z, Wu B, Zhang S, Li L, Jin K, Sun C. Apatinib Induces Ferroptosis of Glioma Cells through Modulation of the VEGFR2/Nrf2 Pathway. *Oxid Med Cell Longev.* 2022;2022(9):925919. doi: 10.1155/2022/925919. [PMC free article] [PubMed]
83. Zhang K, Wu Y, Chen G, Wang H, Liu Y, Zhou Y. Heat shock protein 27 deficiency promotes ferrous ion absorption and enhances acyl-Coenzyme A synthetase

- long-chain family member 4 stability to promote glioblastoma cell ferroptosis. *Cancer Cell Int.* 2023 Jan 1323(1):5. doi: 10.1186/s12935-023-02848-3. [\[PMC free article\]](#) [\[PubMed\]](#)
84. Liang X, Wang G, Xue C, Zhou Y. RBMS1 interference inhibits malignant progression of glioblastoma cells and promotes ferroptosis. *Discov Oncol.* 2024 Oct 1115(1):548. doi: 10.1007/s12672-024-01430-1. [\[PMC free article\]](#) [\[PubMed\]](#)
 85. Carvalho SM, Mansur AAP, da Silveira IB, Pires TFS, Victória HFV, Krambrock K, Leite MF, Mansur HS. Nanozymes with Peroxidase-like Activity for Ferroptosis-Driven Biocatalytic Nanotherapeutics of Glioblastoma Cancer: 2D and 3D Spheroids Models. *Pharmaceutics.* 2023 Jun 1015(6):. doi: 10.3390/pharmaceutics15061702. [\[PMC free article\]](#) [\[PubMed\]](#)
 86. Miki K, Yagi M, Noguchi N, Do Y, Otsuji R, Kuga D, Kang D, Yoshimoto K, Uchiumi T. Induction of glioblastoma cell ferroptosis using combined treatment with chloramphenicol and 2-deoxy-D-glucose. *Sci Rep.* 2023 Jun 2813(1):10497. doi: 10.1038/s41598-023-37483-5. [\[PMC free article\]](#) [\[PubMed\]](#)
 87. Wang H, Zhao P, Zhang Y, Chen Z, Bao H, Qian W, Wu J, Xing Z, Hu X, Jin K, Zhuge Q, Yang J. NeuroD4 converts glioblastoma cells into neuron-like cells through the SLC7A11-GSH-GPX4 antioxidant axis. *Cell Death Discov.* 2023 Aug 159(1):297. doi: 10.1038/s41420-023-01595-8. [\[PMC free article\]](#) [\[PubMed\]](#)
 88. Liu Y, Duan X, Zhang C, Yuan J, Wen J, Zheng C, Shi J, Yuan M. KAT6B May Be Applied as a Potential Therapeutic Target for Glioma. *J Oncol.* 20222022(2):2500092. doi: 10.1155/2022/2500092. [\[PMC free article\]](#) [\[PubMed\]](#)
 89. Wang C, Zhang M, Liu Y, Cui D, Gao L, Jiang Y. CircRNF10 triggers a positive feedback loop to facilitate progression of glioblastoma via redeploying the ferroptosis defense in GSCs. *J Exp Clin Cancer Res.* 2023 Sep 1942(1):242. doi: 10.1186/s13046-023-02816-9. [\[PMC free article\]](#) [\[PubMed\]](#)
 90. Yang YH, Li W, Ren LW, Yang H, Zhang YZ, Zhang S, Hao Y, Yu DK, Tong RS, Du GH, Shi JY, Wang JH. S670, an amide derivative of 3-O-acetyl-11-keto- β -boswellic acid, induces ferroptosis in human glioblastoma cells by generating ROS and inhibiting STX17-mediated fusion of autophagosome and lysosome. *Acta Pharmacol Sin.* 2024 Jan45(1):209-222. doi: 10.1038/s41401-023-01157-9. [\[PMC free article\]](#) [\[PubMed\]](#)
 91. Moses A, Malek R, Kendirli MT, Cheung P, Landry M, Herrera-Barrera M, Khojasteh A, Granucci M, Bukhari SA, Hooper JE, Hayden-Gephart M, Dixon SJ, Recht LD, Beinat C. Monitoring of cancer ferroptosis with [(18)F]hGTS13, a system xc- specific radiotracer. *Theranostics.* 202515(3):836-849. doi: 10.7150/tno.101882. [\[PMC free article\]](#) [\[PubMed\]](#)
 92. Dumitru CA, Schröder H, Schäfer FTA, Aust JF, Kreße N, Siebert CLR, Stein KP, Haghikia A, Wilkens L, Mawrin C, Sandalcioglu IE. Progesterone Receptor Membrane Component 1 (PGRMC1) Modulates Tumour Progression, the Immune Microenvironment and the Response to Therapy in Glioblastoma. *Cells.* 2023 Oct 2012(20):. doi: 10.3390/cells12202498. [\[PMC free article\]](#) [\[PubMed\]](#)
 93. Stringer BW, De Silva MI, Greenberg Z, Noreña Puerta A, Adams R, Milky B, Zabolocki M, van den Hurk M, Ebert LM, Fairly Bishop C, Conn SJ, Kichenadasse G, Michael MZ, Ormsby RJ, Poonoose S, Bardy C. Human cerebrospinal fluid affects chemoradiotherapy sensitivities in tumor cells from patients with glioblastoma. *Sci Adv.* 2023 Oct 279(43):eadf1332. doi: 10.1126/sciadv.adf1332. [\[PMC free article\]](#) [\[PubMed\]](#)
 94. Williams CH, Neitzel LR, Cornell J, Rea S, Mills I, Silver MS, Ahmad JD, Birukov KG, Birukova A, Brem H, Tyler B, Bar EE, Hong CC. GPR68-ATF4 signaling is a novel prosurvival pathway in glioblastoma activated by acidic extracellular microenvironment. *Exp Hematol Oncol.* 2024 Jan 3113(1):13. doi: 10.1186/s40164-023-00468-1. [\[PMC free article\]](#) [\[PubMed\]](#)
 95. Deng L, Di Y, Chen C, Xia J, Lei B, Li N, Zhang Q. Depletion of the N(6)-Methyladenosine (m6A) reader protein IGF2BP3 induces ferroptosis in glioma by modulating the expression of GPX4. *Cell Death Dis.* 2024 Mar 115(3):181. doi: 10.1038/s41419-024-06486-z. [\[PMC free article\]](#) [\[PubMed\]](#)
 96. Guo F, Ling G, Qiu J, Li J, Gan Y, Yu Y, Tang J, Mo L, Piao H. Juglone induces ferroptosis in glioblastoma cells by inhibiting the Nrf2-GPX4 axis through the phosphorylation of p38MAPK. *Chin Med.* 2024 Mar 2219(1):52. doi: 10.1186/s13020-024-00920-2. [\[PMC free article\]](#) [\[PubMed\]](#)
 97. Liang B, Ding X, Yang S, Feng E. Endothelial cell ferroptosis influences IDH wild-type glioblastoma growth in recurrent glioblastoma multiforme patients. *Braz J Med Biol Res.* 202457(1):e13961. doi: 10.1590/1414-431X2024e13961. [\[PMC free article\]](#) [\[PubMed\]](#)
 98. Neitzel LR, Fuller DT, Williams CH, Hong CC. Inhibition of GPR68 kills glioblastoma in zebrafish xenograft models. *BMC Res Notes.* 2024 Aug 2317(1):235. doi: 10.1186/s13104-024-06900-x. [\[PMC free article\]](#) [\[PubMed\]](#)
 99. Abu-Serie MM, Osuka S, Heikal LA, Teleb M, Barakat A, Dudeja V. Diethyldithiocarbamate-ferrous oxide nanoparticles inhibit human and mouse glioblastoma stemness: aldehyde dehydrogenase 1A1 suppression and ferroptosis induction. *Front Pharmacol.* 202415(1):1363511. doi: 10.3389/fphar.2024.1363511. [\[PMC free article\]](#) [\[PubMed\]](#)
 100. Mansuer M, Zhou L, Wang C, Gao L, Jiang Y. Erianin induces ferroptosis in GSCs via REST/LRSAM1 mediated SLC40A1 ubiquitination to overcome TMZ resistance. *Cell Death Dis.* 2024 Jul 2215(7):522. doi: 10.1038/s41419-024-06902-4. [\[PMC free article\]](#) [\[PubMed\]](#)
 101. Cao W, He Y, Lan J, Luo S, Sun B, Xiao C, Yu W, Zeng Z, Lei S. FOXP3 promote the progression of glioblastoma via inhibiting ferroptosis mediated by linc00857/miR-1290/GPX4 axis. *Cell Death Dis.* 2024 Apr 115(4):239. doi: 10.1038/s41419-024-06619-4. [\[PMC free article\]](#) [\[PubMed\]](#)
 102. Lu T, Yee PP, Chih SY, Tang M, Chen H, Aregawi DG, Glantz MJ, Zacharia BE, Wang HG, Li W. LC3-associated phagocytosis of neutrophils triggers tumor ferroptotic cell death in glioblastoma. *EMBO J.* 2024 Jul43(13):2582-2605. doi: 10.1038/s44318-024-00130-4. [\[PMC free article\]](#) [\[PubMed\]](#)
 103. Chen H, Huang J, Wang H, Xu Y, Chen J, Deng T, Su Z, Lin R, Huang C, Wu J. Multifunctional liposome boosts glioma ferroptosis and immunotherapy through reinforcement of chemo-dynamic therapy strategy. *Mater Today Bio.* 2025 Apr31(1):101521. doi: 10.1016/j.mtbio.2025.101521. [\[PMC free article\]](#) [\[PubMed\]](#)
 104. Jamali AW, Zhanzhan Z, Sun B, Song Z, Mehmood A, Liu L. The role of ALKBH5 in regulating proliferation and invasion in U251 glioblastoma cells. *Contemp Oncol (Pozn).* 202529(2):195-205. doi: 10.5114/wo.2025.150649. [\[PMC free article\]](#) [\[PubMed\]](#)
 105. Liu T, Zhu C, Chen X, Guan G, Zou C, Shen S, Wu J, Wang Y, Lin Z, Chen L, Cheng P, Cheng W, Wu A. Ferroptosis, as the most enriched programmed cell death process in glioma, induces immunosuppression and immunotherapy resistance. *Neuro Oncol.* 2022 Jul 124(7):1113-1125. doi: 10.1093/neuonc/noac033. [\[PMC free article\]](#) [\[PubMed\]](#)
 106. Xie Y, Xiao Y, Liu Y, Lu X, Wang Z, Sun S, Liu L, Tang X, Xiao H, Liu H. Construction of a novel radiosensitivity- and ferroptosis-associated gene signature for prognosis prediction in gliomas. *J Cancer.* 202213(8):2683-2693. doi: 10.7150/jca.72893. [\[PMC free article\]](#) [\[PubMed\]](#)
 107. Xu P, Ge FH, Li WX, Xu Z, Wang XL, Shen JL, Xu AB, Hao RR. MicroRNA-147a Targets SLC40A1 to Induce Ferroptosis in Human Glioblastoma. *Anal Cell Pathol (Amst).* 20222022(1):2843990. doi: 10.1155/2022/2843990. [\[PMC free article\]](#) [\[PubMed\]](#)
 108. Yao L, Li J, Zhang X, Zhou L, Hu K. Downregulated ferroptosis-related gene SQLE facilitates temozolomide chemoresistance, and invasion and affects immune regulation in glioblastoma. *CNS Neurosci Ther.* 2022 Dec28(12):2104-2115. doi: 10.1111/cns.13945. [\[PMC free article\]](#) [\[PubMed\]](#)
 109. Liu X, Cao Z, Wang W, Zou C, Wang Y, Pan L, Jia B, Zhang K, Zhang W, Li W, Hao Q, Zhang Y, Zhang W, Xue X, Lin W, Li M, Gu J. Engineered Extracellular Vesicle-Delivered CRISPR/Cas9 for Radiotherapy Sensitization of Glioblastoma. *ACS Nano.* 2023 Sep 1217(17):16432-16447. doi: 10.1021/acsnano.2c12857. [\[PMC free article\]](#) [\[PubMed\]](#)
 110. Ye R, Zhang W, Zhang H, Qu S, Xu J, Xu R, Zhu Y, Huang G, Zhang XA, Yi GZ. The HBP Pathway Inhibitor FR054 Enhances Temozolomide Sensitivity in Glioblastoma Cells by Promoting Ferroptosis and Inhibiting O-GlcNAcylation. *CNS Neurosci Ther.* 2025 Aug31(8):e70546. doi: 10.1111/cns.70546. [\[PMC free article\]](#) [\[PubMed\]](#)
 111. Liu S, Sun K, Li M, Liu X, Wang P, Li M, Peng B, Wang B, Chang YX, Yu XA. Quadruple synergistic amplification of ferroptosis for precision glioblastoma therapy: a luteolin-coordinated ferric ion nanoplatfrom. *J Nanobiotechnology.* 2025 Sep 2523(1):605. doi: 10.1186/s12951-025-03688-1. [\[PMC free article\]](#) [\[PubMed\]](#)
 112. Piotrowsky A, Burkard M, Hammerschmidt K, Ruple HK, Nonnenmacher P, Schumacher M, Leischner C, Berchtold S, Marongiu L, Kufer TA, Lauer UM, Renner O, Venturelli S. Analysis of High-Dose Ascorbate-Induced Cytotoxicity in Human Glioblastoma Cells and the Role of Dehydroascorbic Acid and Iron. *Antioxidants (Basel).* 2024 Sep 1013(9):. doi: 10.3390/antiox13091095. [\[PMC free article\]](#) [\[PubMed\]](#)
 113. Quijano-Rubio C, Silginer M, Weller M. CD95 gene deletion may reduce clonogenic growth and invasiveness of human glioblastoma cells in a CD95 ligand-independent manner. *Cell Death Discov.* 2022 Jul 298(1):341. doi: 10.1038/s41420-022-01133-y. [\[PMC free article\]](#) [\[PubMed\]](#)

114. Richards DM, Merz C, Gieffers C, Krendyukov A. CD95L and Anti-Tumor Immune Response: Current Understanding and New Evidence. *Cancer Manag Res*. 2021;13(1):2477-2482. doi: 10.2147/CMAR.S297499. [PMC free article] [PubMed]
115. Wisniewski P, Ellert-Miklaszewska A, Kwiatkowska A, Kaminska B. Non-apoptotic Fas signaling regulates invasiveness of glioma cells and modulates MMP-2 activity via NFkappaB-TIMP-2 pathway. *Cell Signal*. 2010 Feb;22(2):212-20. doi: 10.1016/j.cellsig.2009.09.016. [PubMed]
116. Ferguson TA, Griffith TS. A vision of cell death: insights into immune privilege. *Immunol Rev*. 1997 Apr;156(1):167-84. doi: 10.1111/j.1600-065x.1997.tb00967.x. [PubMed]
117. Motz GT, Santoro SP, Wang LP, Garrabrant T, Lastra RR, Hagemann IS, Lal P, Feldman MD, Benencia F, Coukos G. Tumor endothelium FasL establishes a selective immune barrier promoting tolerance in tumors. *Nat Med*. 2014 Jun;20(6):607-15. doi: 10.1038/nm.3541. [PMC free article] [PubMed]
118. Fujita H, Koji T, Kitagawa N, Tsutsumi K, Abe K, Kaminogo M, Shibata S. Possible involvement of Fas system in the induction of apoptosis in human astrocytic brain tumors. *Cell Mol Neurobiol*. 2002 Aug;22(4):393-406. doi: 10.1023/a:1021007503779. [PMC free article] [PubMed]
119. Tausin S, Debure L, Moreau JF, Legembre P. CD95-mediated cell signaling in cancer: mutations and post-translational modulations. *Cell Mol Life Sci*. 2012 Apr;69(8):1261-77. doi: 10.1007/s00018-011-0866-4. [PMC free article] [PubMed]
120. Zhang Y, Jin T, Dou Z, Wei B, Zhang B, Sun C. The dual role of the CD95 and CD95L signaling pathway in glioblastoma. *Front Immunol*. 2022;13(10):29737. doi: 10.3389/fimmu.2022.1029737. [PMC free article] [PubMed]
121. Nie Q, Chen W, Zhang T, Ye S, Ren Z, Zhang P, Wen J. Iron oxide nanoparticles induce ferroptosis via the autophagic pathway by synergistic bundling with paclitaxel. *Mol Med Rep*. 2023 Oct;28(4):. doi: 10.3892/mmr.2023.13085. [PMC free article] [PubMed]
122. Stockwell BR, Friedmann Angeli JP, Bayir H, Bush AI, Conrad M, Dixon SJ, Fulda S, Gascón S, Hatzios SK, Kagan VE, Noel K, Jiang X, Linkermann A, Murphy ME, Overholzer M, Oyagi A, Pagnussat GC, Park J, Ran Q, Rosenfeld CS, Salnikow K, Tang D, Torti FM, Torti SV, Toyokuni S, Woerpel KA, Zhang DD. Ferroptosis: A Regulated Cell Death Nexus Linking Metabolism, Redox Biology, and Disease. *Cell*. 2017 Oct;151(2):273-285. doi: 10.1016/j.cell.2017.09.021. [PMC free article] [PubMed]
123. Zhang C, Liu X, Jin S, Chen Y, Guo R. Ferroptosis in cancer therapy: a novel approach to reversing drug resistance. *Mol Cancer*. 2022 Feb;21(1):47. doi: 10.1186/s12943-022-01530-y. [PMC free article] [PubMed]
124. Gao M, Monian P, Quadri N, Ramasamy R, Jiang X. Glutaminolysis and Transferrin Regulate Ferroptosis. *Mol Cell*. 2015 Jul;59(2):298-308. doi: 10.1016/j.molcel.2015.06.011. [PMC free article] [PubMed]
125. Li M, Wang ZW, Fang LJ, Cheng SQ, Wang X, Liu NF. Programmed cell death in atherosclerosis and vascular calcification. *Cell Death Dis*. 2022 May;13(5):467. doi: 10.1038/s41419-022-04923-5. [PMC free article] [PubMed]
126. Yao Y, Ji P, Chen H, Ge J, Xu Y, Wang P, Xu L, Yan Z. Ferroptosis-based drug delivery system as a new therapeutic opportunity for brain tumors. *Front Oncol*. 2023;13(10):1084289. doi: 10.3389/fonc.2023.1084289. [PMC free article] [PubMed]
127. Battaglia AM, Sacco A, Perrotta ID, Faniello MC, Scalise M, Torella D, Levi S, Costanzo F, Biamonte F. Iron Administration Overcomes Resistance to Erastin-Mediated Ferroptosis in Ovarian Cancer Cells. *Front Oncol*. 2022;12(10):868351. doi: 10.3389/fonc.2022.868351. [PMC free article] [PubMed]
128. Costa I, Barbosa DJ, Benfeito S, Silva V, Chavarria D, Borges F, Remião F, Silva R. Molecular mechanisms of ferroptosis and their involvement in brain diseases. *Pharmacol Ther*. 2023 Apr;244(10):108373. doi: 10.1016/j.pharmthera.2023.108373. [PubMed]
129. Chen X, Kang R, Kroemer G, Tang D. Broadening horizons: the role of ferroptosis in cancer. *Nat Rev Clin Oncol*. 2021 May;18(5):280-296. doi: 10.1038/s41571-020-00462-0. [PubMed]
130. Zhao H, Ji B, Chen J, Huang Q, Lu X. Gpx 4 is involved in the proliferation, migration and apoptosis of glioma cells. *Pathol Res Pract*. 2017 Jun;213(6):626-633. doi: 10.1016/j.prp.2017.04.025. [PubMed]
131. Yi R, Wang H, Deng C, Wang X, Yao L, Niu W, Fei M, Zhaba W. Dihydroartemisinin initiates ferroptosis in glioblastoma through GPX4 inhibition. *Biosci Rep*. 2020 Jun;20(6):. doi: 10.1042/BSR20193314. [PMC free article] [PubMed]
132. Sharma S, Carmona A, Skowronek A, Yu F, Collins MO, Naik S, Murzeau CM, Tseng PL, Erdmann KS. Apoptotic signalling targets the post-endocytic sorting machinery of the death receptor Fas/CD95. *Nat Commun*. 2019 Jul;10(1):3105. doi: 10.1038/s41467-019-11025-y. [PMC free article] [PubMed]
133. Rossin A, Durivault J, Chakhtoura-Feghali T, Lounnas N, Gagnoux-Palacios L, Hueber AO. Fas palmitoylation by the palmitoyl acyltransferase DHHC7 regulates Fas stability. *Cell Death Differ*. 2015 Apr;22(4):643-53. doi: 10.1038/cdd.2014.153. [PMC free article] [PubMed]
134. Hadji A, Ceppi P, Murrmann AE, Brockway S, Pattanayak A, Bhinder B, Hau A, De Chant S, Parimi V, Kolesza P, Richards J, Chandel N, Djabballah H, Peter ME. Death induced by CD95 or CD95 ligand elimination. *Cell Rep*. 2014 Apr;10(7):208-22. doi: 10.1016/j.celrep.2014.02.035. [PMC free article] [PubMed]
135. Muzio M, Chinnaiyan AM, Kischkel FC, O'Rourke K, Shevchenko A, Ni J, Scaffidi C, Bretz JD, Zhang M, Gentz R, Mann M, Krammer PH, Peter ME, Dixit VM. FLICE, a novel FADD-homologous ICE/CED-3-like protease, is recruited to the CD95 (Fas/APO-1) death-inducing signaling complex. *Cell*. 1996 Jun;148(6):817-27. doi: 10.1016/s0092-8674(00)81266-0. [PubMed]
136. Milhas D, Cuivillier O, Therville N, Clavé P, Thomsen M, Levade T, Benoist H, Ségui B. Caspase-10 triggers Bid cleavage and caspase cascade activation in FasL-induced apoptosis. *J Biol Chem*. 2005 May;280(20):19836-42. doi: 10.1074/jbc.M414358200. [PubMed]
137. Song JJ, Lee YJ. Differential cleavage of Mst1 by caspase-7/-3 is responsible for TRAIL-induced activation of the MAPK superfamily. *Cell Signal*. 2008 May;20(5):892-906. doi: 10.1016/j.cellsig.2008.01.001. [PMC free article] [PubMed]
138. Sánchez-Osuna M, Martínez-Escardó L, Granados-Colomina C, Martínez-Soler F, Pascual-Guiral S, Iglesias-Guimaraes V, Velasco R, Plans G, Vidal N, Tortosa A, Barcia C, Bruna J, Yuste VJ. An intrinsic DFF40/CAD endonuclease deficiency impairs oligonucleosomal DNA hydrolysis during caspase-dependent cell death: a common trait in human glioblastoma cells. *Neuro Oncol*. 2016 Jul;18(7):950-61. doi: 10.1093/neuonc/nov315. [PMC free article] [PubMed]
139. Shen Z, Liu T, Li Y, Lau J, Yang Z, Fan W, Zhou Z, Shi C, Ke C, Bregadze VI, Mandal SK, Liu Y, Li Z, Xue T, Zhu G, Munasinghe J, Niu G, Wu A, Chen X. Fenton-Reaction-Acceleratable Magnetic Nanoparticles for Ferroptosis Therapy of Orthotopic Brain Tumors. *ACS Nano*. 2018 Nov;12(11):11355-11365. doi: 10.1021/acsnano.8b06201. [PubMed]
140. Huo M, Wang L, Chen Y, Shi J. Tumor-selective catalytic nanomedicine by nanocatalyst delivery. *Nat Commun*. 2017 Aug;8(1):357. doi: 10.1038/s41467-017-00424-8. [PMC free article] [PubMed]
141. Alborzina H, Flórez AF, Kreth S, Brückner LM, Yildiz U, Gartlgruber M, Odoni DI, Poschet G, Garbowicz K, Shao C, Klein C, Meier J, Zeisberger P, Nadler-Holly M, Ziehm M, Paul F, Burhenne J, Bell E, Shaikhkarami M, Würth R, Stainczyk SA, Wecht EM, Kreth J, Büttner M, Ishaque N, Schlesner M, Nicke B, Stresmann C, Llamazares-Prada M, Reiling JH, Fischer M, Amit I, Selbach M, Herrmann C, Wölfl S, Henrich KO, Höfer T, Trumpp A, Westermann F. MYCN mediates cysteine addiction and sensitizes neuroblastoma to ferroptosis. *Nat Cancer*. 2022 Apr;3(4):471-485. doi: 10.1038/s43018-022-00355-4. [PMC free article] [PubMed]
142. Bao Z, Hua L, Ye Y, Wang D, Li C, Xie Q, Wakimoto H, Gong Y, Ji J. MEF2C silencing downregulates NF2 and E-cadherin and enhances Erastin-induced ferroptosis in meningioma. *Neuro Oncol*. 2021 Dec;23(12):2014-2027. doi: 10.1093/neuonc/noab114. [PMC free article] [PubMed]
143. Floros KV, Cai J, Jacob S, Kurupi R, Fairchild CK, Shende M, Coon CM, Powell KM, Belvin BR, Hu B, Puchalapalli M, Ramamoorthy S, Swift K, Lewis JP, Dozmorov MG, Glod J, Kobinski JE, Boikos SA, Faber AC. MYCN-Amplified Neuroblastoma Is Addicted to Iron and Vulnerable to Inhibition of the System Xc-/Glutathione Axis. *Cancer Res*. 2021 Apr;81(7):1896-1908. doi: 10.1158/0008-5472.CCR-20-1641. [PMC free article] [PubMed]
144. Wan S, Zhang G, Liu R, Abbas MN, Cui H. Pyroptosis, ferroptosis, and autophagy cross-talk in glioblastoma opens up new avenues for glioblastoma treatment. *Cell Commun Signal*. 2023 May;19(1):115. doi: 10.1186/s12964-023-01108-1. [PMC free article] [PubMed]
145. Zhou Y, Wu H, Wang F, Xu L, Yan Y, Tong X, Yan H. GPX7 Is Targeted by miR-29b and GPX7 Knockdown Enhances Ferroptosis Induced by Erastin in Glioma. *Front Oncol*. 2021;11(1):802124. doi: 10.3389/fonc.2021.802124. [PMC free article] [PubMed]

Annex 1: Methods

1.1 Approach

The search strategy was designed according to the PRISMA (Preferred Reporting Items for Systematic Reviews and Meta-Analyses) guidelines [1]. The systematic literature review was automatically generated on demand using the Synthory AI service. All components listed below were identified, extracted, assessed, and analyzed automatically as part of the review process. The review was created for research purposes.

1.2 Criteria of Inclusion and Exclusion

Inclusion criteria

- Publications available in PubMed and PubMed Central™.
- Publications related to ferroptosis, glioblastoma, and associated aspects.
- Primary research studies, including randomized controlled trials, cohort studies, and qualitative research.

Exclusion criteria

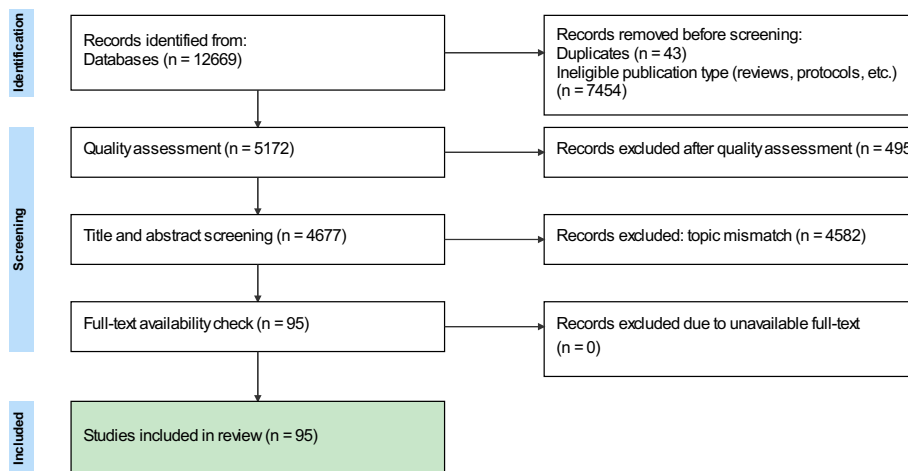
- Articles published before 2018/01.
- Systematic literature reviews, case series, case reports, expert opinions, study protocols, and any unidentified study types.
- Studies without full-text availability in PubMed or PubMed Central™.
- Articles that have been previously included and analyzed in existing reviews within the defined focus areas, to avoid duplication and ensure the inclusion of novel research findings.

1.3 Search Strategy and Screening Process

The topic of the request was 'Ferroptosis in glioblastoma'. The search employed 18 keywords. The search was conducted across the PubMed and PubMed Central™ databases, covering the publication period from 2018/01 to 2025/10.

1. Identification: 5172 records were retrieved from PubMed using the inclusion criteria.
2. Screening:
 - a. Articles were excluded based on the criteria.
 - b. Articles of low quality risk were excluded following an Article Quality Assessment.
3. Eligibility: Assessment of alignment with defined topics.

Figure 1. PRISMA 2020 Flow Diagram



A total of 95 articles were included in the final review, based on the inclusion and exclusion criteria.

- Ferroptosis and Immune Modulation: Mechanisms and Therapeutic Strategies in Glioblastoma – 7
- Ferroptosis in Glioblastoma: Pathways, Immune Interactions, and Overcoming Resistance – 86
- CD95 Gene Deletion: Reducing Malignancy in Glioblastoma Cells – 1
- Iron Oxide Nanoparticles and Paclitaxel: Inducing Ferroptosis via Autophagic Pathways in Glioblastoma – 1

1.4 Data extraction

Key study characteristics were extracted from the included articles. A predefined data extraction table was used to document details such as study design and key findings.

1.5 Quality Assessment

The quality of the included articles was assessed as follows:

1. The Newcastle-Ottawa Scale (NOS) was used to assess the quality of non-randomized and cohort studies [2].
2. The risk of bias assessment was used for randomized trials [3].

1.6 Analysis

The analysis proceeded in three phases:

- Phase 1: Identification of potential topics.
- Phase 2: Data extraction from relevant articles.

- Phase 3: Analysis of the relevance of new findings.

A hybrid generative and causal method was employed for data analysis and review generation, with OpenAI™ serving as the generative component. This method combines generative modeling with causal analysis, enhancing both the reliability and interpretability of the outcomes by accounting for underlying cause-effect relationships.

The approach facilitated the integration of various evidence types into a coherent summary. The review process included summarizing and interpreting findings, as well as discussing the limitations identified in the included articles.

[Back to 1. Methods](#)

Annex 2: Table 1. Signaling Networks and Subtype Transition in Glioblastoma

Study ID	Length of intervention	Population of intervention	Intervention	Intervention details	Primary outcome	Secondary outcome
Guo S et al. (2025)	72 hours	Nude mice aged 6–8 weeks, male and female, subcutaneous implantation of PDX tumor tissue cubes	Transfection of DNA constructs to overexpress FOSL1 tagged with GFP	Transfection performed at 50–75% cell confluency, lipofectamine 3000 reagent used, RNA extraction at 72 h using TRIzol reagent, overexpression assessed at 48 or 72 h post-transfection, studies conducted in triplicates	Role of FOSL1 in regulating biological processes and signaling networks during proneural to mesenchymal subtype transition in glioblastoma, including the identification of upregulated_genes and downregulated_genes.	Identification of 8 upregulated and 4 downregulated genes, pathway implications for glioblastoma prognosis
Li H et al. (2023)	15 days	Patients with GBM histologically diagnosed according to WHO classification, underwent surgical treatment in the Department of Neurosurgery, First Affiliated Hospital of Zhengzhou University	Overexpression and knockdown of FTL, overexpression of iPLA2 β lentiviruses, anti-PD-1 therapy	Lentiviruses constructed by Genechem and Obio Technology, transfected into THP-1-induced macrophages and RAW264.7 macrophages, anti-PD-1 Ab administered intravenously at 10 mg/kg 5 times every 3 days starting day 5 post-tumor injection, cells implanted into right corpus striatum using stereotactic frame at 0.25 μ L/min via micro-infusion syringe pump	FTL upregulation in TAMs promotes an immunosuppressive tumor microenvironment by inducing M2 polarization and facilitating glioblastoma progression	FTL inhibition reprograms the tumor microenvironment, attenuates glioma angiogenesis, promotes T cell recruitment, sensitizes glioma to anti-PD1 therapy
de Souza I et al. (2022)	24 hours, 48 hours, 72 hours, 120 hours, 10 days	Human glioma cell lines U251MG and T98G	Treatment of glioblastoma cells with temozolomide (TMZ), Erastin, RSL3, and Ferrostatin-1	Compounds dissolved in DMSO, applied to cultured cells in varying concentrations (5, 10, 20, 100 μ M), durations of 24 h, 48 h, 72 h, 120 h, and 10 days, cells plated in plates of varying sizes (12-well, 24-well, 35-mm dishes, 6-well), washed with PBS, fixed with paraformaldehyde or formaldehyde, stained with crystal violet or specific antibodies, analyzed using flow cytometers, fluorescence measured using GSH/GSSG Ratio Detection Assay Kit	NRF2's role in ferroptosis induction and its therapeutic potential in glioblastoma cells	Elevated NRF2 expression correlating with chemotherapy resistance, sensitivity to ferroptosis and GSH depletion upon system xc- blockage, NRF2 silencing reducing TMZ resistance and ferroptosis sensitivity, ABCC1 silencing increasing TMZ sensitivity and resistance to Erastin, positive correlation of NRF2 and ABCC1 expression with glioma aggressiveness, drug resistance, and poor survival

[Back to 2.1.1. Signaling Networks and Subtype Transition in Glioblastoma](#)

Annex 3: Table 2. Therapeutic Targets and Drug Interactions

Study ID	Length of intervention	Population of intervention	Control	Intervention	Intervention details	Primary outcome	Secondary outcome
Kyani A et al. (2018)	72 hours, 6 hours, 24 hours	Human glioblastoma cell lines U87MG, U118MG, NU04, A172		Treatment of cells with compounds including 35G8, NAC, Z-VAD-FMK, Necrostatin-1, H2O2, catalase, DTT	Cells seeded in 96-well plates, compounds added at specific time intervals, incubation at 37°C and 5% CO2, MTT assay performed for cell viability, PDI activity assessed via reduction reaction, thermal shift assay conducted using microplates and ThermoFluor instrument, Western blotting performed for protein analysis	Validation of PDI as a therapeutic target for glioblastoma, cytotoxicity of pyrimidotriazinedione 35G8	Upregulation of heme oxygenase 1 and SLC7A11, repression of TXNIP and EGR1, induction of autophagy and ferroptosis, activation of Nrf2 antioxidant response and ER stress response
Buccarelli M et al. (2018)	3 weeks	Adult patients with GBM tumors (WHO grade IV), underwent complete or partial surgical resection	Samples treated with vehicle alone	Application of chemical and drug treatments to GSCs, in vitro and in vivo models	Drugs include TMZ, QN, z-VAD-FMK, CA074, TRE, HCQ, calpain inhibitor I, Necrostatin-1, pepstatin A, DFO, ferrostatin 1, delivered in vitro in six-well microtiter plates or intraperitoneally in NOD-SCID mice, GFP-expressing GSCs resuspended in serum-free DMEM, in vitro treatments for 72h and 96h, in vivo treatments three to five times/week for 3 weeks, doses include TMZ 50 mg/kg, QN 10 mg/kg	Modulation of autophagy affects glioblastoma stem-like cell growth and survival, including GSC susceptibility to TMZ.	Induction of ferroptosis in glioblastoma stem-like cells, increased susceptibility to temozolomide
Zhao Z et al. (2023)	24 hours	Human GBM cell line U251 MG		Use of KLT injection for Coix treatment, TMZ treatment	Cells cultured in Dulbecco's Modified Eagle Medium under controlled conditions, seeded at 5000 cells/well in 96-well plates, treated with culture medium containing different concentrations of TMZ and Coix, KLT injection diluted to various concentrations, TMZ dissolved in sterilized water and diluted, incubated for 24 hours	Synergistic effect of Coix and TMZ in inhibiting Glioblastoma cells	Down-regulation of interferon-related genes, activation of ferroptosis, regulation of cholesterol metabolism pathway
Remy J et al. (2022)		Human GBM cell lines A172, MZ-18, MZ-54, MZ-256, MZ-304, U87-MG, U251-MG, U343-MG, U373-MG, LN229, murine GBM cell lines Tu2449 and Tu-9648, GSC lines PB1, FPW1, MN1, RKI1, RN1, MMK1, NCH1425, NCH601, NCH644, NCH421k	Non-mammalian targeting control shRNA	Genetic manipulation via Crispr/Cas9 knockouts, shRNA-mediated STAT3 knockdown, stable expression of mRFP-GFP-MAP1LC3B	Cells cultured in DMEM GlutaMAX with 10% FBS, transfection using Lipofectamine 3000, plasmid cloning into px459 vector, viral transduction with lentiviral supernatant, selection with puromycin and G418, scratch assays performed with Mitomycin C treatment, incubation in humidified incubator at 37°C and 5% CO2	Enhanced cell survival in glioblastoma cells upon STAT3 depletion under Pimozide treatment, demonstrating STAT3's role in lysosomal membrane permeabilization and vulnerability	Influence of STAT3 on autophagy pathways, potential use of STAT3 as a treatment predictor for apoptosis-resistant cancers

[Back to 2.1.2. Therapeutic Targets and Drug Interactions](#)

Annex 4: Table 3. Mechanisms of Ferroptosis in Glioblastoma

Study ID	Length of intervention	Population of intervention	Control	Intervention	Intervention details	Primary outcome	Secondary outcome
Chen Y et al. (2019)	14 days	Patients with malignant glioma undergoing surgical treatment; specific pathogen-free athymic nude BALB/c mice injected with glioma cells		Use of antibodies, chemical compounds (DHA, ferrostatin-1, liproxstatin-1, GSK2606414, EGCG, deferoxamine), siRNA transfections	Transfections via Lipofectamine 2000, compound treatments, flow cytometry staining for ROS and lipid ROS, biochemical assays for glutathione and GPX4 activity, incubations at 37°C (4 hours for assay, 30 minutes for ROS staining, 10 minutes for lipid ROS staining), tumor generation through cell injections (2×10 ⁶ cells in 0.2 ml PBS per mouse), protocols followed based on manufacturer's recommendations	Induction of ferroptosis in glioma cells by DHA, characterized by iron-dependent cell death, ROS generation, and lipid peroxidation	Activation of protective PERK-ATF4-HSPA5-GPX4 pathway, increased ferroptosis sensitivity upon pathway inhibition
Zhou Y et al. (2021)	3 weeks	Patients with primary gliomas who underwent surgery without prior treatment		Transfection with siGPX7, miR-29 mimics, pcDNA3.1-GPX7 plasmid, erastin treatment	Transfection conducted using Lipofectamine 2000, erastin administered intraperitoneally every other day for 3 weeks, stable GPX7 knockdown cell line established via lentivirus vectors, wound healing assay performed by scratching 12-well plates and culturing in serum-free medium for 24h, CCK-8 agent incubated at 0, 24, 48, 72h, luciferase activities measured 48h post-transfection, tools used include 96-well plates, lentivirus vectors, poly-L-lysine-coated glass coverslips, confocal microscope, GP-miRGLO vector	Prognostic role of GPX7 in glioma, enhanced ferroptosis-related oxidative stress via GPX7 silencing, increased erastin sensitivity through GPX7 suppression	miR-29b-mediated suppression of GPX7 expression, enhanced erastin sensitivity
Yuan F et al. (2022)	48 hours	Patients with glioblastoma (GBM) from Renmin Hospital of Wuhan University		Use of Erastin, APR-246, Pifithrin-α, Nutlin-3, CRISPR/CAS9-mediated SQSTM1/p62 depletion	Transfections performed using Lipofectamine 3000, CRISPR/CAS9 applied following Zhang Feng Lab's protocol, cells selected with 8 mg/mL puromycin for at least 48 h, cultured in high-glucose DMEM containing 10% foetal bovine serum and 1% penicillin/streptomycin, plasmid transfections with pcDNA3.1 or HA-P62, treatment with DMSO or erastin or erastin combined with APR-246 or PFT-α, staining with Trypan blue, viable cells counted using hemocytometer	Dual regulatory role of p62 in ferroptosis based on p53 mutation status in glioblastoma	Survival benefit in p62 knockout models, reversal of p62-mediated ferroptosis enhancement by APR-246 in p53 mutant GBM
Xu Y et al. (2022)	2 hours, 24-72 hours	Human glioma cell lines U87 and U251 treated with Sev gas and ATF4 siRNA		Treatment of glioma cells with Sev gas and transfection with ATF4 siRNA	Sev gas concentrations of 1.7%, 3.4%, and 5.1% applied for 2 h, ATF4 siRNA transfected via Lipofectamine 2000 followed by 5.1% Sev gas treatment for 2 h, Erastin treatment at 10 μM applied for 24, 48, and 72 h	Induction of ferroptosis in glioma cells via the ATF4-CHAC1 pathway	Interruption of ferroptosis and CHAC1 activation by ATF4 suppression, reversal of interruption by Erastin
Kram Het al. (2022)	30 weeks	Patients with primary and recurrent GBM, median age 58 years, treated with the Stupp scheme		Standard Stupp scheme with radiochemotherapy and temozolomide	Formalin-fixed paraffin-embedded tissue sections, deparaffinization, epitope unmasking in citrate buffer at 95°C for 30 minutes, blocking with horse serum and avidin, primary antibodies incubated overnight at 4°C, secondary antibodies incubated for 30 minutes at 1:400 dilution, double immunofluorescence staining with shortened primary antibody incubation to reduce background staining	Increased susceptibility of recurrent GBM tumors to ferroptosis, demonstrated by changes in GPX4 and ACSL4 expression	Significant increase in ALDH1A3 expression in recurrent GBM, correlation of ferroptosis markers with overall survival

Sun S et al. (2022)	2 weeks	Male BALB/c nude mice, 4-week-old	Placebo control group, intraperitoneally administered with DMSO and orally given saline twice a day	PX-478 and SAS treatments, lentivirus-mediated overexpression of SLC7A11, intracranial injection of luciferase-transfected U87 cells, subcutaneous implantation of U87 cells	PX-478 and SAS administered intraperitoneally and orally twice daily for 2 weeks, lentivirus infection used for stable overexpression of SLC7A11, glioma cells treated in culture plates for 24 hours, intracranial injection performed using stereotactic head frame at 3mm depth, subcutaneous implantation in right flanks of nude mice, tumor size monitored every 3 days, cells stained with Crystal Violet Solution or TUNEL kit, imaging by TEM and Xenogen IVIS Spectrum system, flow cytometry used for cell analysis	Suppression of SAS-induced ferroptosis by hypoxia through upregulation of SLC7A11 expression and activation of the PI3K/AKT/HIF-1 α pathway	Synergistic anticancer effect of PX-478 and SAS combination therapy in glioma xenograft mouse models
Zhang F et al. (2023)	48 hours, 24 hours, 10–15 days	Patients with glioma, 54 participants		Treatment of glioma cells with erastin and Ferrostatin-1, transfection with FHOD1 shRNAs or Flag-HSPB1	Transfection with FHOD1 shRNAs or Flag-HSPB1 using TransIT-X2, shRNA vector, psPAX2, and pMD2.G plasmid, treatment with erastin (10 μ M) and Fer-1 (1 μ M) for 24 hours, cells cultured in DMEM medium with FBS and penicillin-streptomycin at 37°C with 5% CO ₂ , colony formation incubated for 10–15 days, glioma xenograft models constructed by injecting glioma cells into nude mice	Regulatory role of the FHOD1-HSPB1 axis in ferroptosis	Impact of FHOD1 expression levels on prognosis and therapeutic response in glioma, enhanced ferroptosis sensitivity linked to FHOD1 knockdown
Minami JK et al. (2023)		Female immunocompromised NOD scid gamma (NSG) mice, 8–9 weeks old		Establishment and maintenance of patient-derived GBM tumors and gliomaspheres, lentiviral transduction, puromycin selection, ferrostatin-1 treatment, intracranial implantation of gliomaspheres	Gliomasphere media prepared with DMEM/F12, B27, heparin, EGF, FGF, GlutaMAX, penicillin-streptomycin, maintained at 37°C, 20% O ₂ , 5% CO ₂ , lentiviral spinfection at 800g for 1 hour and 30 minutes with Polybrene, puromycin selection at 1 μ M, ferrostatin-1 refreshed every 2–3 days, intracranial stereotactic injection coordinates set at 2 mm lateral, 1 mm posterior to bregma, depth 2 mm	CDKN2A deletion remodels the GBM lipidome, redistributing polyunsaturated fatty acids into distinct compartments, increasing lipid peroxidation, and priming tumors for ferroptosis	Identification of exploitable link between molecular lesion and lipid metabolism, creation of molecular and lipidomic resource for GBM specimens
Banu MA et al. (2023)	30 days for mice, 18 hours for patient-derived slices	Male and female C57BL/6 mice, aged 6–8 weeks	Patient-derived tumor slices treated with DMSO, drug vehicle control group	PDGF-BB – IRES – Cre retrovirus injection into subcortical white matter, orthotopic cell transplantation with p53–1 or N1C-1 cells, cell labeling and incubation using specific reagents	Retrovirus injected at 0.33 μ L/min at specified coordinates, cells injected at 0.25 μ L/min at specified coordinates, cells plated in media and incubated for 24–48 hours, various reagents including BODIPY-C11, MitoTracker Red CMXRos, H2DCFDA, FCCP, DMSO used for labeling, Promega Cytotox Glo solution and Seahorse XF base media used, imaging every 30 seconds for 30 minutes, metabolomics processing after overnight plating	Identification of glioma cell state-specific metabolic liabilities rendering N1C cells sensitive to GPX4 inhibition and ferroptosis. The analysis revealed a significant p-value, indicating the robustness of the findings.	Selective depletion of quiescent astrocyte-like glioma cells via GPX4 inhibition in patient-derived organotypic slices
Banu MA et al. (2024)	30 days, 24–48 hours, 18 hours	6–8-week-old male and female C57BL/6 mice		Injection of PDGF-BB retrovirus and orthotopic cell transplantation, drug treatments, siRNA transfections	Retrovirus injections at specific brain coordinates with flow rate of 0.33 μ L/min, orthotopic cell transplantation with 100,000 cells resuspended in PBS at coordinates and flow rate of 0.25 μ L/min, drug treatments applied to cells in poly-L-lysine-coated plates for 24–48 hours, siRNA transfections performed in vitro for 18 hours, slice culture media used for drug treatments, mice anesthetized with isoflurane and monitored for respiration and body temperature	Increased sensitivity of quiescent astrocyte-like glioma cells to GPX4 inhibition and induction of ferroptosis	Selective depletion of quiescent astrocyte-like glioma cells, therapeutic vulnerability linked to mitochondrial redox imbalance, resistance to standard treatments
Yang Y et al. (2024)	48 hours	Low-grade glioma tissues, 534 samples		Transfection of si-Control or METTL16 siRNAs (siMETTL16-1 and siMETTL16-2) using GoldenTran-R	siRNAs transfected using GoldenTran-R reagent, duration of transfection 48 hours, METTL16 siRNA sequences provided for consistency	METTL16 knockdown inhibited glioma progression, induced ferroptosis, and reduced NFE2L2 mRNA stability and levels	Correlations of METTL16 and NFE2L2 with immune cell proportions and immune checkpoints in low-grade gliomas

Gao W et al. (2024)	44 days	C57BL/6N mice, aged 6–8 weeks, average weight 24 g		Implantation of GL261-luciferase cells into mouse striatum, oral gavage treatment for GBM-bearing mice	Stereotactic injection into striatum using Hamilton syringe, gavage at 15 mg/kg daily for 44 days, D-luciferin injection at 15 mg/mL followed by live imaging, NRF2 protein diluted to 10 µg/mL at pH 4.0 and immobilized at 30–50 µg/mL with flow rate of 10 µL/min, Procyanidin B1 injected with 120 s contact and 180 s dissociation time regenerated with glycine solution, OxiRed Probe diluted to 10 µM incubated for 30 min in the dark, LPS diluted to 50 mM incubated for 1 h in the dark, cell observation using confocal and fluorescence microscopy	Suppression of GBM tumor growth and induction of ferroptosis by procyanidin B1 as a novel NRF2 inhibitor, prolongation of survival in GBM-bearing mice, including tumor size assessment.	PSMC3-mediated ubiquitin-dependent degradation of NRF2 proteins, enhanced H ₂ O ₂ accumulation during ferroptosis, anti-tumor effects through downregulation of NRF2
Katz JL et al. (2024)	12–24 hours	Human-derived glioma cell lines U87 and U251, murine glioma cell line GL261, patient-derived xenograft glioma cell lines GBM39 and GBM43		Treatment of glioma cell lines with CKi (20 µM) and GSHee (2 mM) under hypoxic conditions	Incubation in hypoxic chamber at 37 °C and 1% O ₂ , DMEM medium supplemented with fetal bovine serum and penicillin-streptomycin, use of Cell Counting Kit-8 and annexin-V FITC staining, BioTek Cytation 5 plate reader for analysis, silicone inserts and transwell plates for migration assays, treatments applied for 12–24 hours or 8 hours, cells washed and stained for consistency	Disruption of promigratory and anti-ferroptotic mechanisms in GBM by CKi	Hindrance of radiation-induced migration, decrease in invasion-related genes, increase in glutathione metabolism and ferroptosis protection genes, combinatorial blockade abrogating cell survival
Meng X et al. (2024)	4 weeks	Experimental nude mice, 6 weeks old, injected with U87 cells	6 mice, placebo control group	Administration of PMX205 to experimental nude mice with intracranial glioma xenografts	PMX205 dissolved in DMSO or H ₂ O, intraperitoneal injection every two days for four weeks starting on day 7 post-inoculation, U87 cells engineered to express luciferase injected into right striatum to establish xenograft model, injection site standardized at 3.5 mm lateral to midline, 2 mm anterior to coronal suture, and 3 mm depth	Upregulation of C5aR1 promotes glioma progression by inhibiting ferroptosis and stabilizing GPX4 expression	PMX205 promotes ferroptosis alterations and inhibits glioma progression in a mouse model
Zhang Y et al. (2023)	7 days	Female BALB/c nude mice, 6–8 weeks old	Female BALB/c nude mice, 6–8 weeks old, no treatment control group	Silencing SLC39A14 in glioma cells, SAS treatment in mice	siRNA transfection using Lipofectamine 3000, erastin and fer-1 dissolved in DMSO applied for 48 h, SAS administered intraperitoneally twice daily for 7 days, RNA isolation with Trizol reagent, apoptosis analysis with Annexin V-FITC and PI staining, protein analysis with Western blot, tumor preservation with paraffin embedding	Inhibition of glioma progression and induction of ferroptosis through SLC39A14 knockdown, leading to glioma cell proliferation inhibition, ferroptosis induction, tumor volume suppression, cell viability reduction, proliferation reduction, migration reduction, invasion reduction, apoptosis increase, enhanced MDA concentration, reduced GSH levels, protein level suppression, lower cGMP levels, and suppressed cGMP-PKG pathway proteins.	Suppression of cGMP-PKG signaling pathway, reduction in cGMP levels, decreased expression of pathway-associated proteins
Wang W et al. (2024)	14 days	BALB/c nude mice, male, 4–5 weeks old, raised in a pathogen-free environment, injected with 1 × 10 ⁶ U87 glioblastoma cells.		Evaluation of SHG140 and U87 cell growth, migration, invasion, and biochemical properties using cell assays, staining protocols, and imaging techniques.	Cultured cells in plates or chambers, treated with CCK-8 reagent, crystal violet, paraformaldehyde, and other reagents, incubated at specified intervals (e.g., 0 h, 24 h, 48 h), utilized Matrigel for invasion assays, followed reagent-specific protocols, analyzed using flow cytometry, imaging systems, and TEM	KCNA1 promotes tumor growth and invasion by upregulating SLC7A11 and inhibiting ferroptosis	Inhibition of tumor growth and infiltration, extended survival time in vivo

Chen X et al. (2024)		Human glioma cell lines U118, U251, U87.		RSL3 treatment, siRNA targeting SIRT1, AROS, ATF3, use of NAC, ferrostatin-1, FK866, EX527, NAD+, ferric ammonium citrate.	siRNA delivered using Lipofectamine 3000 or GoldenTrans R, cells treated with RSL3 followed by fixation and antibody incubation, FerroOrange staining for ferrous iron detection with 30 min incubation, intracellular GSH and cysteine measured with assay kits, MDA and ROS levels analyzed using specific probes, NAD+/NADH measured using homogenization and chromogenic solution protocols	SIRT1 activation sensitized glioma cells to ferroptosis via ATF3 activation, leading to inhibition of SLC7A11 and GPX4	NAD+ consumption reinforced ATF3 activation, ROS-dependent upregulation of AROS promoted SIRT1 activation, ferroptosis-related factors modulated (ferrous iron, lipid peroxidation, cysteine/GSH depletion)
Miao Z et al. (2022)	6 hours	Patients with low-grade glioma (LGG) or glioblastoma (GBM), specimens derived from excess surgical materials.		Treatment of cells with erastin at varying concentrations.	Cells treated with erastin for 6 hours, mitochondrial membrane potential determined using JC-1 assay and flow cytometry, cell viability assessed using CCK-8 assay, lipid ROS measured using ROS assay kit and lipid peroxidation assay, cells cultured in DMEM with 10% FBS at 37°C with 5% CO2, assays conducted following manufacturer's protocols	Regulation and stabilization of Acs14 expression by Hsp90 and Drp1 in erastin-induced ferroptosis in gliomas	Promotion of ferroptosis through mitochondrial morphology alterations, increased Acs14-mediated lipid peroxidation, augmented anticancer activity of erastin
Vo VTA et al. (2022)	19 days	Glioblastoma stem cells from fresh tissue samples of glioblastoma patients.	Vehicle-treated control group.	Drug treatments with dopamine, erastin, NAC, flupenthixol, RSL3, siRNA targeting DRD5.	Cells grown in DMEM/F-12 supplemented with B27, EGF, bFGF, penicillin, streptomycin, cultured at 37 °C with 5% CO2, hypoxic experiments performed at 1.0% oxygen in Whitley H35 Hypoxystation, co-culture using Falcon®Permeable Support or labeled cells with CMTPX and Hoechst 33342, siRNA transfection with XtremeGENE™ siRNA Transfection Reagent for 3 days, cells treated with drugs for 24 h or 12 h, mice intraperitoneally treated daily with drugs for 19 days, orthotopic transplantation of cells into mouse striatum followed by daily drug administration	Coordination of GBM heterogeneity via dopamine and transferrin secretion by PN-GSCs, inducing MES-GSC proliferation and ferroptosis susceptibility	Iron-dependent proliferation mechanisms, DA receptor D1 activity, TF receptor 1 expression, prognosis analysis of patients with high iron uptake

[Back to 2.2.1. Mechanisms of Ferroptosis in Glioblastoma](#)

Annex 5: Table 4. Prognostic Markers and Risk Models

Study ID	Length of intervention	Population of intervention	Control	Intervention	Intervention details	Primary outcome	Secondary outcome
Liu HJ et al. (2020)		U87MG glioma cell line, U251MG glioma cell line, temozolomide-resistant U87TR and U251TR glioblastoma sub-lines		Use of Erastin, a ferroptosis activator, to treat glioma cell lines	Treated for 24 hours with varying Erastin concentrations, fresh medium replaced, CCK-8 solution added, migration assay using Transwell system, cells pretreated with Erastin or without Erastin, upper chamber with serum-free medium, lower chamber with 10% FBS and Erastin, migrated cells analyzed using microscopy and Image J	Identification of ferroptosis-specific markers and their relationship with glioma progression, including risk score model development and predictive metrics.	Predictive accuracy of the gene signature, association with temozolomide resistance, autophagy, glioma cell migration, overall survival differences
Zhuo S et al. (2020)		Patients with gliomas from CGGA cohort, divided into high-risk group based on median risk score		Risk stratification of glioma patients using ferroptosis-related gene clustering, prognostic analysis, and survival modeling	RNA-seq data from CGGA and TCGA cohorts merged and batch-corrected, genes filtered by median absolute deviation ($MAD \leq 0.5$), NMF clustering performed for subtype assignment, t-SNE validation used for clustering, risk score calculated using LASSO method, Kaplan-Meier analysis used for survival outcomes, functional annotation of 25 genes conducted using GO and KEGG visualization	Prognostic value of ferroptosis-related gene risk signature for glioma patients	Association of gene risk signature with clinical features, independent prognostic indicator role
Chen Z et al. (2021)		Patients with gliomas (LGG and GBM), 665 participants		Application of prognostic gene signature model based on ferroptosis-related genes to stratify glioma patients into high- or low-risk groups	Risk score calculated using $riskScore = \sum_{i=1}^n Coef(X_i) \cdot Exp(X_i)$, stratification using median risk score as cutoff, immune cell infiltration and immune function analysis performed using ssGSEA, RNA-seq data and TPM-transformed expression matrix utilized, GSVA version 1.36.3 applied	Predictive performance of the 11-gene ferroptosis-related signature for overall survival in glioma patients	Diagnostic potential of the 11-gene signature, correlation with iron-related molecular functions, immune-related biological processes, and immune cell infiltration
Hu Y et al. (2021)	2020–2021	Glioma patients treated by surgical excision, living longer than 30 days from diagnosis		Establishment of FRSig-based prognostic model for glioma patients	Patients stratified into subgroups based on FRSig scores, univariate and Lasso Cox regression used to identify significant FRGs, risk score formula constructed using FRG coefficients and TPM values, ssGSEA performed to analyze immune cell infiltration, prognostic nomogram model validated using multivariate Cox regression and 'rms' R package	Prognostic value of FRSig in glioma patients, stratification into subgroups with distinct clinical outcomes	Correlations between FRSig and immune-related indexes, tumor mutation burden, copy number alterations, immune checkpoint expression, nomogram model construction for prognostic prediction
Peng X et al. (2023)		Glioma patients from the TCGA-GBM dataset, diagnosed with glioma		Development of ferroptosis-related gene signature for glioma prognosis, classification of patients into subgroups based on PCA score	Screening prognostic ferroptosis genes via Cox regression, unsupervised clustering using ConsensusClusterPlus package, PCA score calculation based on gene expression profiles, classification into high- and low-score groups, survival analysis using KM curves and log-rank tests, ssGSEA analysis with gsva package to assess immune cell infiltration and pathway activity	Survival differences between ferroptosis-related gene clusters and gene score subgroups	Prediction of clinicopathological features of immune activity, correlations of infiltrating immune cells with PCA and gene scores
Wang X et al. (2023)		99 participants with GBM tumor tissues		Ipatasertib used to suppress HSPB1 phosphorylation, inducing ferroptosis in glioma cells	Pan-Akt inhibitor ipatasertib targeting HSPB1 phosphorylation, inducing ferroptosis	Identification of five ferroptosis regulators (HSPB1, GPX4, ACSL3, IL33, ELAVL1) as prognostic biomarkers significantly correlated with overall survival in glioblastoma multiforme	Validation of risk scoring model efficiency in RNA-seq datasets and external cohorts, analysis of drug response differences in high- and low-expression groups
Zuo Z et al. (2022)		28 patients with glioma in a high-risk group		Use of deep learning network based on 3D-ResNet for predictive performance evaluation	Derived from ResNet50 with stages (stage0, stage1–stage4, AvgPool3d+Reshape+FC), trained using threefold cross-validation with alternating training and validation sets, input images cropped by TC/WT mask ($96 \times 96 \times 96$ pixels), random flip operations for data enhancement, learning rate set to 10^{-4} , batch size of 8, maximum of 70 epochs	Association of FRG-related risk score with glioma prognosis, classification of patients into high- and low-risk subgroups, survival rate differences among stratified groups	Efficiency of FRG-related risk score in prognostic prediction, diagnostic accuracy of deep learning network

Nie XH et al. (2022)	4 weeks, 24 hours, 72 hours	4-to-5-week-old athymic nude mice in a subcutaneous xenograft tumor model		PF treatment (1.0 g/kg/day), RSL3 treatment (100 mg/kg, 2 times/week), transfection with oeNEDD4L, shNEDD4L, oeSTAT3 plasmids	Cells cultured in DMEM medium with FBS and penicillin-streptomycin, transfection performed using Lipo2000 reagent, tumor models created via subcutaneous inoculation of U251 cells into athymic nude mice, PF administered daily, RSL3 administered twice weekly, tumor volumes measured every 4 days, biochemical assays and staining performed using manufacturer protocols	Antitumor activity of paeoniflorin in glioma cells through ferroptosis induction via upregulation of NEDD4L and repression of Nrf2, GPX4, and STAT3	Enhanced tumor inhibition through combination therapy with PF and RSL3, correlation of low NEDD4L expression with poor glioma prognosis, increased intracellular ROS levels, elevated MDA and Fe ²⁺ levels
Song L et al. (2022)	15 days	TMZ-resistant GBM cell lines (T98G-R and U118-R)		Transfection using Lipofectamine 3,000 reagent and siRNAs targeting FANCD2	Performed according to manufacturer's protocol, siRNAs sequences provided by Genescript, cells re-inoculated in six-well plates at 1 × 10 ⁵ /well density after 24 h, incubated at 37°C with 5% CO ₂ for 15 days	Up-regulation of FANCD2 correlates with poor prognosis in GBM and promotes TMZ resistance by attenuating ferroptosis	Knockdown of FANCD2 increases ROS levels, inhibits cell survival, links to ferroptosis, correlates with immune features and cancer-associated pathways
Xiao D et al. (2021)		74 patients diagnosed with grade III or grade IV gliomas, age at diagnosis 21-89 years (median 60)		Grouping patients with GBM based on FRGPRS values, analysis of prognosis-related genes influencing progression-free survival	FRGPRS constructed using prognostic gene expression levels and regression coefficients from multivariate Cox proportional hazards regression analysis, univariate Cox regression models and Lasso-logistic regression used to identify prognosis-related core genes, FRGPRS calculated using risk score formula, relationship between FRGPRS and overall survival evaluated using log-rank test	Prediction of overall survival and progression-free survival in GBM patients using the FRGPRS model	Associations with immunity, tumor tissue proportions, immune response, chemotherapeutic response, predictive performance during immune checkpoint therapy
Zhou L et al. (2021)		Patients with glioma, 660 participants		Identification of autophagy-ferroptosis genes, construction of prognostic risk model for overall survival (OS), creation of nomogram based on prognosis-related genes	Genes screened using univariate and lasso regression analysis with p < 0.01, patients divided into high and low expression groups based on median expression levels, nomogram constructed using five prognosis-related genes and risk score	Prognostic risk model for predicting overall survival (OS) in glioma	Validation of risk model efficacy through Kaplan-Meier survival analysis and ROC analysis, confirmation of association with clinical factors, improved accuracy in prognosis prediction using nomogram
Sun W et al. (2022)		Cases with gene expression profiles and clinicopathological data		Construction of predictive model based on AD-FRGs to evaluate glioma prognosis	Screening AD-FRGs using univariate Cox analysis, predictive model established using LASSO-penalized Cox regression, patients divided into risk groups based on median risk scores, nomogram constructed for prognosis prediction, biological pathway enrichment analyzed using GSEA software, immune response assessed using ssGSEA, CIBERSORT method, and ESTIMATE algorithm, computational analysis delivered via R packages and software tools	Prediction of 1-, 3-, and 5-year survival rates in glioma patients using autophagy-dependent ferroptosis-related gene signature	Correlation of high-risk group with immunosuppressive tumor microenvironment, macrophage infiltration, and immunotolerance
Cai Y et al. (2021)	48 hours	Patients with glioma, categorized into LGG and HGG		Erastin treatment of human glioma cell lines, investigation of subcellular protein distribution and expression	Glioma cell lines cultured in DMEM medium with 10% FBS at 37°C with 5% CO ₂ , erastin added after 24 h, CCK-8 assay performed at 24 and 48 h, reagent-to-medium ratio of 1:9, 100 µl solution added per well, incubated for 2 h, immunofluorescence and immunohistochemistry staining performed	Prognostic implications of ferroptosis-related gene prognostic index (FRGPI) in glioma patients, including overall survival prediction, temozolomide sensitivity, and immune checkpoint inhibitor response	Correlation of FRGPI with immune cell infiltration, tumor mutational burden, PD-L1 expression, and microsatellite instability

Huang L et al. (2022)		GBM cell lines U251 and KNS-89		Infection and selection of U251 and KNS-89 cell lines with puromycin	Infection of cell lines, selection after 48 hours, 2 µg/ml puromycin (cat# A1113803, Thermo Fisher) applied to cell culture	Development of a 3-FRLs signature to classify glioma patients into high-risk and low-risk groups with stable prognostic accuracy for overall survival	Differences in cellular immunity, immune cell numbers (NK cells, CD4+, CD8+ T-cells, macrophages), immune-related gene expression, somatic mutation rates in glioma prognosis-related genes IDH1 and ATRX, inhibition of ferroptosis after LINC01426 knockdown
Zhang X et al. (2022)	24 hours	Human glioblastoma cell lines U87MG and U251MG	Control solvent	Pretreatment of U251MG and U87MG cells with ferroptosis activator erastin (10 µM)	Cells cultured in DMEM medium supplemented with 10% FBS, incubated at 5% CO2 and 37°C, migration assays performed using Transwell system (24-well, 8 µm pore size polycarbonate membrane), cells fixed with 4% PFA and stained with crystal violet, migrated cells photographed with light microscope and counted using ImageJ software, experiments repeated more than three times	Prognostic value of ferroptosis-related genes associated with IDH1 status in GBM patients	Association with immune-related factors, involvement in p53 signaling, senescence, autophagy, negative regulation of kinase activity, identification of therapeutic drugs
Tong S et al. (2022)	24 h, two weeks	Patients with gliomas, untreated before surgery		Transfection of human U251 and U87 glioblastoma cells using Lip3000 and plasmids, followed by experimental assays including cell viability testing, colony formation, Edu incorporation, ROS detection, lipid peroxidation analysis, wound healing assay, transwell migration assay, and western blot	Cultured in DMEM supplemented with 10% FBS, 100 U/ml penicillin, 100 µg/ml streptomycin, transfected with 2 µg plasmids using Lip3000 for 6 h, harvested after 24 h, seeded in plates at specific densities, cultured for 24 h to two weeks, stained with paraformaldehyde and crystal violet, Edu diluted in culture medium and incubated for 2 h, fluorescence observed under microscope, cells stained with H2DCFDA dye and C11-BODIPY dye, flow cytometry and microscopy used for imaging, transwell assay performed using Matrigel-coated upper wells, cells fixed and stained, western blot conducted using primary and secondary antibodies, membranes visualized with ECL detection kit	Positive correlation between IRF2 expression and glioma grade, IRF2 overexpression protects glioma cells from ferroptosis, enhances invasive and migratory abilities	IRF2 identified as a potential biomarker for diagnosis and treatment in glioma, novel ferroptosis-related signature predicts prognosis
Feng S et al. (2022)		GBM patients receiving anti-PD-1 checkpoint inhibition therapy		Evaluation of tumor immune escape and ICB therapy response using computational analysis	Consensus clustering using ConsensusClusterPlus tool in R, prognostic model construction via ridge regression, immune infiltration analysis using TIMER, MCP-counter, EPIC, xCell, quanTiseq, CIBERSORT, gene enrichment analysis via GSVA and GSEA, TIDE analysis to assess CTL dysfunction and rejection	Association between higher risk scores and worse prognosis in GBM patients, including overall survival, progression-free survival, and disease-specific survival	Predictive performance of risk signature for 1-, 3-, and 5-year survival, GBM subtypes, IDH status, and response to ICB treatment
Su J et al. (2022)		Glioma cell line U87		siRNA transfection targeting SSBP1 using Lipofectamine® RNAiMAX, knockdown of SSBP1 for 72 hours, exposure to TMZ, mitochondrial ROS and MMP detection	Transfection performed with Lipofectamine® RNAiMAX Reagent, siRNA sequences specified, mitochondrial ROS detected using MitoSOX™ Red, mitochondrial membrane potential assessed using MitoTracker™ Red, cells cultured at 37°C with 5% CO2, serum-free medium in upper chambers and 20% FBS in lower chambers, incubation with MitoSOX™ Red and MitoTracker™ Red for 30 minutes, exposure to TMZ for 48 hours, cell viability measured using Cell Counting Kit-8, manufacturer's instructions followed	Prognostic risk score model based on 12 DE-MRGs demonstrated excellent performance in predicting GBM patient prognosis	Association of risk score with inflammatory response, extracellular matrix, immune pathways, gene mutations, immune cell infiltration, therapeutic potential of SSBP1, SSBP1 knockdown increased TMZ sensitivity by enhancing ferroptosis

Wu Y et al. (2025)		Patients with GBM tumor tissue samples, 415 participants	Control group consisted of normal brain tissue samples from the GTEx database, totaling 1152 samples.	Injection of 5×10^6 cells into mice brains, lentivirus transfection of cells, weekly bioluminescence imaging of intracranial tumors	Injected using stereotactic device, lentivirus transfection (MOI = 10) with polybrene for 4 h followed by medium replacement after 24 h, transfection efficiency observed after 48 h using luciferase reporter genes, stable transduced lines selected with ampicillin, weekly imaging from day 7 onward, housed in pathogen-free environment at 20°C–25°C and 60%–65% humidity, polarized macrophages collected after 24 h co-culture, analyzed using flow cytometer	Prognostic value of a five-gene risk model in GBM, stratification of patients into high-risk and low-risk groups based on survival outcomes	Biological significance of ferroptosis-related genes in tumor progression, therapeutic target identification, correlation analysis between gene expression and immune checkpoints, distinct gene expression patterns between GBM and normal tissues, gene distribution across cell types via scRNA-seq
Lv Y et al. (2025)	38 hours, 24 hours, 2 hours, 5 days, 1 week, 24–48 hours	Patients with primary and recurrent GBM after chemotherapy, 80 participants		Transfection of U251 and LN229 cells with MFAP4 siRNA or siRNA negative control using Lipofectamine 3,000	siRNA mixed with Lipofectamine 3,000 in serum-free medium, added to medium with 10% FBS, incubated for 38 h under standard conditions, cell viability assessed using CCK-8 solution and absorbance at 450 nm, scratches made in confluent cell monolayers with pipette tip, cells imaged at 0, 24, and 48 h, Transwell assay conducted with regulated cell concentration in serum-free medium, incubated for 24–48 h in 37°C 5% CO2 incubator	MFAP4 identified as an independent prognostic indicator, correlated with glioma progression and adverse clinicopathological features	Significant associations between MFAP4 levels, immune infiltration, ferroptosis, immune checkpoint genes, and survival metrics (OS, DSS, PFI)
Clavreul A et al. (2024)		Patients aged ≥ 18 years, newly diagnosed unilateral supratentorial IDH-wildtype glioblastoma, underwent tumor resection, received first-line chemoradiotherapy according to the Stupp protocol, sourced from the French GB biobank		Subsequent adjuvant chemotherapy with oral TMZ depending on tolerance and radiological response	Administered orally, based on tolerance and radiological response, following complete concomitant chemoradiotherapy according to the Stupp protocol	Prognostic utility of circulating MDH1 and RNH1 biomarkers for survival in IDH-wildtype glioblastoma patients	Differential expression of tumor and serum proteins associated with ROS detoxification, identification of therapeutic pathways driven by MDH1, RNH1, and FABP7
Xu Z et al. (2022)	48 h, 24 h, 14 days	Glioma patients admitted for operation in Beijing Tiantan Hospital, 325 participants		siRNA transfection targeting MXRA8, polarization of macrophages to M1 and M2 phenotypes, TMZ drug treatment at varying concentrations, co-incubation of macrophages and glioma cells in a Transwell plate	siRNAs transfected into glioma cells using Lipofectamine 3000 for 48 h, macrophages polarized to M1 using PMA for 6 h and to M2 using IL-4 plus IL-13 for 72 h, TMZ added to medium at concentrations of 0–400 μ M for 48 h, macrophages seeded in upper chamber of Transwell plate without serum for 12 h, glioma cells incubated in bottom chamber with 10% FBS for 24 h, infiltrated macrophages fixed in formalin and stained with crystal violet	Identification and validation of MXRA8 as a novel prognosis indicator associated with ferroptosis and glioma progression	Correlation of MXRA8 with immune infiltration cells, immune score, enrichment in immunity-related pathways, association with unfavorable survivals

[Back to 2.2.2. Prognostic Markers and Risk Models](#)

Annex 6: Table 5. Therapeutic Strategies and Treatment Outcomes

Study ID	Length of intervention	Population of intervention	Control	Intervention	Intervention details	Primary outcome	Secondary outcome
Ye L et al. (2021)	24 months	Patients with gliomas (low-grade glioma WHO grade II–III and GBM WHO grade IV), collected at Renmin Hospital of Wuhan University, Wuhan, China, no chemotherapy or radiotherapy before surgery	Patients with cerebral hemorrhage, 6 participants, no treatment control group	Investigation of CYP2E1 mRNA expression levels in glioma tissues, analysis of its clinical significance, and molecular docking of TCM compounds targeting CYP2E1	RNA extracted using TRIzol reagent, cDNA synthesized using PrimeScript RT Reagent Kit, CYP2E1 mRNA levels detected using SYBR Premix Ex Taq II and Bio-Rad real-time PCR Systems, relative Ct method used for comparison, gene expression analyzed using R packages, molecular docking performed using AutoDock 4.2 and PyMOL software, correlation analysis conducted for immune checkpoints, miRNA prediction performed using MiDRB and TargetScan, functional enrichment analyzed using GO and KEGG pathways	Prognostic significance of CYP2E1 expression in glioma patients, correlation with poor prognosis, clinical features, survival outcomes, and statistical significance	Involvement of CYP2E1 in lipid metabolism, ferroptosis, tumor immune microenvironment, correlation with methylation levels and copy number variation, miRNA targeting by hsa-miR-527, identification of compounds targeting CYP2E1
Chen Q et al. (2021)	45 days	U87 and U251 glioblastoma cells, 4-week-old specific pathogen-free male nude mice injected with U87 and U251 cells		Incubation of U87 and U251 glioblastoma cells, transfection with NC, hsa-miR-27a-3p angomir, si-TMEM161B-AS1, si-TMEM161B-AS1 + hsa-miR-27a-3p angomir, migration assay, invasion assay, apoptosis assay, lipid ROS detection, subcutaneous implantation of transfected cells in nude mice	Cells incubated at 37°C under 5% CO ₂ in DMEM containing 10% FBS and 1% penicillin-streptomycin, seeded in 96-well plates, migration assay in Transwell inserts with serum-free DMEM and 10% FBS-DMEM in bottom chamber, invasion assay with Matrigel-coated membrane, apoptosis assay using PI and FITC staining and Caspase-Glo 3/7 reagent, lipid ROS detection using C11 BODIPY dye, subcutaneous injection of 4×10 ⁵ transfected cells into nude mice, tumor volume measured after 45 days	Regulation of malignant biological behavior (proliferation, migration, invasion, apoptosis, ferroptosis) and temozolomide resistance through the TMEM161B-AS1-hsa-miR-27a-3p-FANCD2/CD44 axis	Tumor growth inhibition in nude mice, identification of potential therapeutic targets for glioblastoma
Van Loenhout Jet al. (2021)	14 days	Mice inoculated subcutaneously with 1 × 10 ⁶ SB28 GBM cells in the shaved abdominal flank	Spheroids in untreated PBS, vehicle control	AF (0–10 μM) mono- or combination treatments with plasma-treated PBS (pPBS) generated by atmospheric pressure plasma jet systems or microsecond-pulsed dielectric barrier discharge (DBD) system	Plasma generated using kINPenIND® with argon gas or COST jet with He/5% H ₂ O vapor mixture, plasma applied directly to spheroids or indirectly to 2D cell cultures in PBS, AF administered via oral gavage or pretreatment for 4 h, plasma applicator held above tumors for 10 s, standardized plasma jet parameters (flow rate, gap distance, pulse width, frequency), IncuCyte® system used for reagent applications, mice sedated during DBD treatments	Synergistic therapeutic strategy for glioblastoma via combination of oxidative stress-inducing treatments, reducing tumor growth kinetics and prolonging survival	Decrease in TrxR activity and GSH levels, intracellular ROS accumulation, apoptosis and ferroptosis induction, increase in danger signals and dendritic cell maturation, inhibited phagocytotic capacity of dendritic cells

Moujalied D et al. (2022)	5 days, 48 hours, 24 hours	Six GBM cell lines, including U251 and SNB-19; 6-week-old female NOD/SCID/ <i>yc-/-</i> mice with intracranially implanted U251-Ch-Luc GBM tumors	Mice gavaged with vehicle, health status: after detectable engraftment of tumour cells	Treatment with Temozolomide, JQ1, A1331852, ferroptosis/apoptosis inducing and preventing compounds, gavage of BCL-XL inhibitor A1331852	Cells treated in RPMI-1640 medium supplemented with FBS, penicillin, streptomycin, and DMSO, compounds added at specified concentrations, cells treated for 48 hours and harvested by trypsinisation, mice gavaged daily for 5 consecutive days with A1331852 formulated in Phosal 50 PG, polyethylene glycol 400, ethanol, and DMSO, flow cytometry performed using Annexin V and DAPI staining, apoptosis and viability evaluated using MTT assay	Enhanced apoptosis and cell killing observed in GBM cell lines with dual targeting of pro-survival proteins BCL-XL and MCL-1 using BH3 mimetic drugs compared to conventional therapies	Synergistic cell killing with ferroptosis inducers and BH3 mimetic drugs, activation of apoptosis markers caspase-3 and PARP1 cleavage, dependence on intrinsic apoptosis executioners BAX and BAK
Su IC et al. (2023)	3 weeks	Female BALB/C nude mice aged 5–6 weeks, injected with tumor xenografts (GBM cells)	shScramble xenografts treated with vehicle, 5 participants, no treatment control group	Induction of ferroptosis using IKE administered intraperitoneally, generation of TMZ-resistant U87MGR cells through increasing TMZ doses	IKE administered intraperitoneally at 25 mg/kg/day for 3 weeks, TMZ-resistant cells maintained with 100 μ M TMZ, cells cultured in Dulbecco's modified Eagle's medium supplemented with fetal bovine serum and penicillin/streptomycin, subcutaneous injection of Matrigel mixture containing 1×10^6 scrambled or shSOD2 U87MG-R cells, mitochondrial ROS production analyzed using MitoSOX red, immunofluorescence staining performed	CYBB orchestrated mesenchymal shift and promoted TMZ resistance by modulating the Nrf2/SOD2 axis, reducing erastin-mediated ferroptosis sensitivity	Upregulation of CYBB and SOD2 in mesenchymal GBM subtype, association of CYBB with poor clinical outcomes, protective role of SOD2 against erastin-triggered ferroptosis in TMZ-resistant GBM cells
Zhou Y et al. (2023)	21 days	Male nude mice, 5 weeks old, injected with U87 glioma cells, treated with myristiglan	U87-injected nude mice, DMSO-treated control group	Stereotactic implantation of U87 glioma cells into the striatum, intraperitoneal injection of myristiglan (5 mg/kg) every 3 days	U87 cells suspended in 3 μ L PBS, stereotactically implanted under isoflurane anesthesia, myristiglan administered intraperitoneally starting 7 days post-tumor injection, injections repeated every 3 days for 21 days	Suppression of glioblastoma growth through EMT-mediated ferroptosis in a Slug-dependent manner	Inhibition of NF- κ B signaling, induction of ferroptosis via Slug-SLC7A11 pathway, suppression of glioblastoma progression in xenograft mouse model
Liu B et al. (2022)	9 days	6 weeks old C57 mice, GBM-bearing	Normal saline group	Use of Fe3O4-siPD-L1@M-BV2 nanoparticles for PD-L1 silencing and ferroptosis induction	Fe3O4-siPD-L1@M-BV2 nanoparticles, siPD-L1, IFN- γ , Fer-1, DFO, APC-CD11c antibody, FITC-CD80 antibody, PE-CD86 antibody, delivered via tail vein injections every three days (4 times total) and serum-free DMEM for 48 hours, enzyme-linked immune analyzer and flow cytometer used, standardized concentrations (Fe3O4: 10–200 μ g/mL; IFN- γ : 10 ng/mL; Fer-1: 10 μ M; DFO: 100 μ M), incubation at 37 $^{\circ}$ C	Inhibition of orthotopic drug-resistant GBM growth, prolonged survival time, increased siPD-L1 and Fe2+ accumulation, decreased PD-L1 protein expression, enhanced ferroptosis, immune reactivation	Altered invasion-related protein expressions, ferroptosis-related protein expressions, increased effector T cell to regulatory T cell ratio, increased M1/M2 microglia ratio, maturation of dendritic cells

Jiang Y et al. (2022)	15 days	Patients diagnosed with grade IV glioblastoma, underwent surgery at Shanghai Tenth People's Hospital		Lentiviral-based infections to overexpress or knock down molecules in glioma stem cells	Lentiviral vectors constructed by Gene-Chem, RNAi-mediated lentivirus vectors, treated with necrostatin-1, Z-VAD-FMK, 3-MA, ferrostatin-1, RSL, selection with 10 µg/ml puromycin for 15 days, reagents delivered at specific concentrations and incubation times, stereotaxic apparatus used for orthotopic injections into mouse brains	Inhibition of glioblastoma stem cell viability, proliferation, neurosphere formation, stemness, and tumorigenesis via ferroptosis induction	Potential biomarker for glioblastoma, therapeutic target for molecular or ferroptosis-dependent therapies
Xia L et al. (2022)	24-72 hours	Human glioma U251 and U87 cell lines, female BALB/c nude mice, age 4 weeks	No treatment control group	Treatment of human glioma U251 and U87 cell lines with apatinib	Apatinib transfection at 50% confluence, plasmid transfection at 70% confluence using Lipofectamine 2000, cells seeded at densities of 5×10^3 cells/well (96-well plate) or 1×10^5 cells/mL (6-well plate), treated for 24/48/72 hours, staining with PI solution and fixation with ethanol, flow cytometry performed, biochemical assays conducted using detection kits (ROS, MDA, GSH, LDH, iron), protein analysis with BCA Protein Assay Kit and SDS-PAGE, membranes incubated with antibodies, gliomas fixed in paraformaldehyde and dehydrated with ethanol	Restraint of glioma cell proliferation through induction of ferroptosis via inhibition of VEGFR2/Nrf2/Keap1 pathway. Primary outcome of the study.	Counteraction of ferroptosis induction by overexpression of Nrf2
Zhang K et al. (2023)	2 weeks	Human GBM and brain contusion tissue samples, BALB/c nude mice, 4 weeks old		Culturing human GBM and brain contusion tissues, assessing proliferation and mortality	Cells cultured in DMEM with 10% FBS, seeded in 96-well plates at 5000 cells/well, proliferation tested using CCK8 reagent at 24, 48, 72, and 96 h, mortality assessed with lactate dehydrogenase cytotoxicity assay, JC-1 staining for fluorescence analysis, lentivirus-encoded SHG-140 cells injected into mice skulls, tumor size recorded using IVIS imaging system on days 7, 14, 21, and 28, brains fixed with 4% paraformaldehyde and analyzed with HE/IHC staining	Promotion of ferroptosis induction and retardation of tumor growth rate in GBM cells via HSP27 deficiency	Reduction in tumor growth capacity in intracranial xenograft models
Liang X et al. (2024)	1 hour, 48 hours, 24 hours, 14 days	T98G human glioblastoma cell line, RBMS1 expression reduced using sh-RBMS1 constructs	Negative control group (sh-NC)	Use of ferroptosis inhibitor Fer-1 (1 µM) to treat T98G cells	Transfected using Lipofectamine 2000 reagent at 37 °C for 48 h, inoculated into 6-well plates at specified densities, incubated in serum-free medium pre-coated with Matrigel, exposed to C11-BODIPY probe, washed with pre-cold PBS, homogenized with iron assay buffer, centrifuged at $16,000 \times g$ for 15 min at 4 °C	Inhibition of GBM cell proliferation and promotion of apoptosis through RBMS1 silence, possibly mediated by ferroptosis	Inhibition of migration, invasion, EMT process; promotion of ferroptosis

Carvalho SM et al. (2023)	7 days	U87 glioblastoma cells, treated with MION, Co40-MION, and DOX at concentrations of 0.6, 6, and 60 µg mL ⁻¹	Negative control group (DMEM with 10% FBS and sterile polypropylene chips), positive control group (DMEM with 10% FBS and TBHP)	Synthesis and application of magnetic iron oxide nanoparticles (MION) and cobalt-doped nanoparticles (Co40-MION)	Synthesized using coprecipitation method with NH ₄ OH in alkaline conditions, iron salts dissolved in preheated CMC solution, heated in nitrogen atmosphere, dialyzed for purification, applied to U87 cells and spheroids, spheroids treated on Day 0 and Day 3, reagents include FeSO ₄ , FeCl ₃ , cobalt salts, phosphate-citrate buffer, hydrogen peroxide, DMPO spin trap, MTT reagent, SDS solution, acetic acid, treatments lasting up to 24 hours	Reduction in glioblastoma tumor spheroid volume and enhanced cytotoxicity through cobalt-doped iron oxide nanoparticles	Comparison of nanozyme efficacy with doxorubicin, concentration-dependent cytotoxicity, role of hydroxyl radicals in anticancer activity
Miki K et al. (2023)		Cell lines U87MG, U373, and KNS1451, KNS1451 classified as aggressive mesenchymal glioblastoma		Culturing glioblastoma cell lines under controlled conditions with specific additives and hypoxic environment	DMEM with glucose, CAP, 2-DG, DFO, SS, metformin, DMEM/Ham's F12 for stem-like cells, 6-well dishes, medium replaced every 3 days, hypoxic conditions (1% O ₂ , 5% CO ₂) using personal CO ₂ multi-gas incubator and Gas Cylinder Auto Changer, Coulter counter, TC 20 automated cell counter with trypan blue, Seahorse XF24 Flux analyzer and microplates, cells seeded in triplicate, cultured for 7 days, sphere size and number evaluated on the 7th day, OCR measured after 16 h incubation	Significant inhibition of glioblastoma cell growth with combined CAP and 2-DG treatment under normal glucose conditions	Validation of effectiveness in hypoxic conditions, identification of ferroptosis as a potential mechanism
Wang H et al. (2022)	21 days	Human glioblastoma cells, U251, U87, KNS89		Infection of glioblastoma cells with GFP and GFP+NeuroD4 viruses, stereotactic injection into nude mice	Lentiviral vectors and packaging plasmids transfected into HEK-293T cells, infected glioblastoma cells injected into mice, neuronal induction medium (DMEM, F12, neurobasal, N2, B27, forskolin, dorsomorphin) used for cultivation, medium changed every other day, virus media collected and filtered at 24 and 48 hours, supplemented with polybrene, tumor growth evaluated every 7 days, EdU administered for 2 hours, PI dye used for cell cycle analysis, dihydroethidium applied 30 minutes before flow cytometry	Reprogramming glioblastoma cells into neuron-like cells induced terminal differentiation, inhibited proliferation, and prolonged survival in tumor-bearing mice	Smaller tumor sizes in NeuroD4-infected xenografts, reduced SLC7A11 and GPX4 expression, ferrostatin-1 blocking NeuroD4-mediated reprogramming
Liu Y et al. (2022)	2 weeks	Patients with glioma (astrocytoma, IDH wildtype, grades I-IV), 35 participants	Negative control group	Transfection of glioma cell lines U251 and LN229 with small interference RNA targeting KAT6B and STAT3	Transfected using Lipofectamine 2000 reagent, maintained in DMEM medium with 10% FBS and 1% penicillin/streptomycin, incubated overnight post-transfection, assays performed at indicated time points, lipid ROS measured by flow cytometry, iron levels measured using Iron Assay Kit, ChIP assay performed using Pierce Magnetic ChIP Kit	Contribution of KAT6B to glioma progression by repressing ferroptosis via epigenetic induction of STAT3	Regulation of glioma cell viability, apoptosis, lipid ROS, iron levels, epigenetic mechanisms involving H3K23ac and RNA polymerase II enrichment on STAT3 promoter

Wang C et al. (2023)	24-120 hours	Glioma patients undergoing surgery, grades 2, 3, and 4 gliomas, 60 participants	Normal brain tissue specimens from GBM patients, 10 specimens	Experimental processing of glioma stem cells (GSCs)	GSCs isolated and cultured in StemFlex™ medium at 37°C with 5% CO2 atmosphere for 2 weeks until tumor spheres formed, treated with necrostatin-1, Z-VAD-FMK, 3-MA, ferrostatin-1, transfected with lentiviral vectors synthesized by Gene-Chem, injected into mice brains using stereotactic apparatus at density of 5×10^4 cells in 5 μ L solution, processed using RNA/protein assay kits and detection kits, tumor volume calculated using formula $V = (D \times d^2) / 2$	CircRNF10 upregulation in glioblastoma promotes ferroptosis defense and tumorigenic efficacy	CircRNF10 silencing extends survival rates, establishes circRNF10/ZBTB48/IGF2BP3 feedback loop remodeling iron metabolism
Yang YH et al. (2024)	12 days	Female BALB/c nude mice, xenograft tumor model with U87 cells, 24 participants	Female BALB/c nude mice, placebo control group (DMSO), 6 participants	Administration of S670 via irrigation	Administered via irrigation, once daily for 12 days, tumor volume calculated using $V = 0.5 \times l \times w^2$, Ki67, LC3, and LAMP2 expression analyzed in tumor tissues	Significant inhibition of tumor growth, dose-dependent inhibition of GBM cell proliferation (IC50 value for GBM cell proliferation inhibition), induction of ferroptosis via ROS generation	ROS-mediated Nrf2 activation, TFEB nuclear translocation, autophagosome and lysosome biogenesis, impaired autophagosome-lysosome fusion, autophagy flux inhibition, STX17 suppression
D'Aprile S et al. (2024)	24-48 hours	Patients diagnosed with mesenchymal or proneural GBM subtypes, 153 participants	Vehicle-treated cells	Exposure of cells to FAC and erastin	FAC prepared as 50 mM stock solution in PBS, erastin prepared as 2 mM stock solution in DMSO, cells seeded in 96-well plates, 24-well plates, and T-75 flasks at specified densities, FAC exposure at concentrations of 5–100 μ M for 24–48 h, erastin exposure at 1–20 μ M for 24–48 h, FAC exposure at 100 μ M for 6 h or 24 h, cells collected at 30, 90, or 180 min, use of blocking buffer for membranes, incubation with primary antibodies overnight at 4 °C	Differential response to ferroptosis induction between mesenchymal and proneural GBM subtypes	Up-regulation of antioxidant defense mechanisms in mesenchymal GBM subtypes
Moses A et al. (2025)	12 h	Male and female Sprague Dawley rats, healthy and glioma-bearing, 15 participants	Vehicle control group	Ferroptosis induction using erastin2 and RSL3	Delivered through cell seeding in plates and intravenous administration in rats, monitored using Incucyte SX1 live-cell analysis instrument and PET/CT scanner, BODIPY C11 dye at 1.5 μ M, erastin2 and RSL3 at specified concentrations, [18F]hGTS13 administered intravenously (~20 MBq), IKE prepared in 10% DMSO/50% PEG-400/40% saline and administered at 25 mg/kg 48 h post-[18F]hGTS13	Monitoring ferroptosis sensitivity and engagement of system xc- targeted therapies using [18F]hGTS13	Distinction between sensitive and resistant cell lines, association of [18F]hGTS13 uptake with cellular glutathione content

Dumitru CA et al. (2023)	10 days	Adult patients with newly diagnosed IDH wild type GBM	Transfected cells with control plasmid	Transfection of GBM cell lines with shRNA clone	Transfection in antibiotics-free medium using PANFect A-plus reagent, selection with Puromycin at specified concentrations, conditioned supernatants prepared by culturing GBM cells for 24 h at 37°C, neutrophils isolated from EDTA-anticoagulated blood using Pancoll and purified by sedimentation and osmotic shock, MTT assay performed with 4 h incubation, agarose-based culture setup for 10–11 days, invasion assay using ORISTM system with rat tail collagen I matrix, neutrophil chemotaxis assessed using transwell inserts with 3 µm pores after 3 h incubation, MMP9 release analyzed by gelatine zymography, IL-8 levels measured using ELISA kit	PGRMC1 levels significantly predicted poor overall survival and promoted proliferation, anchorage-independent growth, invasion, and progression of GBM	Increased susceptibility of GBM cells to ferroptosis inducer erastin, decreased susceptibility to temozolomide, enhanced tumor-related inflammation, promoted recruitment of neutrophils, correlation of PGRMC1 levels with ITGB1 expression
Stringer BW et al. (2023)	5 days, 7 days, 24 hours	Patients with GBM undergoing surgery at Flinders Medical Centre or the Royal Adelaide Hospital, South Australia	Cells without radiation, 6 replicates	Drug treatments with TMZ and TFP, ionizing radiation applied to GBM cells	TMZ dissolved in DMSO and diluted in cell medium, TFP dissolved in DPBS and diluted in cell medium, GBM cells seeded in 384-well CellCarrier Ultra imaging plates, treated with 2 Gy radiation daily for 5 days, TMZ treatment for 7 days at 0, 25, and 100 µM, TFP treatment for 24 hours at 0, 4, 7, and 10 µM, half-medium changes every 48 hours, neuronal cultures matured for >100 days, MEA recordings conducted using Maestro Pro system on Lumos MEA plates coated with poly-L-ornithine and laminin	CSF induces therapeutic resistance in GBM cells through NUPR1-mediated ferroptosis inhibition, trifluoperazine enhances killing of resistant GBM cells	Improved survival outcomes for GBM patients suggested by combining trifluoperazine with standard care
Qu S et al. (2023)	72 h, 24 h, 2 weeks	Orthotopic xenograft nude mice implanted with human GBM cells		Combination treatment of ABX and TMZ to suppress GBM progression and prolong survival	Delivered via intracranial injection using Hamilton syringe, conventional skin disinfection and skin suture closure performed, tumor growth monitored using imaging facility, treatments administered for 24–72 h, organoid medium refreshed every 48 h	Suppression of GBM progression (Primary Outcome) and prolonged survival (Secondary Outcome 1) in orthotopic xenograft nude mice through combination treatment of ABX and TMZ (Secondary Outcome 2, Secondary Outcome 3)	Induction of sustained DNA damage, enhancement of ferroptosis, increased drug sensitivity confirmed through GBM PDOs models

Williams CH et al. (2024)	72 hours, 3 days	Glioblastoma cell lines (13 tested), neurosphere lines, PDX models	Standard non-targeting siRNA, transfection control plasmid	Blocking GPR68 signaling using small molecule inhibitor OGM and genetic means	Cells reverse transfected with siRNA, sgRNA, or plasmids using lipofectamine RNAiMAX or lipofectamine 3000, OGM compounds added to media at indicated concentrations, incubation under standard cell culture conditions for 72 hours, exposure to DMSO, OGM, or Erastin, addition of 2.5 µM Liperfluo resuspended in DMSO for 1-hour incubation, cells plated in 96-well plates, 12-well plates, or 100 mm cell culture dishes	Robust cell death induced in glioblastoma cells by blocking GPR68 signaling, irrespective of genetic heterogeneity or temozolomide resistance	Non-toxicity of OGM to zebrafish, selective sparing of non-malignant neural cells
Li X et al. (2024)	24 hours, 12 hours followed by 24 hours, 8 days	GBM cells including U251 and U87MG cell lines, GBM#4 cells isolated from primary surgical GBM biopsy specimens from patients treated at Renji Hospital, Shanghai, China		Treatment of U251 and U87MG cells with erastin, RSL3, DMSO, DFO, NAC, 3-TYP, FerroOrange, FerroGreen, Mito-FerroGreen, DCFH-DA, MitoSOX solutions, injection of 3-TYP and RSL3 into tumor-bearing mice	Cells treated in 96-well plates with prepared solutions, incubated at 37°C in 5% CO ₂ , solutions freshly prepared before treatments, cells washed with serum-free DMEM or PBS before treatments, compounds injected into tumors every 2 days for 8 days	SIRT3 inhibition sensitized GBM cells to RSL3-induced ferroptosis both in vitro and in vivo	Downregulation of SLC7A11, activation of mitophagy pathway, accumulation of ferrous iron and ROS in mitochondria
Deng L et al. (2024)	1-2 weeks, 2 days, 24 hours	Nude mice with subcutaneous injection of U87 IGF2BP3-KD cells	Subcutaneous injection of U87 control cells	IGF2BP3 knockdown in glioma cells, lentiviral infection, xenograft tumor model establishment, co-culture of human microglia and glioma cells	Lentivirus transfection using pLKO.1 vector, filtered through 0.45 µm filter, polybrene added for infection, puromycin selection for 2 days, xenograft model with subcutaneous injection into nude mice, tumor monitoring every two days, co-culture in 6-well plates for 3 days, confocal microscopy used for phagocytosis analysis	IGF2BP3 knockdown impairs glioma cell growth, survival, and tumor formation	Regulation of ferroptosis via GPX4 mRNA binding, stabilization of GPX4 mRNA through m6A modification, increased susceptibility of glioma cells to microglial phagocytosis
Guo F et al. (2024)	17 days, 15 days + 24 hours + 24 hours	LN229 and T98G human glioblastoma cell lines, immunodeficient mice (6 total: 3 females, 3 males, age 6 weeks).	Placebo control group (6 mice: 3 females, 3 males).	Juglone treatment alone or combined with inhibitor applied to LN229 and T98G glioblastoma cell lines and xenograft tumor models.	Cells inoculated into 96-well and 6-well plates, juglone medium maintained for 24 h with pre-treatment using inhibitor for 1 h, medium replaced with normal growth medium, cells fixed with 4% polyformaldehyde and stained with crystal violet solution, total protein extracted using RIPA buffer with protease inhibitors, protein analyzed via SDS-PAGE and NC membrane transfer, primary and secondary antibodies used for detection, intracellular ROS measured with DCFDA incubation and flow cytometry, xenograft tumor model created using LN229 cell suspension injected into nude mice, treatment administered via abdominal injections every other day	Induction of ferroptosis and inhibition of glioblastoma growth by juglone	Activation of p38MAPK phosphorylation, negative regulation of Nrf2-GPX4 signaling pathway

Liang B et al. (2024)	24 hours	HUVEC-NOX4-Si-1 cells (8285 cells) from Cell Resource Center, Peking Union Medical College, China.	HUVEC-siCtrl cells.	Transfection of HUVEC cells with NOX4 gene siRNA and control siRNA using RNAimax.	Cells digested with trypsin-EDTA, resuspended in medium, transfection performed using RNAimax at 50 nM, incubated post-transfection, RNA extracted using Trizol and chloroform, reverse transcription applied using qPCR RT kit, qPCR performed using SYBR Master Mixture for gene analysis	Upregulation of ferroptosis in endothelial cells within recurrent glioblastomas, identified by NOX4 gene overexpression	Reduction of glioblastoma cell growth rate linked to decreased ferroptosis activity
Zhu Y et al. (2024)		U87MG glioblastoma cells, orthotopic U87MG-Luc glioblastoma in vivo models.		Carrier-free Ce6@Cu nanoparticles self-assembled via coordination of Cu ²⁺ and chlorin e6, sonodynamic-triggered combination of cuproptosis and ferroptosis.	Internalization by U87MG cells, glutathione depletion, lipid peroxidation, blood-brain barrier penetration, accumulation in glioblastoma cells, sonodynamic activation	Induction of ferroptosis and irreversible cuproptosis in glioblastoma via sonodynamic activation of Ce6@Cu nanoparticles, resulting in Cu ⁺ concentration increase, proteotoxic stress, and tumor reduction.	Minimal side effects, significant tumor accumulation, proteotoxic stress, increased Cu ⁺ concentration
Neitzel LR et al. (2024)		Orthotopic larval xenograft models in Danio rerio, human glioblastoma cell lines U87-MG and U138-MG overexpressing GPR68.		shRNA-mediated knockdown of GPR68, treatment with ogremorfin (OGM) as a small molecule inhibitor.	Delivered in orthotopic larval xenograft models in zebrafish, shRNA applied for GPR68 knockdown, OGM administered to inhibit GPR68, limited toxicity observed in zebrafish embryos	Reduction in in vivo survival of glioblastoma cells following GPR68 inhibition or knockdown	Induction of ferroptosis linked to increased lipid peroxidation, limited toxicity to zebrafish embryos
Abu-Serie MM et al. (2024)	2 weeks per cycle, repeated up to 6 cycles.	Human glioblastoma stem cells (MGG18, JX39P), mouse glioblastoma stem cells (GS, PDGF-GSC), radioresistant glioblastoma stem cells (MGG18-RR, GSRR, PDGF-GSC-RR, JX39-RT).		Use of DE-FeO nanoparticles (NPs) and TMZ for growth inhibition of glioblastoma stem cells and radioresistant variants.	Applied at specific concentrations during sphere formation assays, incubation for 72 hours in 5% CO ₂ incubator at 37°C, XTT assay to measure cell viability, ROS assay kit for reactive oxygen species detection, ALDH assay for enzyme activity evaluation, fluorescence and phase contrast microscopy for sphere morphology, ImageJ software for sphere area measurement	Potent inhibition of glioblastoma stem cells and their radioresistant variants via ALDH1A1 suppression and ferroptosis induction	Improved sensitivity to chemotherapy and radiotherapy, reduction in self-renewal, chemoresistance, radioresistance, cancer repopulation, inhibition of stemness gene expression, decreased p-AKT/AKT ratio

Shao G et al. (2024)	2 days, 48 hours, 6–7 days, 17 days	C57BL/6N mice aged 6–8 weeks, male and female, health status assessed before the experiment, MS4A4A knockout mice inoculated with CT2A or GL261 tumor cells	Wild-type mice inoculated with CT2A tumor cells, no treatment control group	MS4A4A knockout, combined immune checkpoint blockade therapy, TAM stimulation, macrophage polarization using recombinant cytokines, lentiviral infection of THP-1 cells, subcutaneous and intracranial tumor cell injections	THP-1 cells infected with lentivirus at MOI 0.8, treated with puromycin (10 µg/mL for 48 h), macrophage polarization with PMA (50 ng/mL for M0), LPS and interferon-γ (100 ng/mL and 20 ng/mL for M1), IL-4 or IL-4/IL-13 (20 ng/mL each for M2), TAM stimulation with CT2A/GL261 supernatant for 2 days, subcutaneous injection of CT2A/GL261 tumor cells (2.5–3 × 10 ⁶ cells in 100–200 µL), intracranial injection of CT2A tumor cells (1 × 10 ⁶ cells in 1–5 µL), anti-PD-1 antibodies (200 µg day 6, 50 µg day 12, repeated every 3–4 days), anti-PD-L1 antibodies (100 µg day 6, repeated every 3 days), Clodronate liposomes (150 µL intra-abdominal), injection site protocols (depth 3 mm, posterior to nose bridge, lateral to midline)	Complete tumor eradication, inhibition of tumor growth, reshaped tumor immune microenvironment	Reduction in M2 TAM infiltration, enhanced CD8+ T-cell infiltration, improved GBM response to PD-1 immunotherapy
Mansuer M et al. (2024)	4 months, 14 days per dose, 24 hours	Patients diagnosed with glioma undergoing surgery at the Neurosurgery Department of the Shanghai Tenth People's Hospital from January 2015 to December 2019, 70 participants		Induction of TMZ-resistant glioblastoma cells, gene manipulation targeting REST, LRSAM1, and SLC40A1, treatment with proteasome inhibitor MG132 and cycloheximide	TMZ administered in culture media for 14 days per dose over 4 months, lentiviral vectors transfected using Lipofectamine 3000, MG132 added to culture media for 6 hours, cycloheximide administered at intervals up to 12 hours, standardized protocols for lentiviral transfection and gene manipulation	Eriarin enhances TMZ sensitivity in TMZ-resistant glioma stem cells and induces ferroptosis through REST downregulation and SLC40A1 ubiquitination and degradation	Inhibition of malignant phenotypes, suppression of stemness, reduction in cell proliferation, migration, invasion, neurosphere-forming ability
Cao W et al. (2024)	48 hours, 12 days, 30 days	BALB/c-nude mice, aged 8 weeks, Animal Experimental Center of Guizhou Medical University, 5 participants per experimental group		FOXP3-overexpression or FOXP3-knockdown through lentivirus transfection, siRNA mimics targeting GPX4 and Linc00857	Transfection using polybrene and Lipo2000, stable cell selection with puromycin after 48 hours, RPMI-1640 medium supplemented with 10% FBS, lentivirus and siRNA mimics used, manufacturer's instructions followed for transfection	Impact of FOXP3 on glioblastoma progression by inhibiting ferroptosis and promoting proliferation	Therapeutic potential of FOXP3 inhibition using epirubicin, suppression of proliferation and induction of ferroptosis in GBM cells
Lu T et al. (2024)		Patients with biopsy-proven grade VI high-grade gliomas (GBMs)	Vehicle control, placebo control group	Isolation and generation of patient-derived GBM tumor cells, coculture experiments with neutrophils, treatment with 4-ABAH and Liproxstatin-1	Tumor tissue collected during craniotomy, minced and digested with hyaluronidase and collagenase IV, cells filtered and centrifuged, coculture with neutrophils labeled with fluorescent dyes, intraperitoneal injection of compounds, imaging using Incucyte S3, IX83 Inverted microscope, JEOL JEM1400 Transmission Electron Microscope, SDS lysis buffer and SDS-PAGE used for cell processing, RGDS peptides applied for adherence assays	Reduction in necrosis formation and prolonged mouse survival in glioblastoma models	Identification of LAP-mediated neutrophil engulfment and granule transfer, potential therapeutic targets for glioblastoma prognosis improvement

Chen Het al. (2025)	18 days	C57BL/6J mice induced with intracranial glioblastoma	Tumor-bearing mice, PBS control group	Lpo@Cu2Se and Lpo@Cu2Se-GOx nanocomposites treatment	Cu2Se concentration 2 mg/kg for in vivo treatment, bioluminescence imaging for tumor growth monitoring, GL261 cells pre-treated with 16 µg/mL nanocomposites, co-incubation with DC cells for 48 h, in vitro BBB model using bEnd.3 cells co-incubated with GL261 cells for 24 h, RhB-labeled nanocomposites added to apical chamber for 4 h, cell viability detected via CCK-8 assay, live/dead cells evaluated using Calcein-AM/PI detection kit, serum analysis for liver/renal function markers and blood tests, tumor tissues fixed for staining (H&E, Ki67, TUNEL, CRT, HMGB1), stereotactic injection of GL261-luc cells into striatum	Enhanced anti-tumor effect of Lpo@Cu2Se-GOx nanocomposites demonstrated through oxidative stress induction and tumor inhibition	Improved immune response, efficient penetration through BBB, increased intracellular ROS generation
Jamali AW et al. (2025)	3 weeks	Female mice, 4–6 weeks old, undergoing cisplatin-induced acute kidney injury and tumor formation experiments.	Cells transfected with non-targeting shRNA or empty vector plasmid.	Administration of ALKBH5 inhibitors (DDO-2728, IOX1), transfection of U251 glioblastoma cells targeting ALKBH5.	Intraperitoneal injection of inhibitors dissolved in dimethyl sulfoxide for 3 weeks, transfection of U251 cells using shRNA plasmids and pcDNA3.1-ALKBH5 plasmid, cell viability assessed via CCK-8 assay, proliferation measured using EdU staining, invasive capability evaluated with Transwell chamber assay, tumour volume calculated using callipers and formula, protein expression quantified via SDS-PAGE and image analysis software	Inhibition of proliferation, invasion, tumour growth, and increased ferroptotic sensitivity in U251 glioblastoma cells through ALKBH5 knockdown-mediated regulation of MUC1	Enhancement of proliferation, invasion, tumour growth, and MUC1 expression with ALKBH5 overexpression, rescue of inhibitory effects of ALKBH5 knockdown via MUC1 overexpression
Wang X et al. (2024)	24 hours	Human glioma cell lines LN229, U251, and U87.	Mice bearing U87 tumor xenografts, placebo control group.	RSL3 pretreatment, X-ray irradiation to enhance IR-induced DSBs.	RSL3 administered to cells and mice, X-ray irradiation using X-RAD 320 irradiator, pretreatment at concentrations of 0.05, 0.1, 0.2 µM for 24 hours, irradiation doses of 2, 4, 6, and 8 Gy at 1.02 Gy/min, additional pretreatment with DFO, FAC, Lip-1 for 1 hour prior to RSL3, Western blot analysis of cellular markers	Radiosensitization of glioma cells via RSL3-enhanced IR-induced DNA double-strand breaks by suppressing TGM2-mediated repair mechanisms	Inhibition of epithelial-mesenchymal transition in glioma cells, synergistic inhibition of glioma cell growth with RSL3/IR combination

Liu T et al. (2022)	5 days	Male C57BL6 and SCID Beige mice, GBM-bearing murine models.		Anti-PD1/L1 Ab and Ferrostatin-1 administration.	Anti-PD1/L1 Ab injected intraperitoneally at 10 µg/g after GBM implantation for 5 days, Ferrostatin-1 injected intraperitoneally at 10 mg/kg every 2 days after GBM implantation for 5 days, SB cells (5×10^4) and GL261 cells (5×10^5) intracranially injected to establish murine models, conditional medium prepared with RPMI-1640 medium containing 10% FBS, GBM cells treated with ferrostatin-1 or erastin for 48 h, supernatant collected after 24 h incubation	Correlation of ferroptosis with glioma outcomes	Synergistic therapeutic effect of ferroptosis inhibition combined with PD-1/PD-L1 blockade in GBM murine models
Xie Y et al. (2022)		169 tumor tissues, RNA sequencing data from TCGA database.	Non-intervention normal tissues.	Exposure of cells to Erastin and X-rays.	Cells incubated with 10 µM Erastin for 10 hours, X-rays applied at doses of 0–8 Gy or 2 Gy, cultured further for 24 hours or 10 days, fixed with paraformaldehyde, stained with crystal violet, EdU, Apollo dye solution, and DAPI, seeded onto 96-well and 6-well plates at specific concentrations, images captured using fluorescence microscope	Identification of seven radiosensitivity- and ferroptosis-associated biomarkers as risk signature genes with survival prediction capabilities in glioma patients	Functional enrichment of DEGs in glioma-related biological processes, differences in immune function status between high-risk and low-risk groups, validation of prognostic model
Xu P et al. (2022)	4 h + 72 h	Human glioblastoma cell lines U87MG and A172, human normal brain astroglia cells HA1800 and SVGp12.	Negative control using DMSO.	Transfection with miR-147a mimic/inhibitor, stimulation with ferroptotic inducers.	Transfection with miR-147a mimic/inhibitor (50 nmol/L) using Lipofectamine™ 3000 for 4 h, stimulation with erastin (5 µmol/L) or RSL3 (2 µmol/L) for 72 h, treatment with Fer-1 (1 µmol/L) or Lip-1 (0.2 µmol/L) for 72 h, infection with AdSLC40A1 at MOI 20 for 4 h followed by miR-147a mimic transfection, TMZ treatment (100 µmol/L) for 48 h	Suppression of glioblastoma cell growth and induction of ferroptosis by miR-147a mimic, enhanced sensitivity to TMZ chemotherapy	Prevention of ferroptosis and increased cell viability by miR-147a inhibitor, targeting of SLC40A1 to inhibit iron export, facilitation of iron overload and lipid peroxidation
Yao L et al. (2022)	2 weeks, 24 hours, 12 hours, 8 hours	Glioma cell lines (T98G-R, U118MG-R)	U87 siCtrl cell line treated with DMSO	KO-947 dissolved in DMSO, colony formation assay, invasion assay, wound-healing assay	Cells seeded in plates or chambers under 5% CO2 at 37°C, colony formation for 2 weeks, invasion assay for 24 hours, wound-healing assay for 12 hours, wound created manually using sterile pipette tips, cell starvation in FBS-free medium for 8 hours, fixation with paraformaldehyde, staining with crystal violet, Matrigel-coated membranes used for invasion assay, protein extraction and immunoblotting performed as per prior protocol	Roles and mechanism of ferroptosis-related genes in chemoresistance and metastasis of glioblastoma multiforme, highlighting SQLE suppression of ERK-mediated TMZ chemoresistance and metastasis, and its prognostic significance, association with WHO grade, and ERK-mediated chemoresistance.	Prognostic and therapeutic potential of SQLE in glioblastoma multiforme

Liu X et al. (2023)	48 h, 72 h	Mice implanted with GBM cells expressing luciferase		Delivery of CRISPR genome editing via modified extracellular vesicles loaded with Cas9/sgRNA complex	Cas9/sgRNA complex loaded into Angiopep-2 and TAT peptide-modified EVs, transduction at low MOI (~0.3), cells inoculated overnight in culture flasks, 20 mm confocal dish, or 96-well plates, treated with irradiation or drugs, incubation for 48 h or 72 h	Identification of synthetic lethal genes associated with radiotherapy resistance in glioblastoma using genome-wide CRISPR screening. The primary outcome of this study is to identify synthetic lethal genes that contribute to radiotherapy resistance. The secondary outcome involves assessing the impact of these genes on treatment efficacy. Additionally, the correlation with patient prognosis will be evaluated to determine how these genes influence overall survival and treatment outcomes.	Role of glutathione synthetase (GSS) in suppressing radiotherapy-induced ferroptosis, correlation of high GSS levels with poor prognosis and relapse in glioma patients
Ye R et al. (2025)		Female nude mice, 4–6 weeks old		Combination of FR054 (PGM3 inhibitor) with TMZ	Administered in vitro and in vivo using GBM organoid and intracranial xenograft models, GBM organoids derived from surgical tumor tissues cultured on ultra-low attachment plates under orbital shaking at 100 rpm, tumor progression monitored via bioluminescence imaging, animal experiments conducted following IACUC-approved protocols	Suppression of tumor progression and prolonged survival in orthotopic xenograft mice treated with FR054 combined with TMZ	Enhanced TMZ sensitivity via inhibition of protein O-GlcNAcylation, induction of ferroptosis through HMOX1 upregulation and GPX4 downregulation, minimal side effects
Liu S et al. (2025)		6-week-old BALB/c nude mice	3 mice, PBS control group	Intravenous injection of Lut NPs, FL NPs, FLD NPs, laser irradiation	Groups randomized, Lut NPs/FL NPs/FLD NPs injected intravenously at 1 mg Lut equivalent/kg, laser irradiation applied to G4 and G6 groups (808 nm, 1.0 W/cm ² , 5 min)	Amplification of ferroptosis and blood-brain barrier penetration for glioblastoma therapy	Enhanced ferroptosis via quadruple mechanisms, improved tumor targeting through multimodal imaging
Piotrowsky A et al. (2024)	24 hours, 48 hours, 3–6 hours, 6 hours, 8 hours	Human-derived glioblastoma cell lines (SF268, SF295, U251)	Positive control group treated with 0.1% Triton®X-100	Use of ascorbate at various concentrations with FeCl ₃ , MgCl ₂ , or DFO	Pre-incubation with FeCl ₃ or MgCl ₂ for 24 h, ascorbate treatment up to 4 mM for 3–8 h or 24 h, cells seeded in 24-well or 12-well plates at specific densities, incubated at 37°C and 5% CO ₂ , washed twice with PBS before treatment, DCFH-DA assay for ROS induction, staining with PI and RNase or Hoechst 33342, hourly imaging for 48 h using Lionheart FX microscope	High-dose ascorbate demonstrated cytotoxicity and antiproliferative efficacy in glioblastoma cells, with evidence of ferroptosis	Increased intracellular ROS formation and cytotoxicity with Fe ³⁺ pre-treatment, weaker effects observed for dehydroascorbic acid, caspase-3 independence of cell death

[Back to 2.2.3. Therapeutic Strategies and Treatment Outcomes](#)